Electronic Supplementary Information

A *Tellura*-Baeyer-Villiger Oxidation: One-step Transformation of Tellurophene into Chiral Tellurinate Lactone

Shitao Wang, Chaoxian Yan, Wenlong Zhao, Xiaolan Liu, Cheng-Shan Yuan, Hao-Li Zhang and Xiangfeng Shao*

State Key Laboratory of Applied Organic Chemistry, Lanzhou University, Tianshui Southern Road 222, Lanzhou 730000 (China)

Email: shaoxf@lzu.edu.cn

Table of contents

1. Materials and General methods

All chemicals and solvents were purified according to the standard procedure.[S1] Tellurium powder was purchased from Adamas Reagent Co. Ltd. The *meta*-chloroperbenzonic acid (*m*CPBA) was purchased from Energy Chemical. The compounds **7** and **8** were synthesized according to our previous report.[S2]

The melting points were determined on a WRS-2 melting point apparatus. The high resolution mass spectral analysis (HRMS) was carried out on Bruker APEX II type mass spectrometer. Thermogravimetric analyses (TGA) were conducted on 1090B type thermal analyzer (Dupont Engineering Polymers). The infrared (IR) spectra were record on the PerkinElmer Spectrum 400 spectrometer with the resolution of 2 cm^{-1}.

The ^{1}H NMR, ^{13}C NMR, and ^{125}Te NMR spectra were recorded on Bruker Advance III 400 MHz or 600 MHz spectrometer (400 MHz or 600 MHz for ^{1}H NMR, 400 MHz for ^{125}Te NMR, 100 MHz or 125 MHz for ^{13}C NMR). Chemical shifts for ^{1}H NMR spectra were reported in parts per million (ppm, δ scale) downfield from tetramethylsilane, and referenced internally to the residual proton in solvents ($CDCl_3$: δ 7.27, CD_2Cl_2: δ 5.32). Chemical shifts for ^{13}C NMR spectra are reported in parts per million (ppm, δ scale) downfield from tetramethylsilane, and are referenced to the ^{13}C resonance of solvenst ($CDCl_3$: δ 77.00, CD_2Cl_2: δ 53.43). Data are reported as follows: chemical shift, multiplicity (s = singlet, d = doublet, t = triplet, q = quartet, m = multiplet); coupling constants, *J*, are reported in hertz. The HSQC and HMBC were recorded on a Bruker Advance III 600 MHz spectrometer. The chemical shifts of ^{125}Te NMR of the compounds in this manuscript were recorded by using ^{125}Te NMR of diphenyl ditelluride (0.5 M solution in $CDCl_3$, δ = 420 ppm) as external reference.[3]

The two pairs of enationmers of compounds **2, 9** and **10** were separated by the means of chiral high-performance liquid chromatography (HPLC, Shimadzu LC-20AT) at 25 ºC. The enantiomers of **2** were separated by the chiral HPLC on CHIRALPAK IG-3 (IG30CD-WE016) column (column size: 0.46 cm I.D. ×15 cm L; eluent: MeOH/DCM=80/20). The **9** and **10** were separated by Daicel CHIRALPAK IF (IF00CE-SL018) column (column size: 0.46 cm I.D. ×25 cm L; eluent: hexane/CH_2Cl_2 = 50/50). The flow rate is 1 mL/min and the wavelength of UV is 254 nm.

Circular dichroism (CD) in CH_2Cl_2 ($c = 6\times10^{-4}$ mol L^{-1}) was measured on an Olis-DSM-1000 Circular Dichroism Spectrometer at 20 ºC. The UV-Vis absorption spectra in CH_2Cl_2 were measured on a UV-2600 UV-Specterophotometer at 20 ºC. The excitation and emission spectra, and emission lifetime in THF solution ($c = 2\times10^{-3}$ mol L^{-1} for **2**, **9**, and **10**; $c = 10^{-6}$ mol L^{-1} for *mono*-**2**, *mono*-**9**, and *mono*-**10**) were measured on a FLS-920 Spectrofluorophotometer at 77 K.

The single-crystal X-ray diffraction was carried out on a SuperNova (Agilent) diffractometer. The crystal structure was solved by a direct method *SIR*2004[S4] and refined by full-matrix least-square method on F^2 by means of *SHELX*L-97.[S5] The calculated positions of the hydrogen atoms were included in the final refinement.

2. Synthesis

2.1 Synthesis of 1

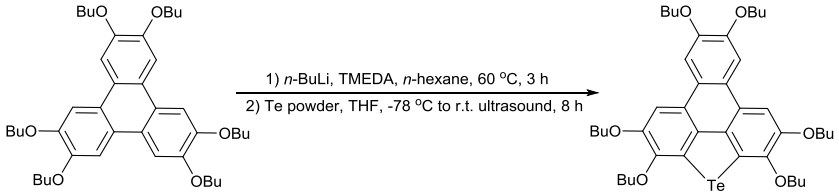

1 (41%)

Under the nitrogen atmosphere, TMEDA (9.00 mL, 0.06 mol) and *n*-butyllithium (2.4 M in *n*-hexane, 25.00 mL, 0.06 mol) were injected to a solution of 2,3,6,7,10,11-hexabutoxytriphenylene (13.2 g, 0.02 mol) in *n*-hexane (100 mL) at room temperature (r.t.). The resulting mixture was stirred at 60 °C for 3 hours, and then cooled to r.t., followed by addition of 100 mL THF. The mixture was further cooled to -78 °C, and tellurium powder (7.62 g, 0.06 mol) was added in one portion. The resulting mixture was allowed to warm up slowly to r.t. and stirred under ultrasound for 8 hours. Finally, the reaction was quenched by adding distilled water and the mixture was extracted with CH_2Cl_2 (3 × 150 mL). The organic layers were combined and dried over anhydrous Na_2SO_4, then concentrated in vacuo. The crude product was purified by column chromatography on silica (eluent, CH_2Cl_2: petro ether, 1 : 4, v/v) to afford **1** as a yellow solid (6.46 g, 41%). mp: 109.1 °C-110.6 °C; ^{1}H NMR (400 MHz, $CDCl_3$): δ(ppm) 7.87 (s, 2H), 7.80 (s, 2H), 4.33-4.26 (m, 12H), 1.98 (m, 8H), 1.91-1.84 (m, 4H), 1.72-1.61(m, 12H), 1.14-1.07 (m, 18H); ^{125}Te NMR (400MHz, $CDCl_3$) δ(ppm) 595.56; ^{13}C NMR (101 MHz, $CDCl_3$) δ(ppm) 150.38, 149.21, 148.48, 133.22, 126.96, 124.12, 119.94, 107.24, 105.22, 72.77, 69.22, 69.19, 32.89, 31.74, 31.5 , 19.61, 19.58, 19.48, 14.13, 14.08; HRMS: calculated for $C_{42}H_{58}O_6Te$, 788.3290; found, 788.3280.

2.2 Synthesis of 2

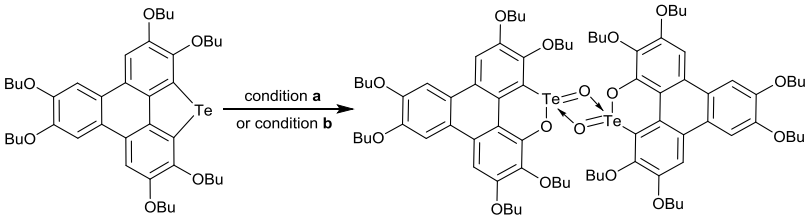

Condition *a*: Compound **1** (0.79 g, 1 mmol) and Oxone (1.23 g, 2 mmol) was dissolved in a mixed solvent of THF (20 mL) and deionized H_2O (5 mL). The resulting mixture was stirred for 4 h at r.t., and then deionized H_2O was added. The mixture was extracted with dichloromethane (CH_2Cl_2, 3 × 30 mL). The organic layers were combined and dried over anhydrous Na_2SO_4, then concentrated under reduced pressure. The crude product was further purified by column chromatography on silica-gel (eluent, CH_2Cl_2) to afford **2** as yellow solid (0.68 g, 82%).

Condition *b*: Compound **1** (0.39 g, 0.5 mmol) and *m*CPBA (85%, 0.20 g, 1 mmol) were dissolved in CH_2Cl_2 (5 mL). The resulting mixture was stirred at r.t. for 4 h. Aqueous Na_2SO_3 and aqueous $NaHCO_3$ were then added to this mixture, which was then extracted with CH_2Cl_2. The organic layer was washed with H_2O, dried over anhydrous Na_2SO_4, and concentrated under reduced pressure. The crude product was further purified by column chromatography on silica-gel (eluent, CH_2Cl_2) to afford **2** as yellow solid (0.21 g, 52%). mp: 186.2-190.1 ^oC; ^1H NMR (600 MHz, $CDCl_3$): δ(ppm) 7.91 (s, 2H), 7.59 (s, 2H), 7.37 (s, 2H), 6.72 (s, 2H), 4.46 (dt, J = 9.2, 6.2 Hz, 2H), 4.35 (dt, J = 8.9, 6.3 Hz, 2H), 4.27 (dt, J = 8.8, 6.5 Hz,, 2H), 4.21 (m, 6H), 4.13 (dt, J = 9.0, 6.6 Hz, 2H), 4.00 (dt, J = 9.4, 6.6 Hz, 2H), 3.54 (dt, J = 9.4, 6.8 Hz, 2H), 3.39 (dt, dt, J = 8.5, 6.0 Hz, 2H), 3.12 (dt, dt, J = 8.1, 6.1 Hz,, 2H), 2.79 (dt, J = 9.5, 6.6 Hz, 2H), 2.08-1.98 (m, 6H), 1.97-1.89 (m, 6H), 1.88-1.81 (m, 4H), 1.75-1.61 (m, 18H), 1.57-1.42 (m, 8H), 1.35-1.23 (m, 4H), 1.12 (t, J = 7.4 Hz, 6H), 1.07 (m, 12H), 1.03 (t, J = 7.4 Hz, 6H), 1.01 (t, J = 7.3 Hz, 6H), 0.94 (t, J = 7.3 Hz, 6H); ^{125}Te NMR (400MHz, $CDCl_3$) δ(ppm) 1222.95; ^{13}C NMR (151 MHz, $CDCl_3$): δ(ppm) 152.41, 149.74, 149.05, 147.82, 146.50, 137.89, 127.50, 125.05, 124.70, 123.78, 123.76, 120.37, 113.53, 110.04, 108.48, 107.52, 97.82, 72.88, 72.13, 71.00, 69.18, 68.68, 67.37, 32.60, 32.35, 31.77, 31.63, 31.57, 19.63, 19.50, 19.47, 19.40, 19.39, 18.83, 14.18, 14.13, 14.11, 14.04, 13.99; HRMS, **2**: calculated for $C_{84}H_{116}O_{16}Te_2$+H, 1639.6443; found, 1639.6437; *mono*-**2**: calculated for $C_{42}H_{58}O_8Te$+H, 821.3267; found, 821.3257.

2.3 Synthesis of 3

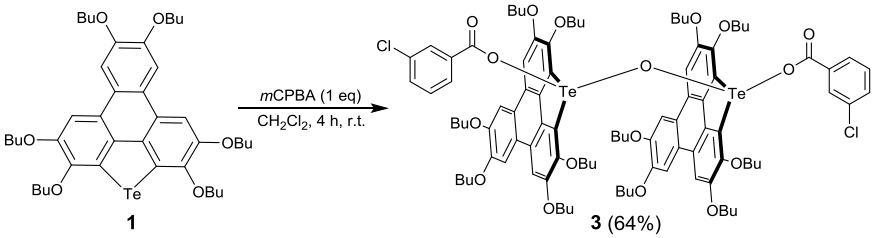

Compound **1** (0.39 g, 0.5 mmol) and *m*CPBA (85%, 101.5 mg, 0.5 mmol) were dissolved in CH_2Cl_2 (5 mL). The resulting mixture was stirred at r.t. for 4 h. Aqueous Na_2SO_3 and aqueous $NaHCO_3$ were then added to this mixture, which was then extracted with CH_2Cl_2. The organic layer was washed with H_2O, dried over anhydrous Na_2SO_4, and concentrated under reduced pressure. The crude product was purified by column chromatography on silica-gel (eluent, CH_2Cl_2 : ethyl acetate (EA) =3:1) to afford yellow solid. After further purification by slowly evaporating the CH_2Cl_2-ethanol (1 : 1, *v*/*v*) solution of the yellow solid at r.t., compound **3** was obtained (0.30 g, 64%). mp: 217.1-219.2 ^oC; ^1H NMR (400 MHz, $CDCl_3$) δ 7.35-7.32 (m, 6H), 7.27 (d, *J* = 7.9 Hz, 2H) 7.13 (s, 6H), 6.97 (t, *J* = 7.9 Hz, 2H), 4.40-4.34 (m, 4H), 4.27-4.20 (m, 8H), 4.17-4.12 (m, 8H), 4.09-4.04 (m, 4H), 2.02-1.92 (m, 16H), 1.90-1.81 (m, 8H), 1.72-1.53 (m, 24H), 1.10 (m, 24H), 1.03 (t, *J* = 7.3 Hz, 12H); ^{13}C NMR (151 MHz, CD_2Cl_2) δ 170.31, 151.29, 149.10, 147.59, 136.56, 134.97, 133.20, 132.44, 130.29, 128.95, 128.68, 127.25, 125.24, 123.36, 108.05, 106.58, 73.72, 69.05, 68.54, 32.54, 31.74, 31.62, 19.66, 19.41, 19.30, 13.88, 13.81;

It should be noted that we cannot observe the ionic peak of compound **3** in HRMS. Instead, the ionic peak of I**M-1 (**$C_{42}H_{58}O_7Te$) appeared in the HRMS as following: calculated for $C_{42}H_{58}O_7Te$+H, 805.3318; found, 805.3340.

2.4 Synthesis of 4

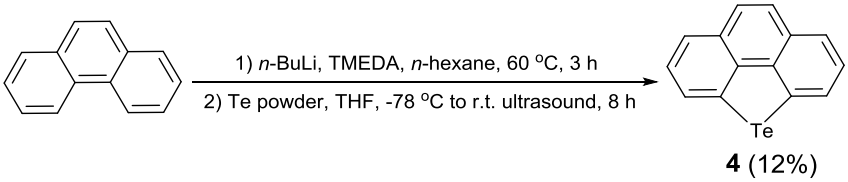

4 (12%)

Under nitrogen atmosphere, TMEDA (13.50 mL, 0.09 mol) and *n*-BuLi (2.4 M in *n*-hexane, 37.5 mL, 0.09 mol) were added to a solution of phenanthrene (5.35 g, 0.03 mol) in *n*-hexane (100 mL) at r.t. The resulting mixture was heated to 60 °C and stirred for 3 h. Afterwards, the reaction was cooled to r.t., followed by addition of THF (100 mL) and then cooled to -78 °C. Te powder (11.43 g, 0.09 mol) was added in one portion. The resulting mixture was warmed up to r.t. and stirred under ultrasound for 8 h. Finally, the reaction was quenched by adding distilled H_2O and the mixture was extracted with CH_2Cl_2 (3 × 150 mL). The organic layers were combined and dried over anhydrous Na_2SO_4, then concentrated in vacuo. The crude product was purified by column chromatography on silica (eluent, petro ether) to afford **4** as a white solid (1.1 g, 12%). mp: 110.1 °C-113.6 °C; ^{1}H NMR (400 MHz, CD_2Cl_2): δ 8.12 (dd, *J* = 7.5, 0.9 Hz, 2H), 7.97 (dd, *J* = 7.8, 1.0 Hz, 2H), 7.87 (s, 2H), 7.70 (t, *J* = 7.6 Hz, 2H); ^{13}C NMR (151 MHz, CD_2Cl_2) δ 139.40 , 133.58 , 129.54 , 128.09 , 127.10 , 126.42 , 123.54 ; HRMS: calculated for $C_{14}H_8Te$, 305.9683; found, 305.9682.

2.5 Synthesis of 5

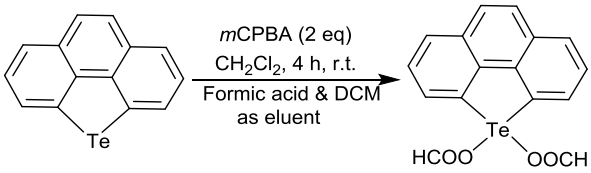

4 **5** (71%)

Compound **4** (152 mg, 0.5 mmol) and *m*CPBA (85%, 203 mg, 1 mmol) were dissolved in CH_2Cl_2 (10 mL). The resulting mixture was stirred at r.t. for 4 h. Aqueous Na_2SO_3 and aqueous $NaHCO_3$ were then added to this mixture, which was then extracted with CH_2Cl_2. The organic layer was washed with water, dried over anhydrous Na_2SO_4, and concentrated in vacuo. The crude product was purified by column chromatography on silica-gel (eluent, CH_2Cl_2 : formic acid=3:1) to afford **5** as a white solid (140.6 mg, 71%). mp: 136.1-138.2 °C; ^{1}H NMR (600 MHz, CD_2Cl_2): δ 8.23 (dd, *J* = 7.3, 0.7 Hz, 2H), 8.16 (dd, *J* = 8.0, 0.7 Hz, 2H), 7.99 (s, 2H), 7.89 (s, 2H), 7.87 (m, 2H); ^{13}C NMR (151 MHz, CD_2Cl_2) *δ*(ppm) 168.08 , 142.51 , 140.35 , 133.48 , 130.26 , 129.97 , 128.39, 127.52; IR (KBr Pellet) 1628 cm^{-1} (C=O); HRMS: calculated for $C_{14}H_8OTe$+H, 322.9710; found, 322.9720. Note that the two ester groups were dissociated in HRMS spectra of **5**, which is similar to that of compound **3**.

2.6 Synthesis of 9

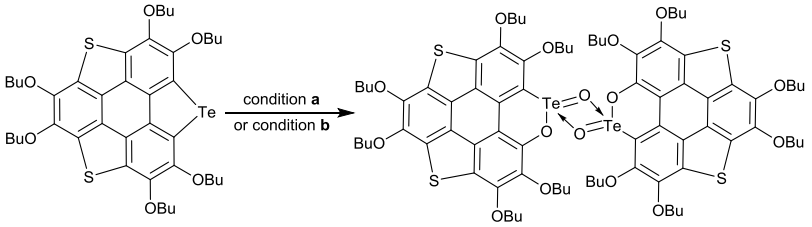

Condition *a*: Compound **7** (0.85 g, 1 mmol) and Oxone (1.23 g, 2 mmol) were dissolved in the mixed solvent of THF (20 mL) and deionized H_2O (5 mL). The resulting mixture was stirred for 4 h at r.t., and then deionized H_2O was added. The mixture was extracted with dichloromethane (CH_2Cl_2, 3 × 30 mL). The organic layers were combined and dried over anhydrous Na_2SO_4, then concentrated under reduced pressure. The crude product was purified by column chromatography on silica-gel (eluent, CH_2Cl_2: petro ether, 4 : 1, *v/v*) to afford **9** as yellow solid (0.70 g, 80%).

Condition *b*: Compound **7** (0.17 g, 0.2 mmol) and *m*CPBA (85%, 81 mg, 0.4 mmol) were dissolved in CH_2Cl_2 (5 mL). The resulting mixture was stirred at r.t. for 4 h. Aqueous Na_2SO_3 and aqueous $NaHCO_3$ were then added to this mixture, which was then extracted with CH_2Cl_2. The organic layer was washed with H_2O, dried over anhydrous Na_2SO_4, and concentrated under reduced pressure. The crude product was further purified by column chromatography on silica-gel (eluent, CH_2Cl_2) to afford **9** as yellow solid (53 mg, 30%). mp: 194.5-197.0 ^oC; ^1H NMR (600 MHz, $CDCl_3$): δ(ppm) 4.55-4.40 (m, 12H), 4.33-4.29 (m, 2H), 4.10-4.06 (m, 2H), 3.69-3.66 (m, 2H), 3.34 (m, 2H), 3.11 (m, 2H), 3.02-2.98 (m, 2H), 2.02-1.94 (m, 8H), 1.93-1.86 (m, 8H), 1.76-1.69 (m, 8H), 1.68-1.59 (m, 8H), 1.51-1.46 (m, 8H), 1.41-1.30 (m, 8H), 1.14-1.05 (m, 24H), 0.96 (m, 12H); ^{125}Te NMR (400MHz, $CDCl_3$) δ(ppm) 1239.43; ^{13}C NMR (151 MHz, $CDCl_3$): δ(ppm) 148.83, 148.73, 148.67, 146.12, 146.01, 145.09, 140.15, 132.63, 127.40, 126.52, 126.14, 125.95, 124.50, 124.47, 123.23, 120.56, 120.40, 111.94, 73.77, 73.09, 72.99, 72.77, 70.32, 32.55, 32.49, 32.43, 32.41, 32.24, 19.43, 19.37, 19.35, 19.31, 19.14, 19.05, 14.19, 14.09, 14.05, 14.00, 13.99, 13.95; HRMS, **9**: calculated for $C_{84}H_{108}O_{16}S_4Te_2$+H, 1759.4700; found, 1759.4736; *mono*-**9**: calculated for $C_{42}H_{54}O_8S_2Te$+H, 881.2395; found, 881.2415.

2.7 Synthesis of 10

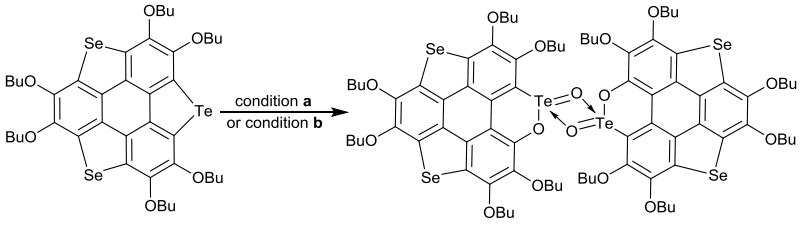

8 **10** (condition **a**: 78%; condition **b**: 8%)

Condition *a*: Compound **8** (0.94 g, 1 mmol) and Oxone (1.23 g, 2 mmol) were dissolved in the mixed solvent of THF (20 mL) and deionized H_2O (5 mL). The resulting mixture was stirred for 4 h at r.t., and then deionized H_2O was added. The mixture was extracted with dichloromethane (CH_2Cl_2, 3 × 30 mL). The organic layers were combined and dried over anhydrous Na_2SO_4, then concentrated under reduced pressure. The crude product was purified by column chromatography on silica-gel (eluent, CH_2Cl_2: petro ether, 4 : 1, *v/v*) to afford **10** as yellow solid (0.76 g, 78%).

Condition *b*: Compound **8** (188.8 mg, 0.2 mmol) and *m*CPBA (85%, 81.2 mg, 0.4 mmol) were dissolved in CH_2Cl_2 (5 mL). The resulting mixture was stirred at r.t. for 4 h. Aqueous Na_2SO_3 and aqueous $NaHCO_3$ were then added to this mixture, which was then extracted with CH_2Cl_2. The organic layer was washed with H_2O, dried over anhydrous Na_2SO_4, and concentrated under reduced pressure. The crude product was further purified by column chromatography on silica-gel (eluent, CH_2Cl_2) to afford **10** as yellow solid (15.8 mg, 8 %). mp: 113.5-116.6 ^oC; ^1H NMR (600 MHz, $CDCl_3$): δ(ppm) 4.51-4.45 (m, 6H), 4.44-4.35 (m, 6H), 4.32 (dt, J = 9.1, 6.7 Hz, 2H), 4.10 (dt, J = 9.4, 6.7 Hz, 2H), 3.53 (m, 4H), 3.10 (m, 4H), 2.04-1.99 (m, 4H), 1.97-1.86 (m, 12H), 1.79-1.68 (m, 8H), 1.66-1.58 (m, 8H), 1.56-1.47 (m, 8H), 1.45-1.33 (m, 8H), 1.17-1.05 (m, 24H), 0.97 (m, 12H); ^{125}Te NMR (400MHz, $CDCl_3$) δ(ppm) 1228.41; ^{13}C NMR (151 MHz, $CDCl_3$): δ(ppm) 150.36, 149.01, 148.97, 148.07, 148.06, 146.37, 140.46, 133.47, 130.02, 129.37, 128.58, 128.45, 125.84, 124.88, 124.01, 122.25, 119.68, 113.58, 73.67, 73.18, 73.05, 72.96 , 72.75, 70.16, 32.69, 32.56, 32.51, 32.44, 19.50, 19.47, 19.38, 19.35, 19.28, 19.18, 14.20, 14.09, 14.06, 14.02, 13.98; HRMS, **10**: calculated for $C_{84}H_{108}O_{16}Se_4Te_2$+H, 1949.2486; found, 1949.2522; *mono*-**10**: calculated for $C_{42}H_{54}O_8Se_2Te$, 976.1206; found, 976.1273.

3. Thermogravimetric Analyses

Thermogravimetric analyses (TGA) were conducted on 1090B type thermal analyzer (Dupont Engineering Polymers).

Table S1 Thermal stability of compounds **2**, **9** and **10**.

Comp	**2**	**9**	**10**
T_d / ºC	200	271	242

T_d : degradation temperature.

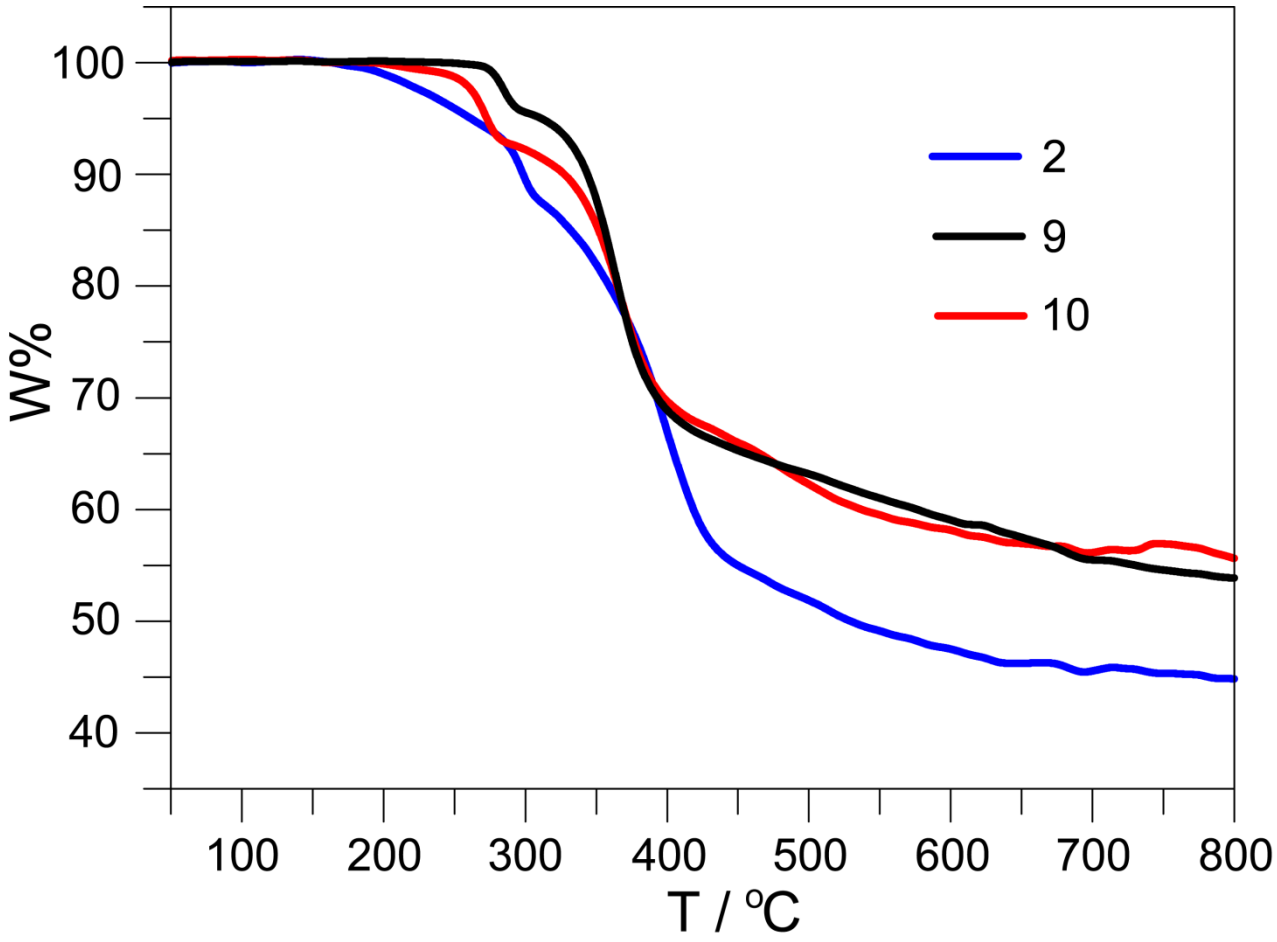

Fig. S1 TGA analyses of compounds **2**, **9** and **10**.

4. Assignment of protons, ^{125}Te NMR, ^{1}H NMR spectra under different conditions

The ^{1}H NMR of compound **2** and **13** were measured in $CDCl_3$ at 25 °C. The protons of –O-C*H*$_2$- on the *n*-butoxy region are assigned through HSQC and HMBC experiments as shown in **Figs. S2, S3, S5,** and **S6**. In addition, the H_{4a}, H_{4b}, H_{5a}, and H_{5b} can be assigned according to the relative position of protons in the crystal structure (**Fig. S4**). **Table S2** summarizes the chemical shifts of ^{1}H NMR, ^{13}C NMR, and the HMBC(H→C) data of **2**. As depicted in **Fig. S5**, there is dynamical transformation between **2** and *mono*-**2**. When the concentration is lower than 8×10^{-5} mol L^{-1}, the ^{1}H NMR spectrum of *mono*-**2** was observed. However, the ^{13}C NMR, HSQC and HMBC spectra of *mono*-**2** can not be obtained at such low concentration. The chemical shifts protons of –O-C*H*$_2$- on the *n*-butoxy region of *mono*-**2** were assigned by comparison with those of the analogue **13** (**Table S3**). The chemical shifts of the ^{125}Te NMR of **2, 9** and **10** are clearly down-field shifted as compared to those of the corresponding **1, 7** and **8** (**Fig. S6-S8**).

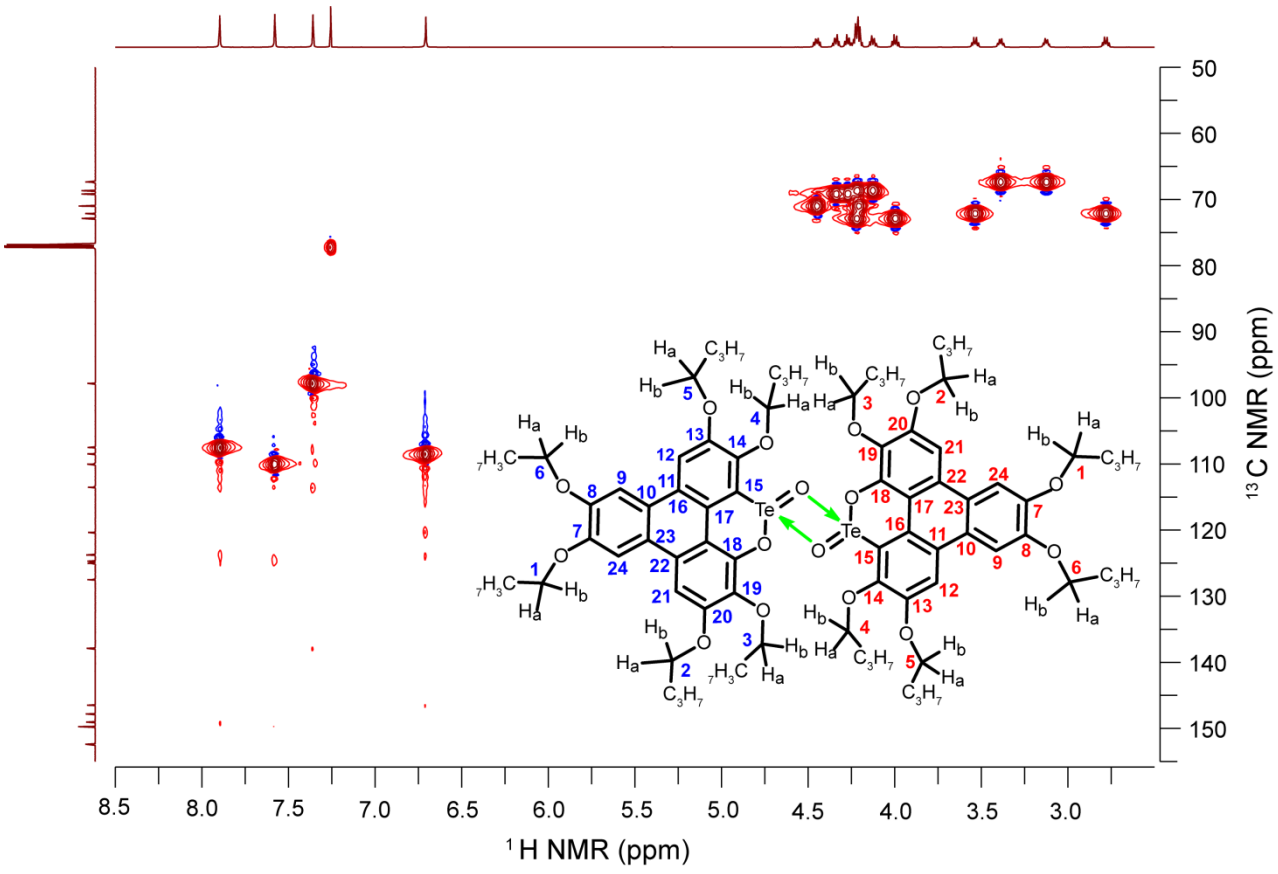

Fig. S2 The HSQC spectrum of compound **2** ($CDCl_3$, 600 MHz).

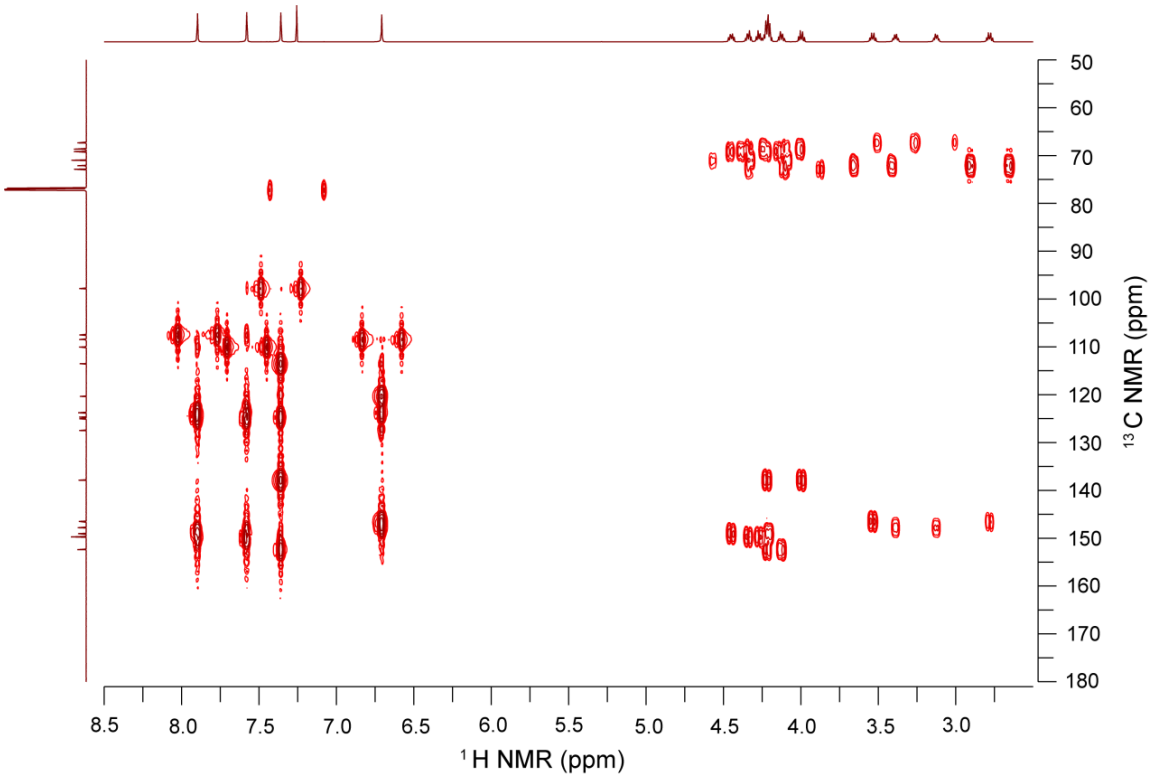

Fig. S3 The HMBC spectrum of compound **2** ($CDCl_3$, 600 MHz).

Table S2 The ^{1}H NMR, ^{13}C NMR and HMBC(H→C) data of compound **2**.

Number	^{1}H NMR (ppm)	^{13}C NMR (ppm)	HMBC(H→C)
1	H_a:4.35 (dt, 8.9, 6.3); H_b:4.27 (dt ,8.8, 6.5)	67.17	7
2	H_a: 4.21 (m); H_b:4.13 (dt, 9.0, 6.6)	68.67	20
3	H_a: 4.21 (m); H_b:4.00 (dt, 9.4, 6.6)	72.87	19
4	H_a: 3.54 (dt, 9.4, 6.8); H_b: 2.78 (dt, 9.5, 6.6)	72.12	14
5	H_a:3.39 (dt, 8.5, 6.0); H_b: 3.12 (dt, 8.1, 6.1)	67.36	13
6	H_a: 4.46 (dt, 9.2, 6.2); H_b:4.21 (m)	70.99	8
9	7.90 (s)	107.51	8, 23, 10, 11, 24, 6
12	6.71 (s)	108.47	13, 14, 15, 10, 11, 16
21	7.36 (s)	97.81	20, 19, 23, 17
24	7.58 (s)	110.03	7, 23, 9, 1

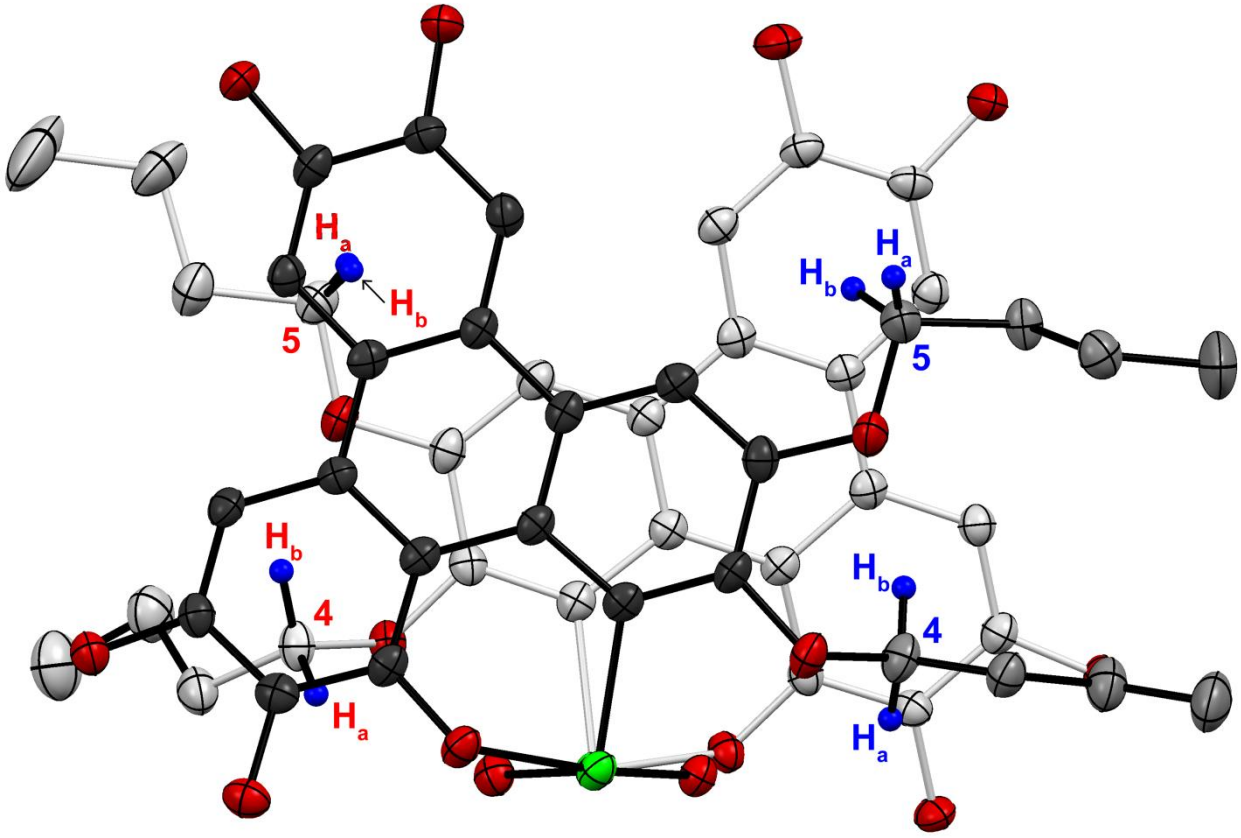

Fig. S4 Crystal structure of the compound **2** (top view). The H_{4a}, H_{4b}, H_{5a}, and H_{5b} are shown in blue. The other *n*-Bu groups and H atoms are omitted for clarity.

The chemical shifts of H-4a, H-4b, H-5a, and H-5b of compound **2** were determined with the aid of crystal structure of **2**. As shown in **Fig. S4**, H-4a, H-4b, H-5a, and H-5b are located in the shielding zone of the other triphenylene as depicted in the crystal structure of **2**. The chemical shift values of H-4b (δH 2.78) implied that H-4b in **2** was significantly shielded by the triphenylene. And the observed deshielding effects provide further evidence for the chemical shifts of H-4a (δH 3.54), H-5a (δH 3.39), and H-5b (δH 3.12).

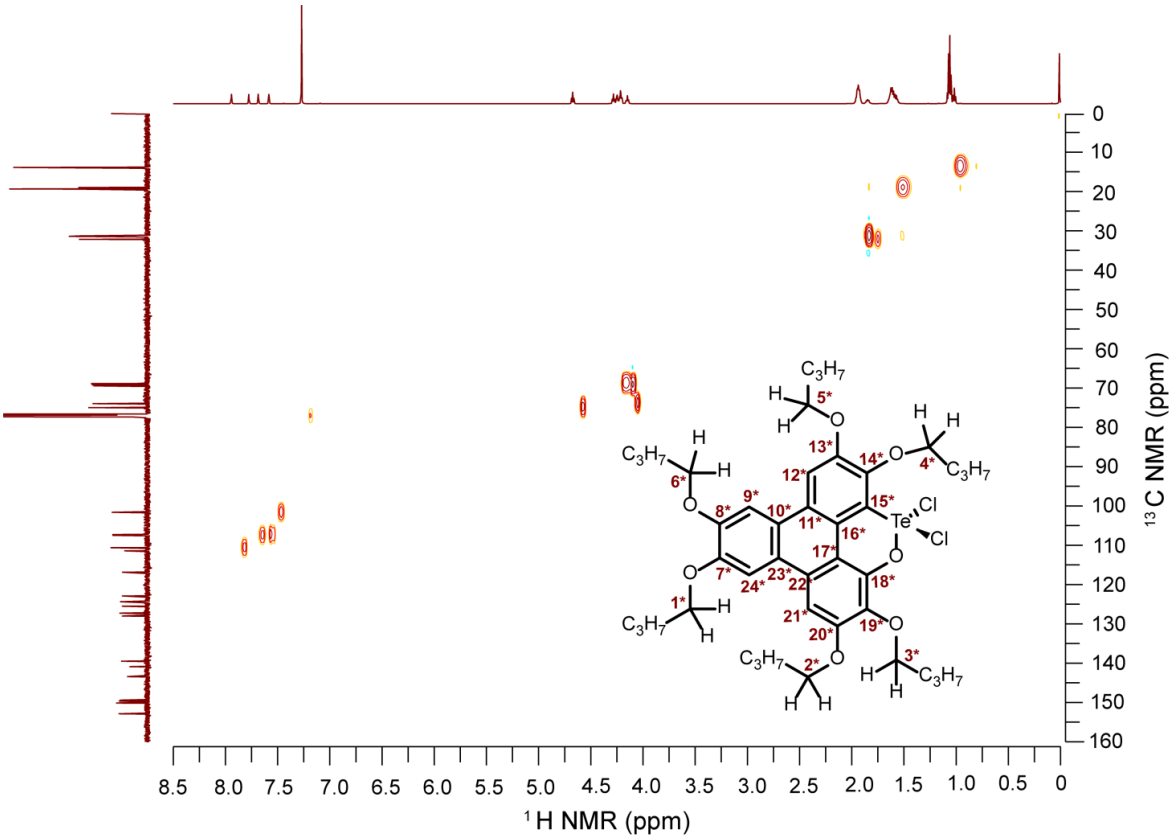

Fig. S5 The HSQC spectrum of compound **13** ($CDCl_3$, 600 MHz).

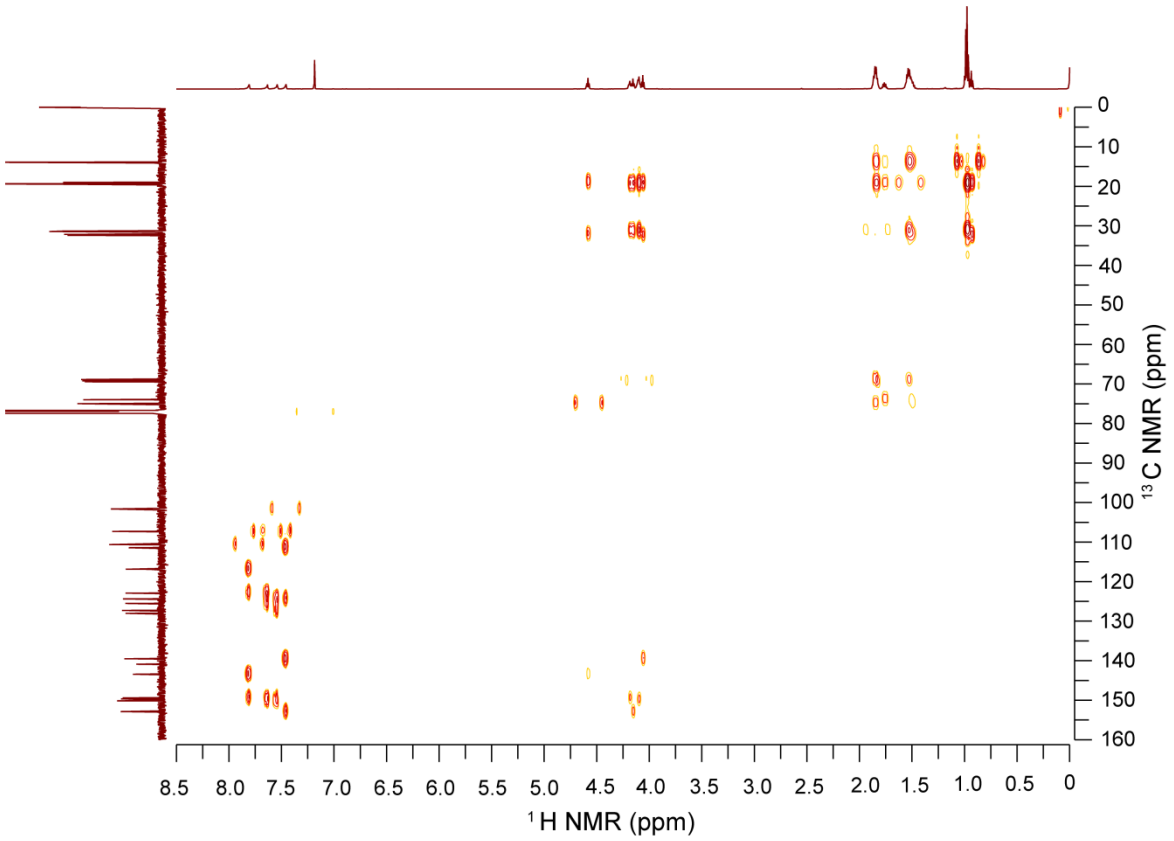

Fig. S6 The HMBC spectrum of compound **13** ($CDCl_3$, 600 MHz).

Table S3 The ^{1}H NMR, ^{13}C NMR and HMBC(H→C) data of compound **13**.

Number	^{1}H NMR (ppm)	^{13}C NMR (ppm)	HMBC(H→C)
1*	4.21 (m)	69.45	7*
2*	4.25 (t, 6.3)	68.87	20*
3*	4.15 (t, 6.5)	73.98	19*
4*	4.67 (t, 6.8)	74.98	14*
5*	4.28 (t, 6.3)	68.90	13*
6*	4.21 (m)	69.20	8*
9*	7.78 (s)	107.50	8*, 11*
12*	7.94 (s)	110.63	13*, 14*, 11*, 16*
21*	7.58 (s)	101.63	20*, 19*, 22*, 17*
24*	7.69 (s)	107.30	7*, 22*

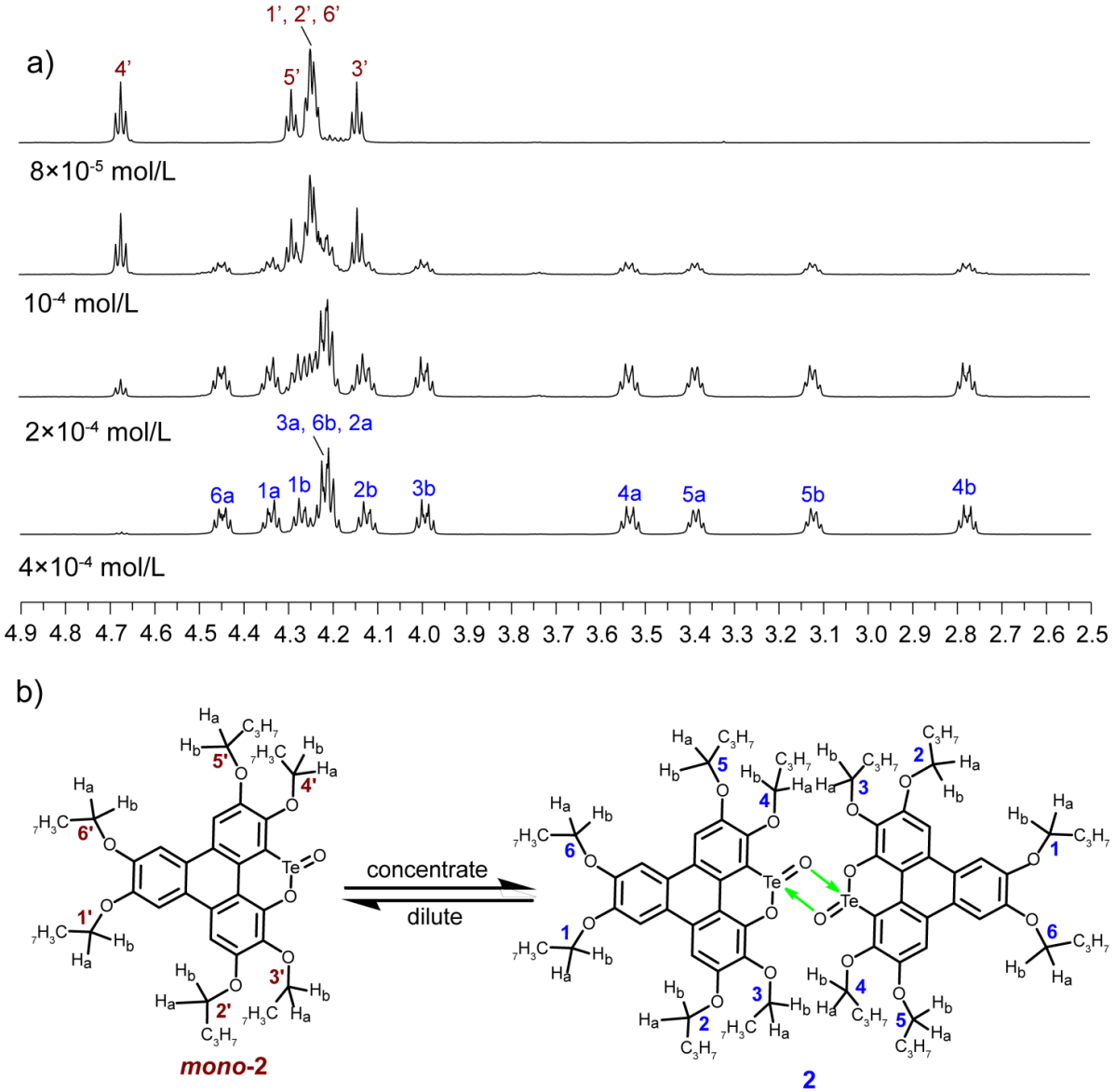

Fig. S7 a) ^{1}H-NMR spectra of **2** at different concentrations; b) transformation between **2** and *mono*-**2** with the numeration of hydrogen atoms (*n*-butoxy region) shown.

Table S4 The ^{125}Te NMR of compounds **1**, **2**, **7**, **8**, **9**, and **10**.

Compound	^{125} Te NMR (ppm)
1	595.56
2	1222.95
7	843.87
8	790.87
9	1239.43
10	1228.41

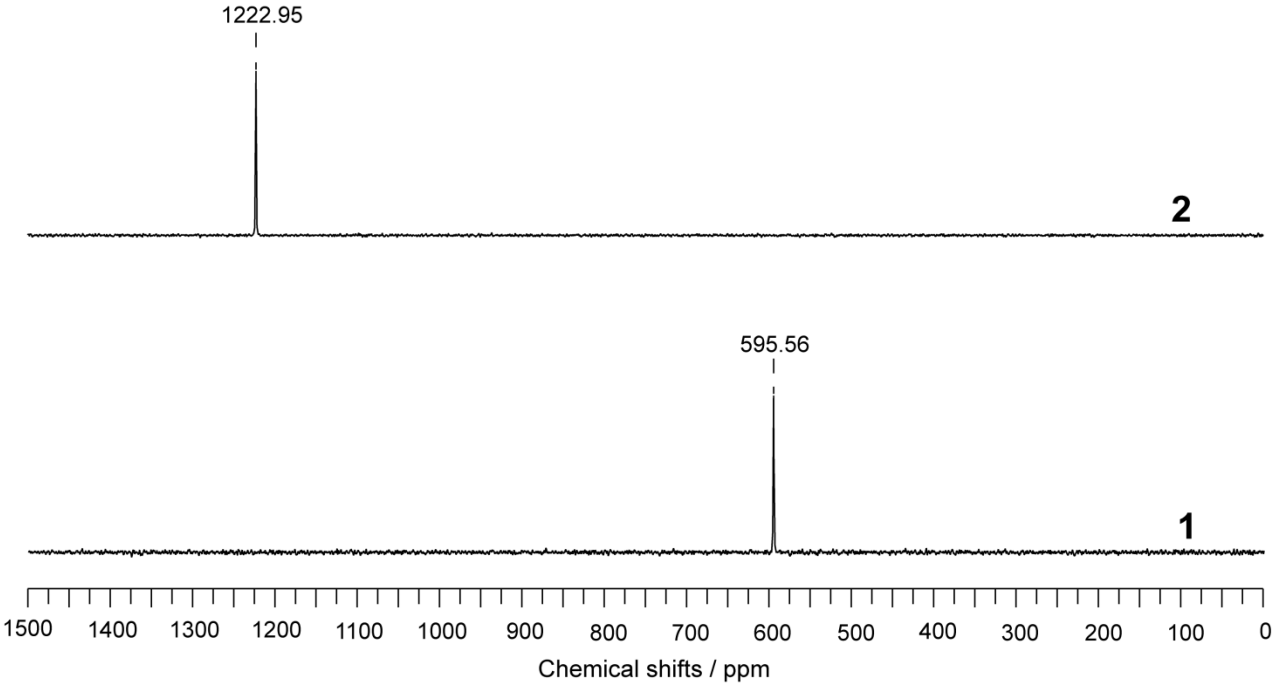

Fig. S8 The ^{125}Te NMR spectra of the compounds **1** and **2**. The chemical shifts were recorded using the ^{125}Te NMR of diphenyl ditelluride (0.5 M solution in $CDCl_3$, δ = 420 ppm) as the external reference.

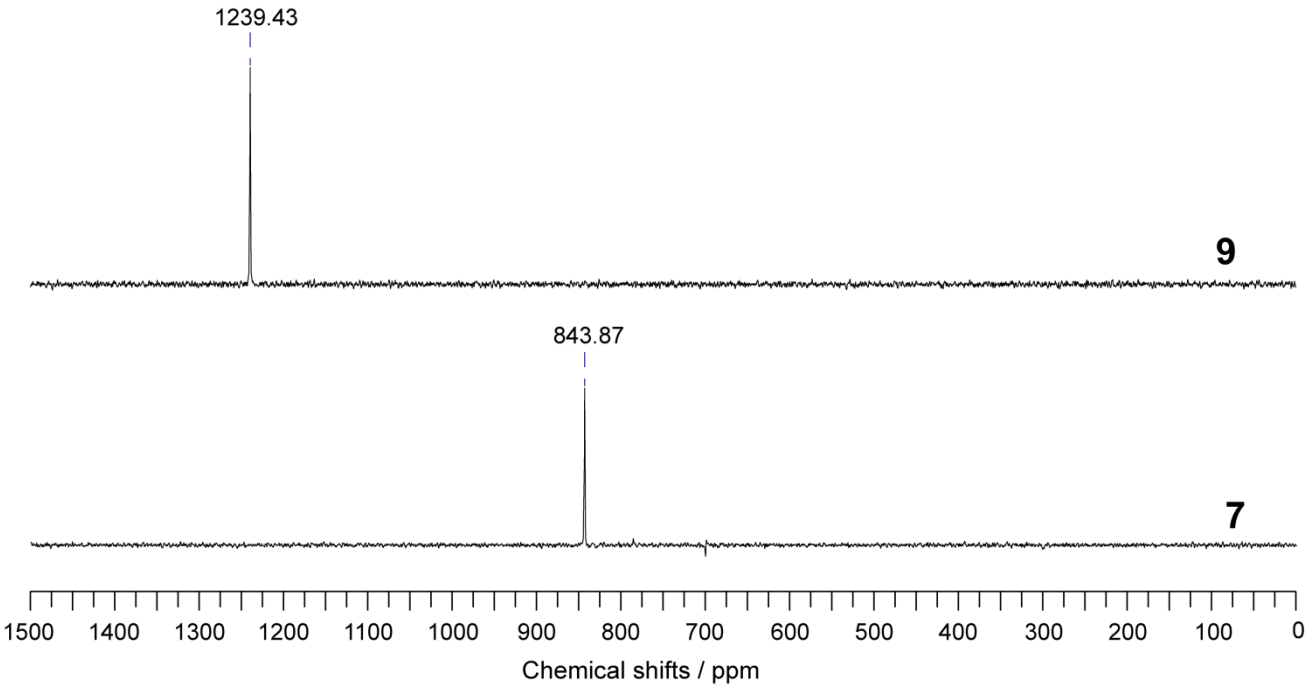

Fig. S9 The ^{125}Te NMR spectra of the compounds **7** and **9**. The chemical shifts were recorded using the ^{125}Te NMR of diphenyl ditelluride (0.5 M solution in $CDCl_3$, δ = 420 ppm) as the external reference.

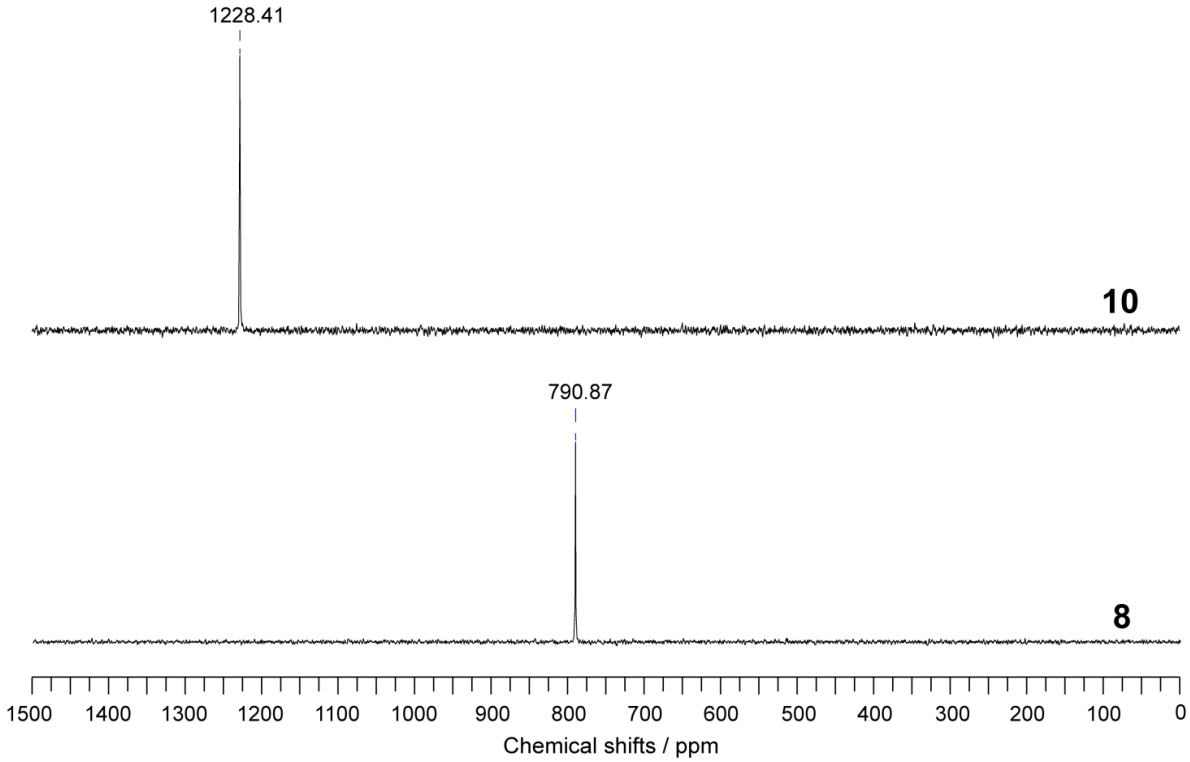

Fig. S10 The ^{125}Te NMR spectra of the compounds **8** and **10**. The chemical shifts were recorded using the ^{125}Te NMR of diphenyl ditelluride (0.5 M solution in $CDCl_3$, δ = 420 ppm) as the external reference.

5. X-ray Crystal Structure Analyses

5.1 Experimental details on crystal growth

The single crystals of **2, 3**, **9**, **10, 11** and **12** were obtained by slowly evaporating their solutions at room temperature as summarized in **Table S5-S6**.

Table S5 Experimental details on crystal growth of compounds **2, 3, 9** and **10**.

Compound	Solvent (*v*/*v*)	Yield (%)	appearance
2 (8.2 mg, 0.005 mmol)	CH_2Cl_2 : EtOH (3 ml : 3 ml)	5.4 mg, 66%	Pale yellow strip
3 (9.5 mg, 0.005 mmol)	CH_2Cl_2 : EtOH (3 ml : 3 ml)	5.1 mg, 54%	Yellow block
9 (8.8 mg, 0.005 mmol)	CH_2Cl_2 : EtOH (1 ml : 4 ml)	6.6 mg, 76%	Yellow block
10 (9.7 mg, 0.005 mmol)	EA: EtOH (1 ml : 4 ml)	6.9 mg, 72%	Pale yellow block

Table. S6 Experimental details on crystal growth of compounds **11** and **12**.

Compound	Reactant	HCl	Solvent (*v*/*v*)	Yield (%)	appearance
11	**9** (17.6 mg, 0.01 mmol)	100 µL	CH_2Cl_2 : EtOH (1 ml : 5 ml)	8.6 mg, 46%	Orange needle
12	**10** (19.4 mg, 0.01 mmol)	100 µL	CH_2Cl_2: EtOH (1 ml : 5 ml)	8.4 mg, 41%	Orange needle

Table S7. Selected crystallographic data of **2**, **3**, **9** and **10**.

	2	**3**	**9**	**10**
CCDC number	2035868	2035866	2035865	2035863
Empirical formula	$C_{84}H_{116}O_{16}Te_2$	$C_{98}H_{124}Cl_2O_{17}Te_2$	$C_{84}H_{108}O_{16}S_4Te_2$	$C_{84}H_{108}O_{16}Se_4Te_2$
Formula weight	1636.96	1900.06	1757.14	1944.74
Temperature [K]	173(1)	170.0	170(2)	100
λ [Å]	0.71073 (Mo-Kα)	0.71073 (Mo-Kα)	0.71073 (Mo-Kα)	0.71073 (Mo-Kα)
Crystal size [mm^3]	0.28×0.15×0.12	0.12×0.08×0.05	0.22×0.21×0.05	0.19×0.15×0.12
Crystal system	monoclinic	monoclinic	triclinic	monoclinic
space group	C2/c	C2/c	*P*-1	$P2_1/n$
a [Å]	39.1328(11)	37.942(2)	19.1567(10)	18.8279(10)
b [Å]	20.3253(7)	17.3698(11)	35.2402(17)	27.9082(16)
c [Å]	29.5440(8)	29.2185(18)	49.703(2)	32.268(3)
α [°]	90	90	97.646(2)	90
β [°]	136.4590(10)	105.560(2)	90.535(2)	106.815(3)
γ [°]	90	90	92.720(2)	90
V [$Å^3$]	16187.7(9)	18550.3(19)	33214(3)	16230(2)
Z	8	8	16	8
d_{calc} [g cm^{-3}]	1.343	1.361	1.406	1.592
μ [mm^{-1}]	0.785	0.752	0.867	2.579
2θmax [°]	52.77	50.056	52.798	50.054
Data/restraints/parameters	16140/1002/967	16335/1372/1243	133760/63527/9454	28467/2716/2067
GooF	1.076	1.026	1.017	1.036
R [I > 2σ(I)]	0.0396	0.0876	0.0874	0.0588
wR_2	0.0731	0.2282	0.2278	0.1427

Table S8 Selected crystallographic data of **11** and **12**.

	11	**12**
CCDC number	2064766	2064765
Empirical formula	$C_{42}H_{54}Cl_2O_7S_2Te$	$C_{42}H_{54}Cl_2O_7Se_2Te$
Formula weight	933.47	1027.27
Temperature [K]	150.00（10）	296.15
λ [Å]	1.54184 (Cu-Kα)	0.71073 (Mo-Kα)
Crystal size [mm^3]	0.04×0.02×0.01	0.12×0.1×0.1
Crystal system	triclinic	triclinic
space group	*P*-1	*P*-1
a [Å]	9.8421(4)	9.902(3)
b [Å]	14.6373(6)	14.643(4)
c [Å]	16.1252(6)	16.120(5)
α [°]	107.209(3)	106.116(9)
β [°]	103.814(3)	104.058(11)
γ [°]	97.239(3)	96.560(9)
V [$Å^3$]	2105.86(15)	2136.5(10)
Z	2	2
d_{calc} [g cm^{-3}]	1.472	1.597
μ [mm^{-1}]	8.059	2.572
$2\theta_{max}$ [°]	144.228	55.434
Data/restraints/parameters	8018/203/522	9758/41/493
GooF	1.046	1.118
R [$I > 2\sigma(I)$]	0.1093	0.0792
*wR*2	0.3028	0.2564

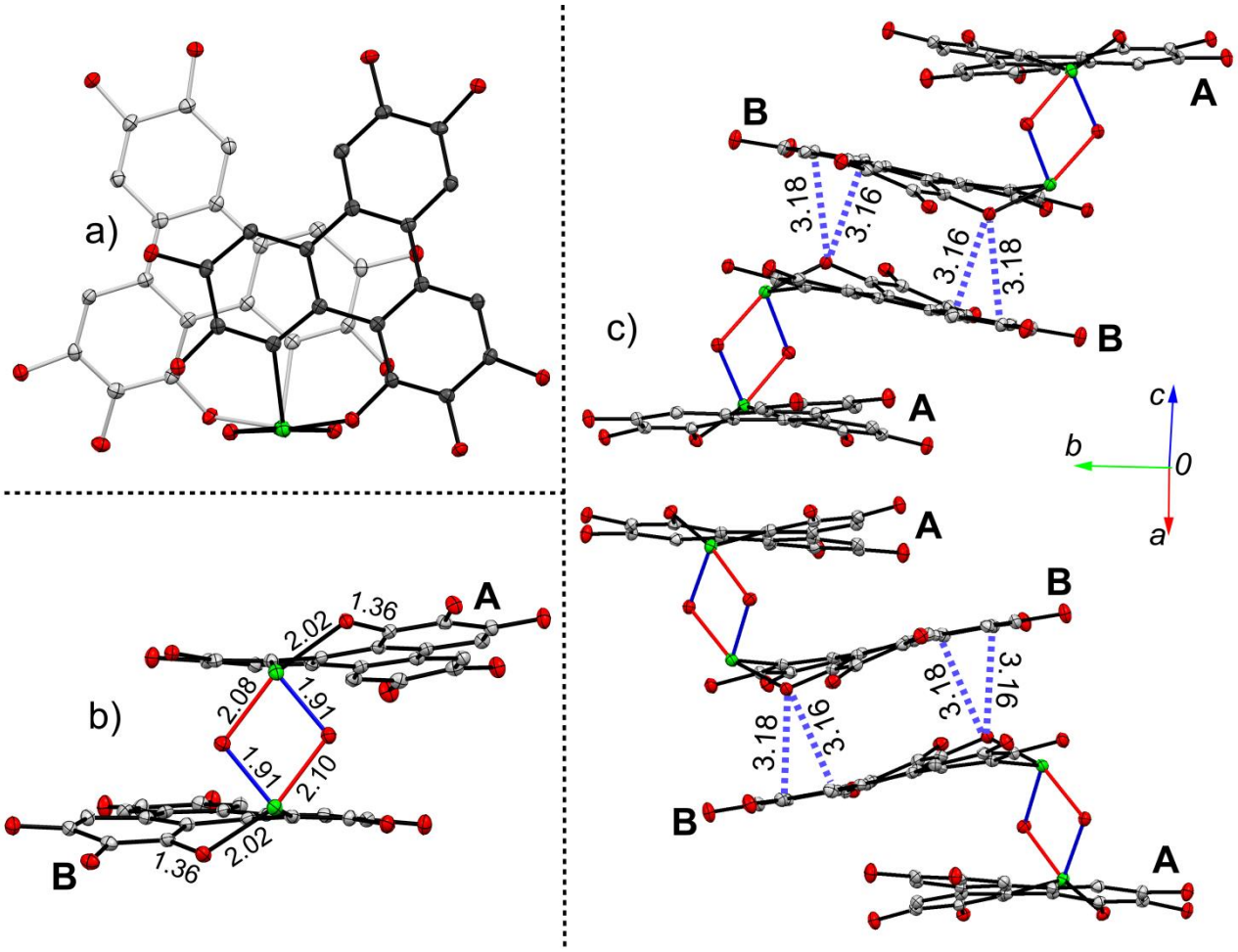

Fig. S11 a) Top view and b) side view of crystal structure of **2**; c) packing motif with atomic contacts shown in blue lines. The C, O and Te atoms are respectively shown in grey, red, and green. The selected bond lengths and intermolecular contacts are in unit of Å. The *n*-Bu groups and H atoms are omitted for clarity.

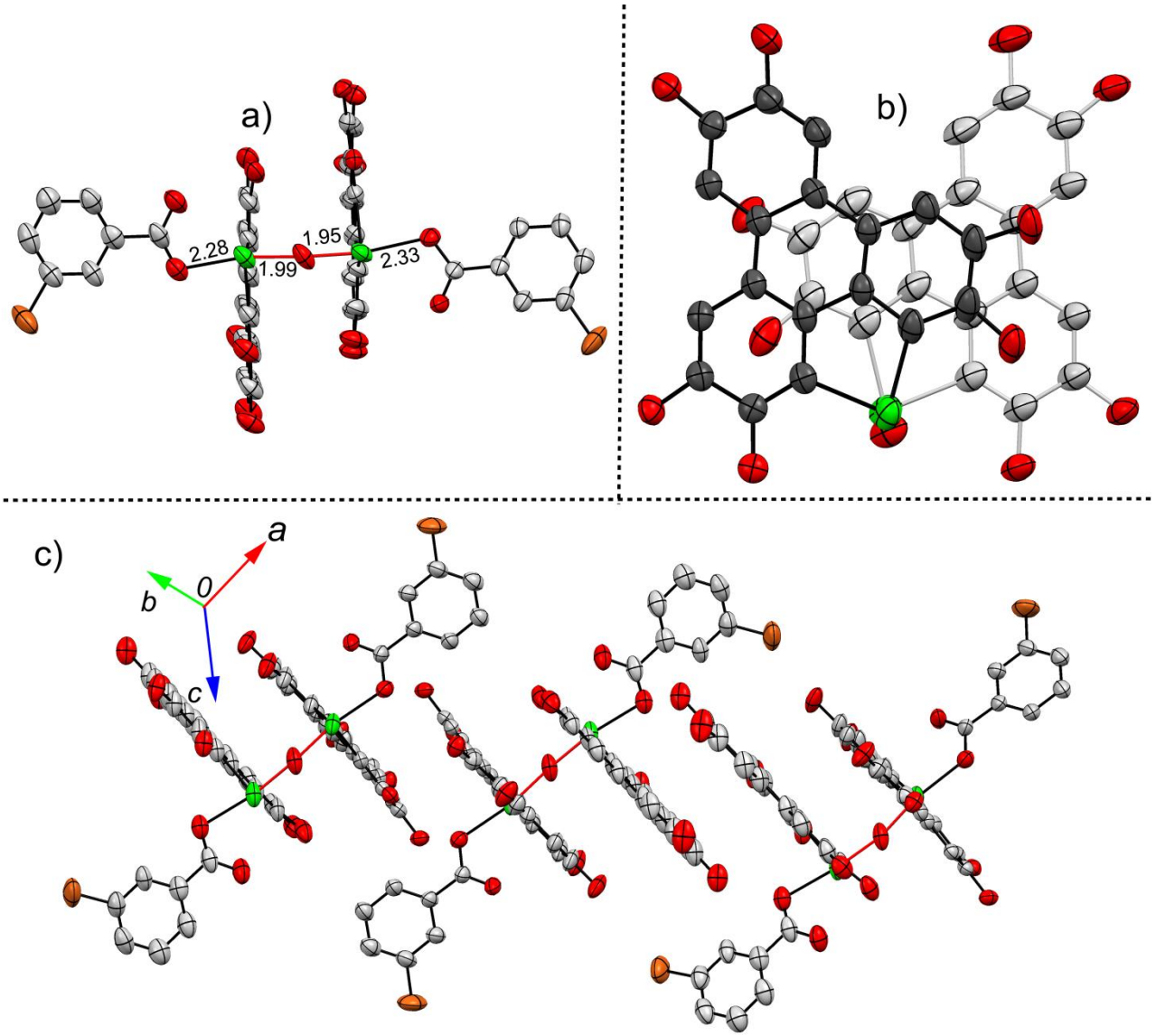

Fig. S12 a) Side view and b) top view of crystal structure of **3**; c) packing motif. The C, O, Cl and Te atoms are respectively shown in grey, red, orange and green. Owing to the large thermo factors of atoms, the Ortep drawn is performed at probability of 30%. The selected bond lengths are in unit of Å. The *n*-Bu groups, H atoms and the *m*CBA ester in b) are omitted for clarity.

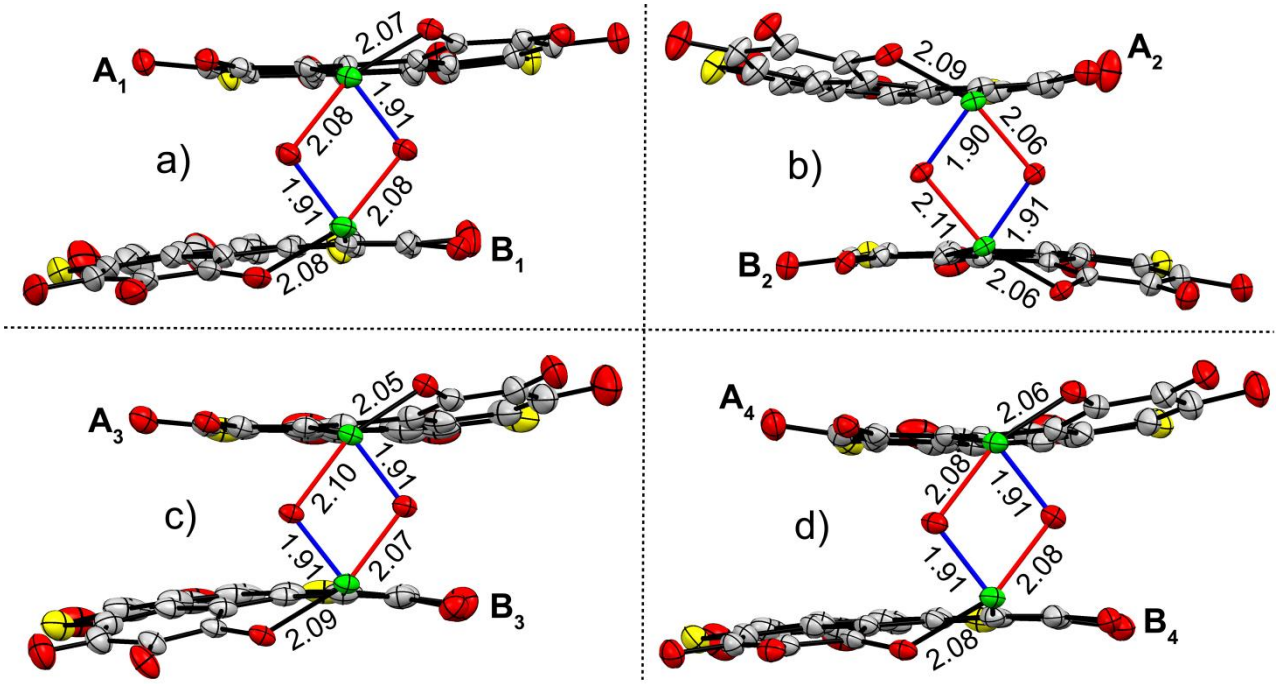

Fig. S13 Side view of molecule ***A₁B₁-A₄B₄*** in **9**. The selected bond lengths are in unit of Å. The bond length of the newly formed C-O is 1.37(2) Å. The C, O, S and Te atoms are respectively shown in grey, red, yellow and green.

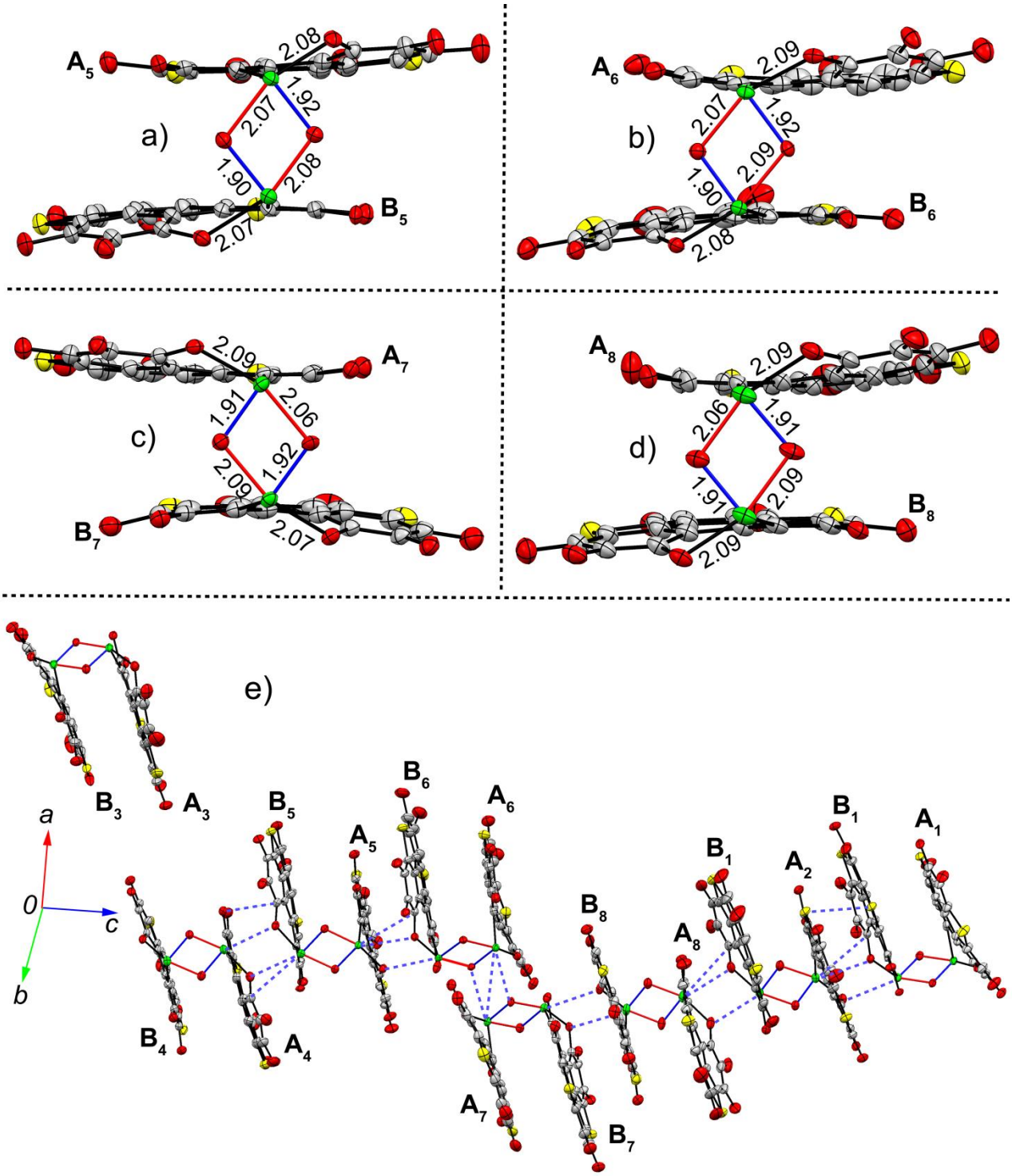

Fig. S14 a), b), c), and d) are side views of molecule ***A*$_5$*B*$_5$-*A*$_8$*B*$_8$** in **9**; e) packing motif of **9** with atomic contacts shown in blue lines. The bond length of the newly formed C-O is 1.37(2) Å. The selected bond lengths and intermolecular contacts are in unit of Å. The C, O, S and Te atoms are respectively shown in grey, red, yellow and green.

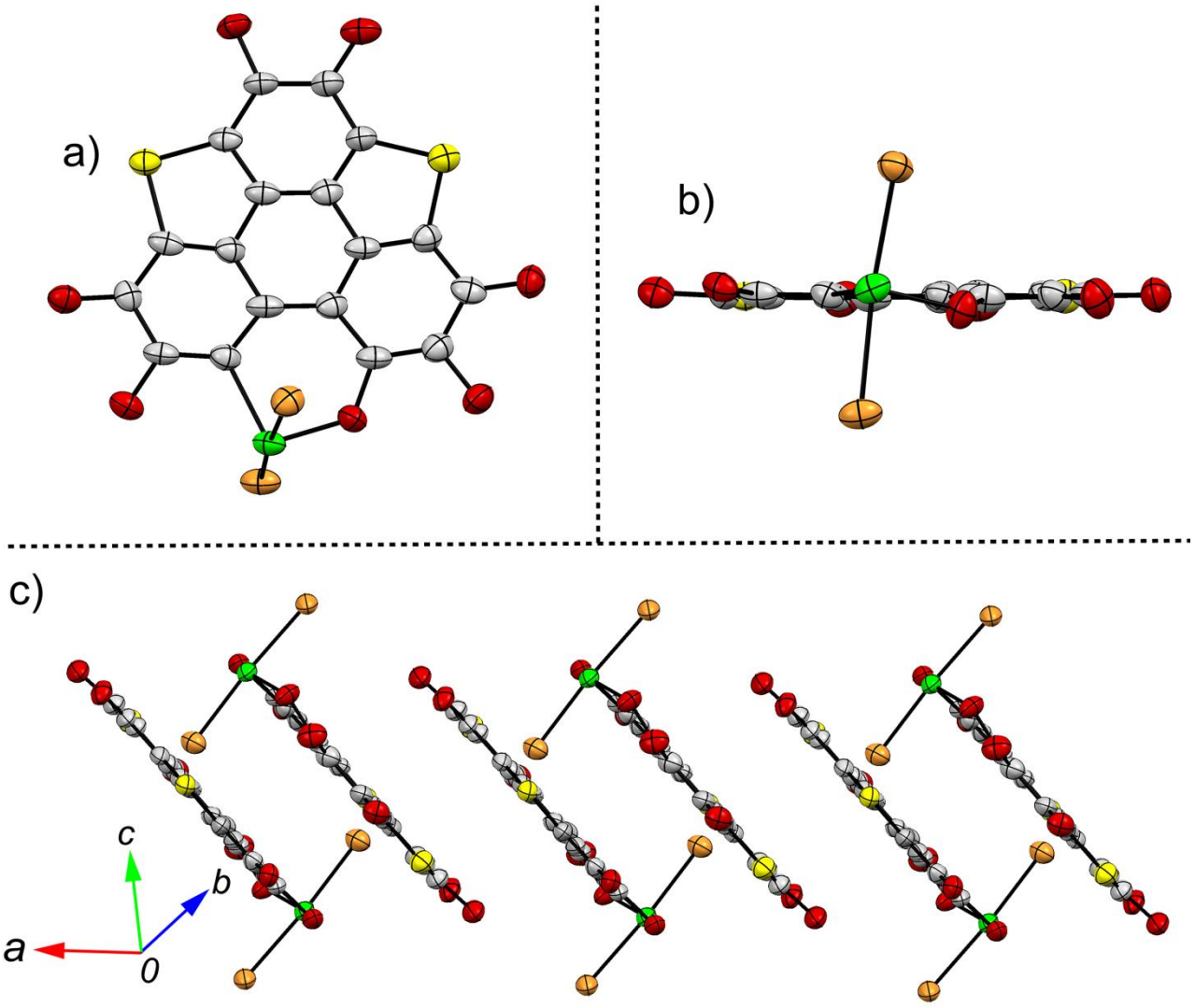

Fig. S15 a) Top view and b) side view of crystal structure of **11**; c) packing motif. The C, O, S, Cl, and Te atoms are respectively shown in grey, red, yellow, orange, and green. The *n*-Bu groups and H atoms are omitted for clarity.

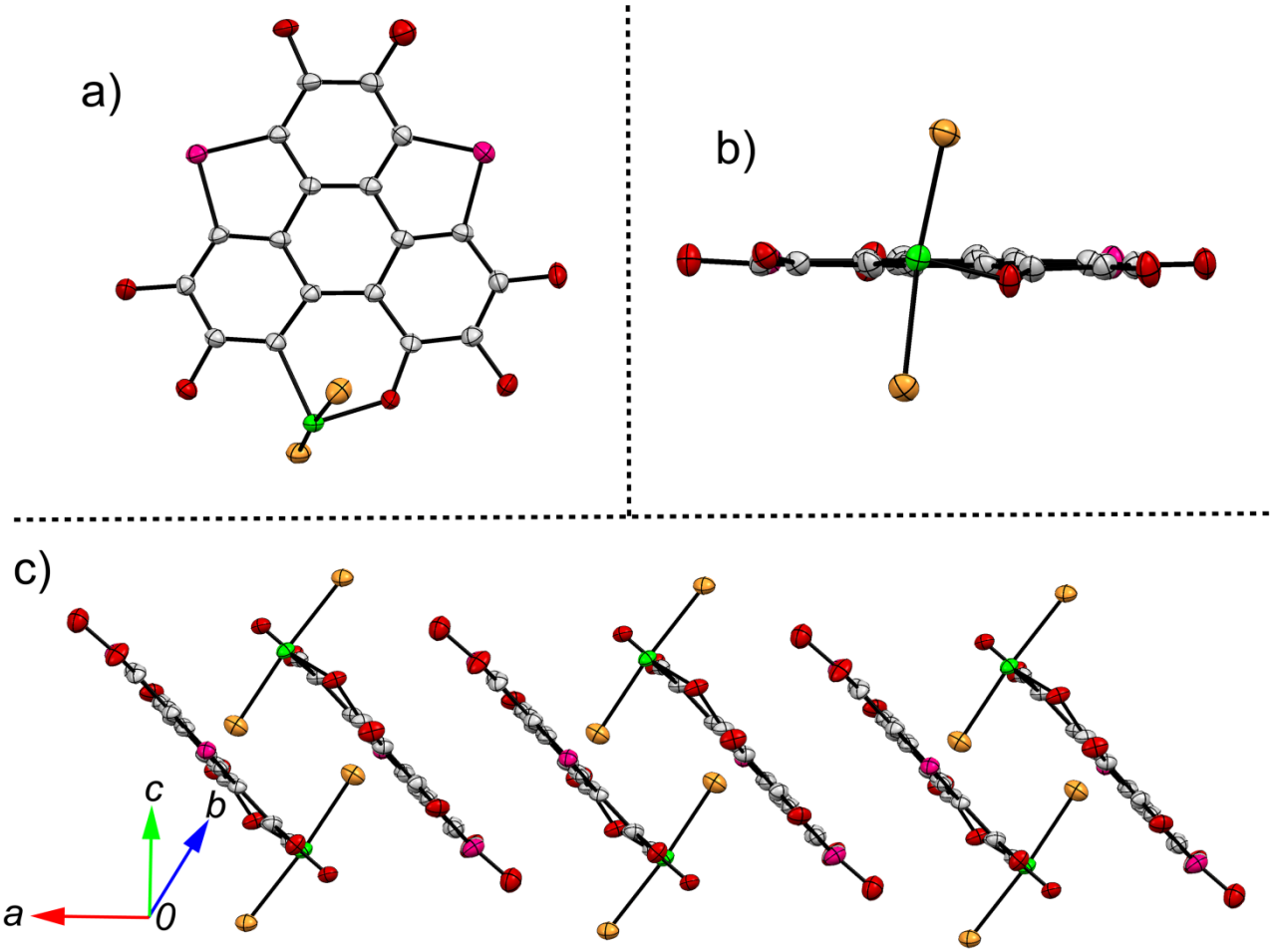

Fig. S16 a) Top view and b) side view of crystal structure of **12**; c) packing motif. The C, O, Se, Cl, and Te atoms are respectively shown in grey, red, pink, orange, and green. The *n*-Bu groups and H atoms are omitted for clarity.

6. Photophysical Studies

6.1 Separation, CD spectra, and molecular structures of the enationmers

The enationmers of compounds **2** and **9** were separated by means of chiral HPLC as shown in **Figs. S17a** and **S18a**, respectively. The circular dichroism (CD) spectra of **2** and **9** were measured in CH_2Cl_2 (c = 6 × 10^{-4} mol L^{-1}) at 20 °C. The CD spectra of **2'** and **9'** were calculated at TD-PBE0/Def2-SVP/IEFPCM(CH_2Cl_2) (nstates = 100, root = 1) level of theory using optimized structures. The molecular structures of (-)-**2'**/(+)-**2'** and (-)-**9'**/(+)-**9'** were respectively shown in **Fig. S17c** and **S18c**.

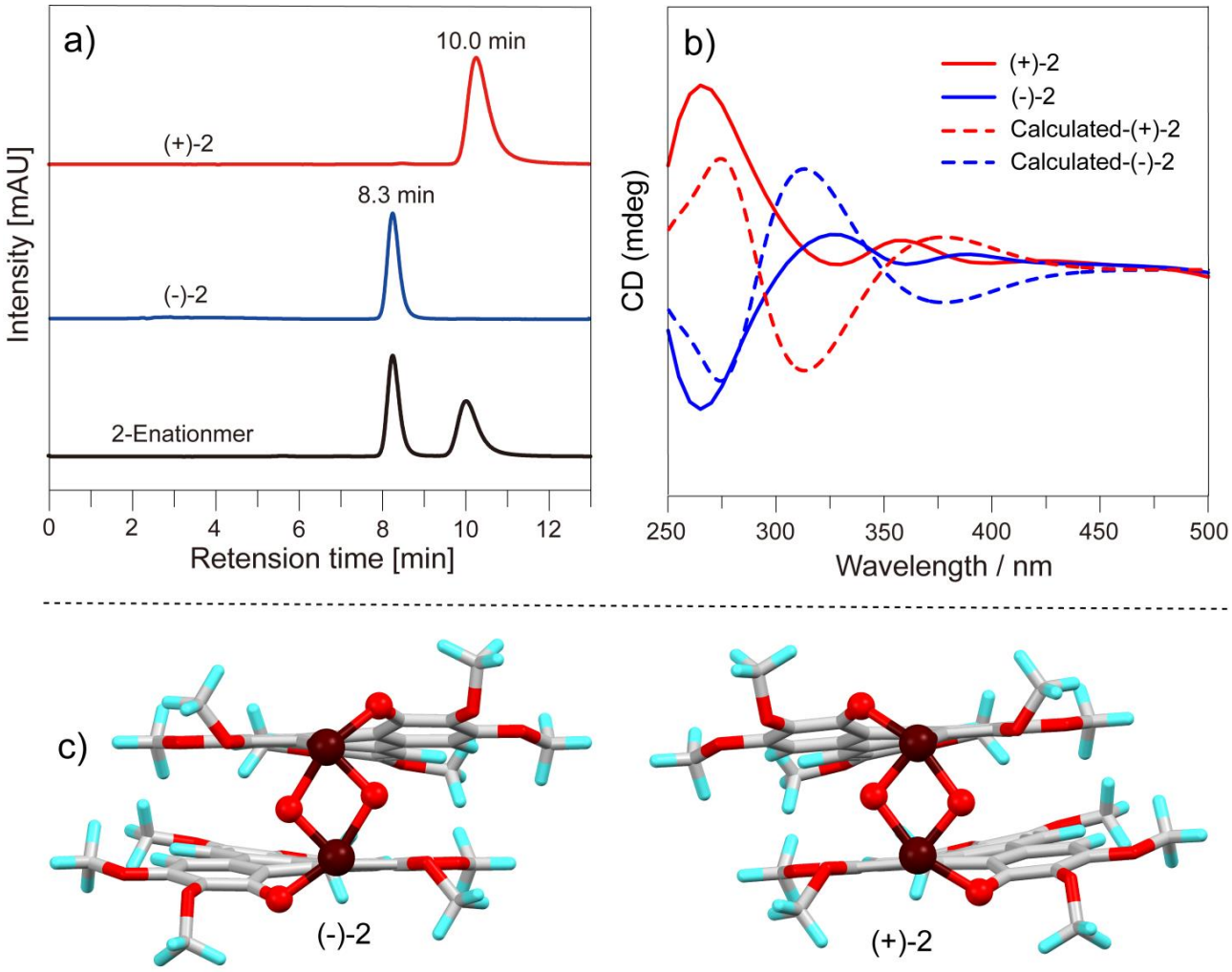

Fig. S17 a) Chiral chromatograms of **2** on a CHIRALPAK IG-3(IG30CD-WE016) column (eluent: MeOH/DCM=80/20); b) CD spectra (solid line) of **(+)-2**/**(-)-2** in CH_2Cl_2 (6×10^{-4} mol L^{-1}) and simulated CD spectra (dash line) of **(+)-2**/**(-)-2** *via* TD-DFT calculation at TD-PBE0/Def2-SVP level; c) molecular structures of (-)-**2',** (+)-**2'**.

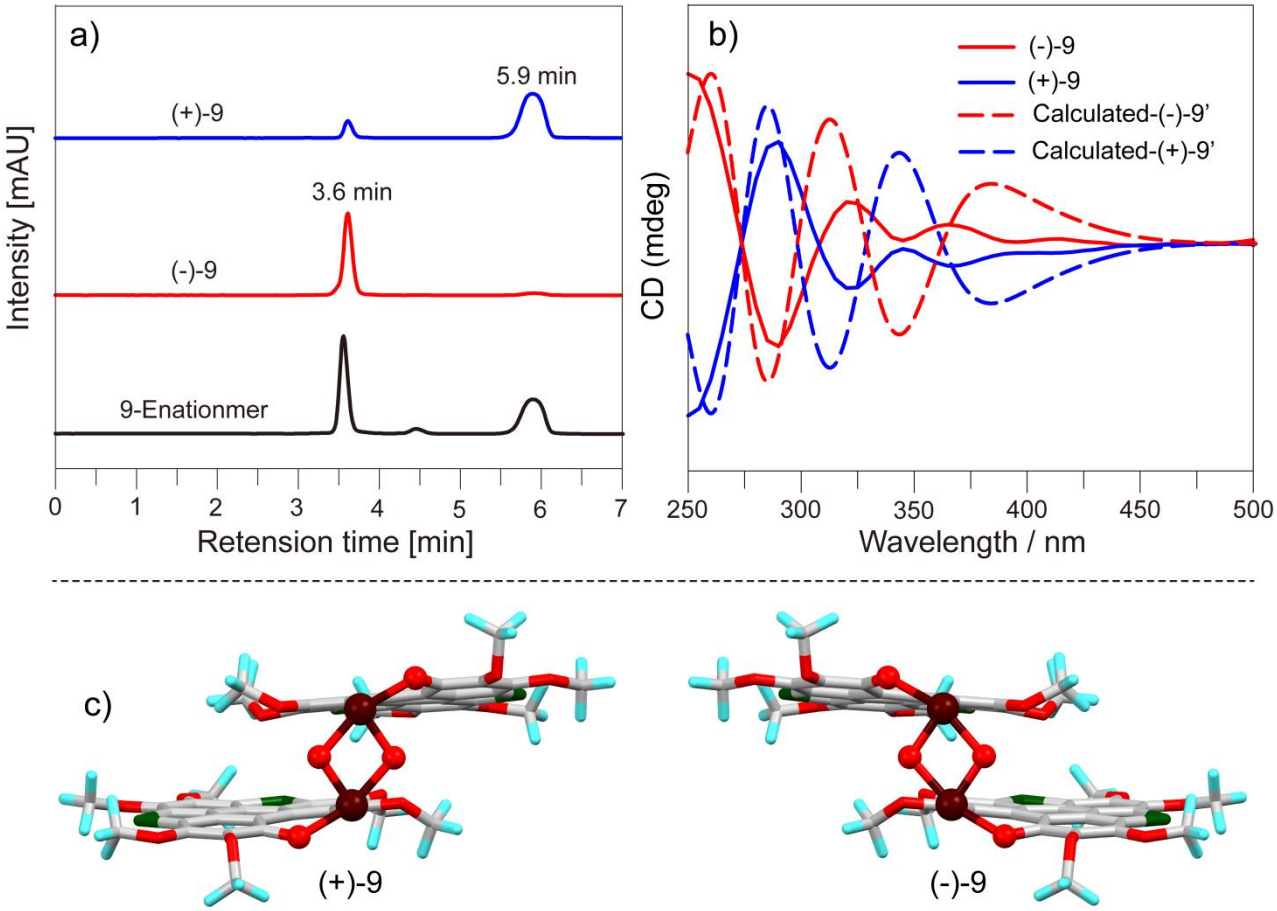

Fig. S18 a) Chiral chromatograms of **9** on Daicel CHIRALPAK IF (IF00CE-SL018) column (eluent: hexane/CH_2Cl_2 = 50/50); b) CD spectra (solid line) of **(+)-9**/**(-)-9** in CH_2Cl_2 (6×10^{-4} mol L^{-1}) and simulated CD spectra (dash line) of **(+)-9**/**(-)-9** *via* TD-DFT calculation at TD-PBE0/Def2-SVP level; c) molecular structures of (+)-**9'**, (-)-**9'**.

6.2 UV-Vis absorption spectra

UV-Vis spectra of **1,** *mono*-**2, 7, 8,** *mono*-**9** and *mono*-**10** were measured in CH_2Cl_2 at 20 ºC on a UV-2600 UV-Vis spectrometer (Shimadzu). The broad absorption bands of *mono*-**2** (376-385 nm) and *mono*-**9** (385-446 nm) are originated from the HOMO-LUMO transitions, and are red-shifted as compared with those of **1** (356-371 nm) and **7** (378-402 nm). This is caused by the electron-withdrawing unit (Te=O) in these structures.

Table S9 UV-Vis absorption spectra of **1,** *mono*-**2, 7, 8,** *mono*-**9** and *mono*-**10** in CH_2Cl_2.

Comp.	λ_{max}/nm	log ε	λ_{max}/nm	log ε	λ_{max}/nm	log ε	λ_{max}/nm	log ε	λ_{max}/nm	log ε
1	256	6.74	282	7.02	356	3.64	371	3.15		
mono-**2**	278	6.92	376	3.97	385	5.92				
7	311	6.84	378	5.16	402	5.19				
8	272	6.50	315	6.80	340	6.43	375	5.24	398	5.12
mono-**9**	258	6.73	294	6.80	314	6.77	416	6.09		
mono-**10**	258	6.74	292	6.74	320	6.76	389	5.95	413	6.08

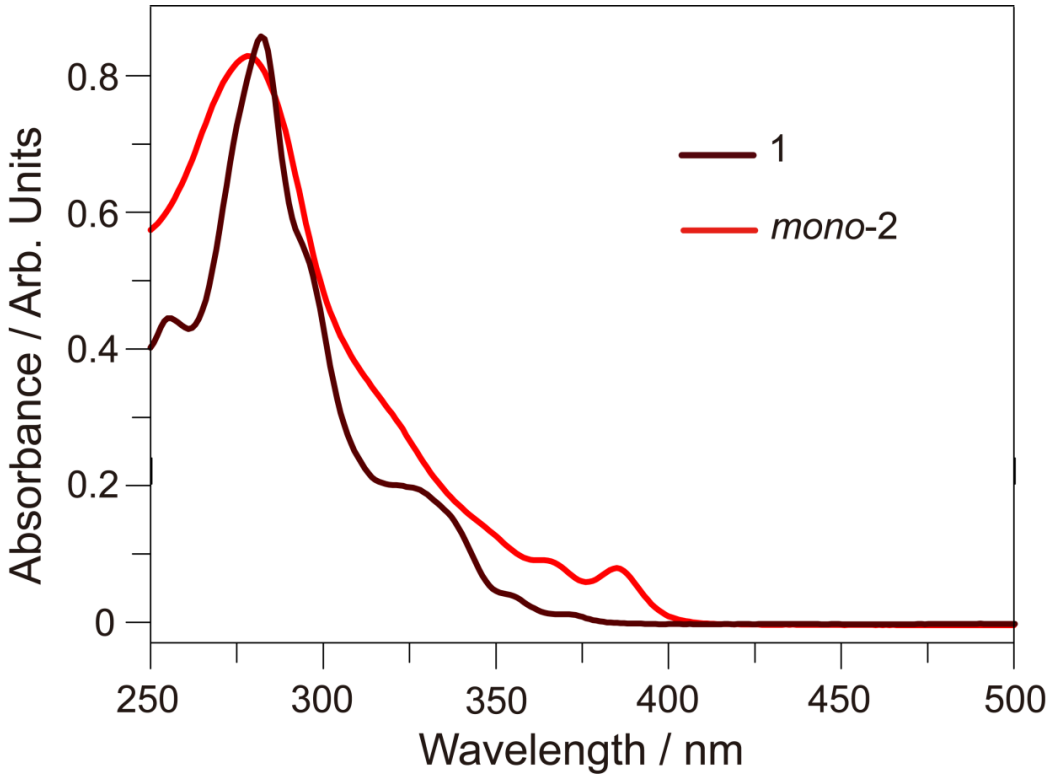

Fig. S19 UV-Vis absorption spectra of **1** and *mono*-**2** in CH_2Cl_2 (10^{-5} mol L^{-1}).

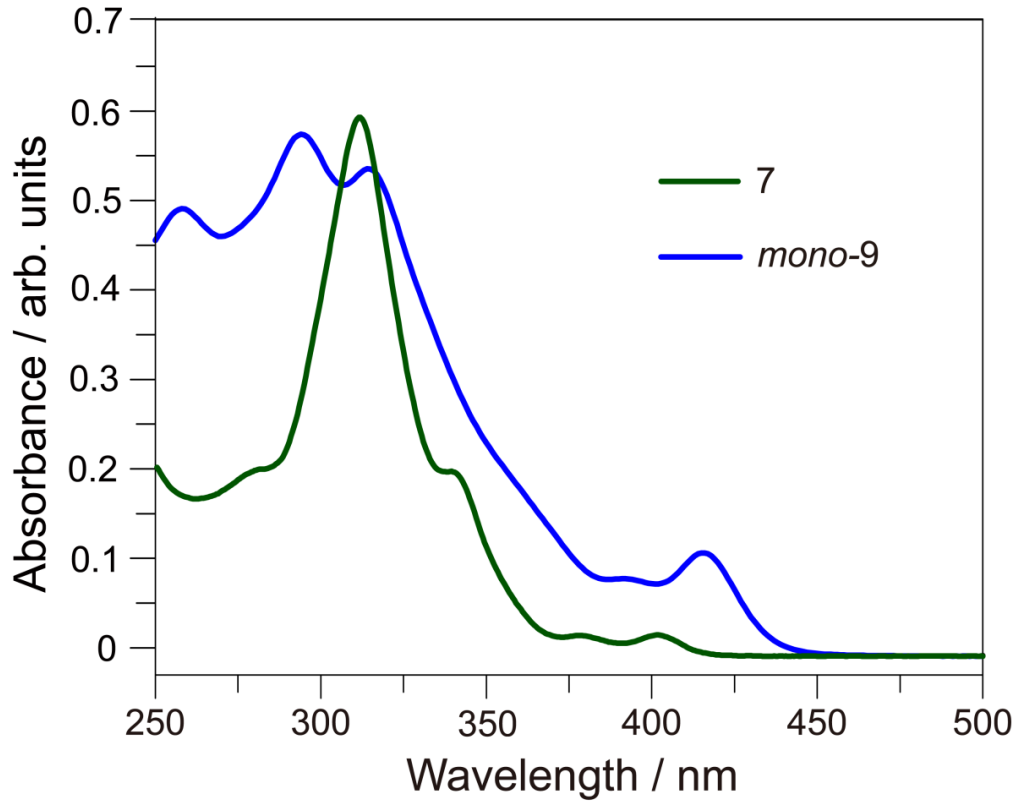

Fig. S20 UV-Vis absorption spectra of **7** and *mono*-**9** in CH_2Cl_2 (10^{-5} mol L^{-1}) .

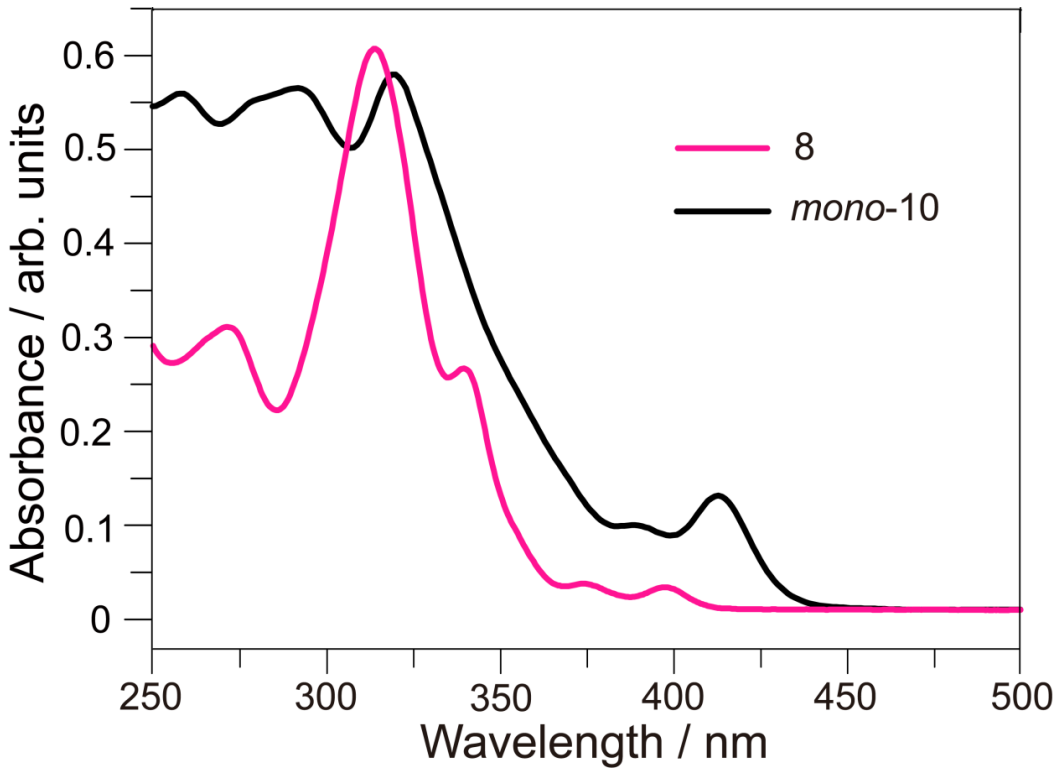

Fig. S21 UV-Vis absorption spectra of **8** and *mono*-**10** in CH_2Cl_2 (10^{-5} mol L^{-1}).

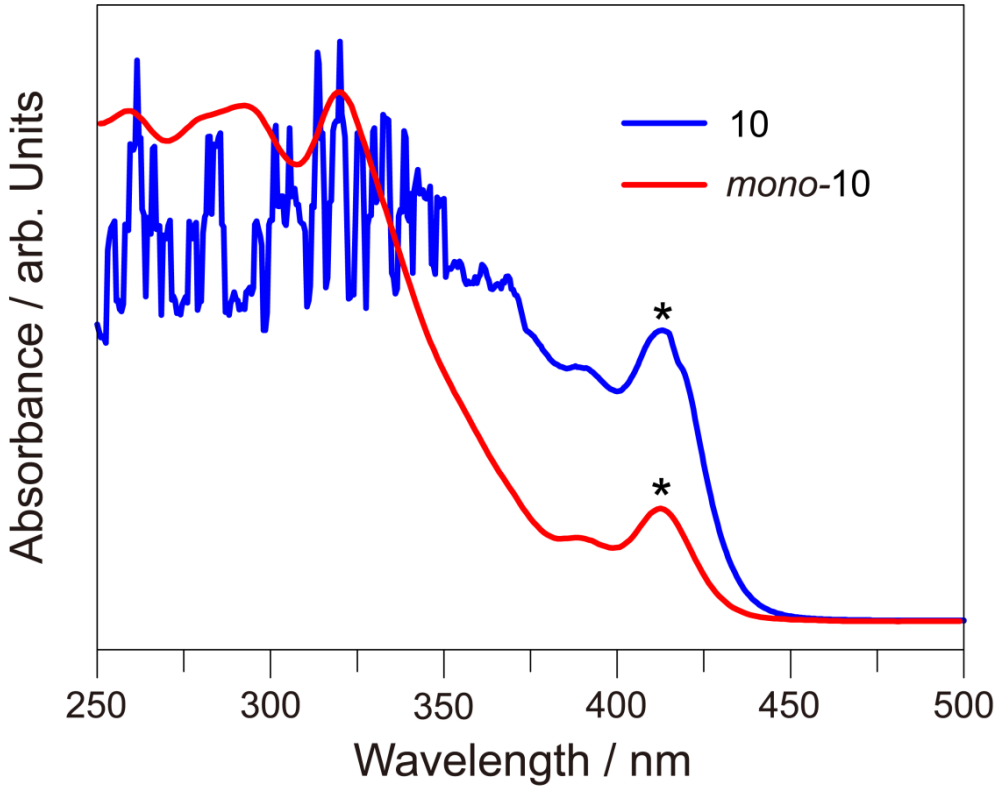

Fig. S22 UV-Vis absorption spectra of the CH_2Cl_2 solution of *mono*-**10** (c = 10^{-5} mol·L^{-1}) and **10** (c = 4×10^{-4} mol·L^{-1}).

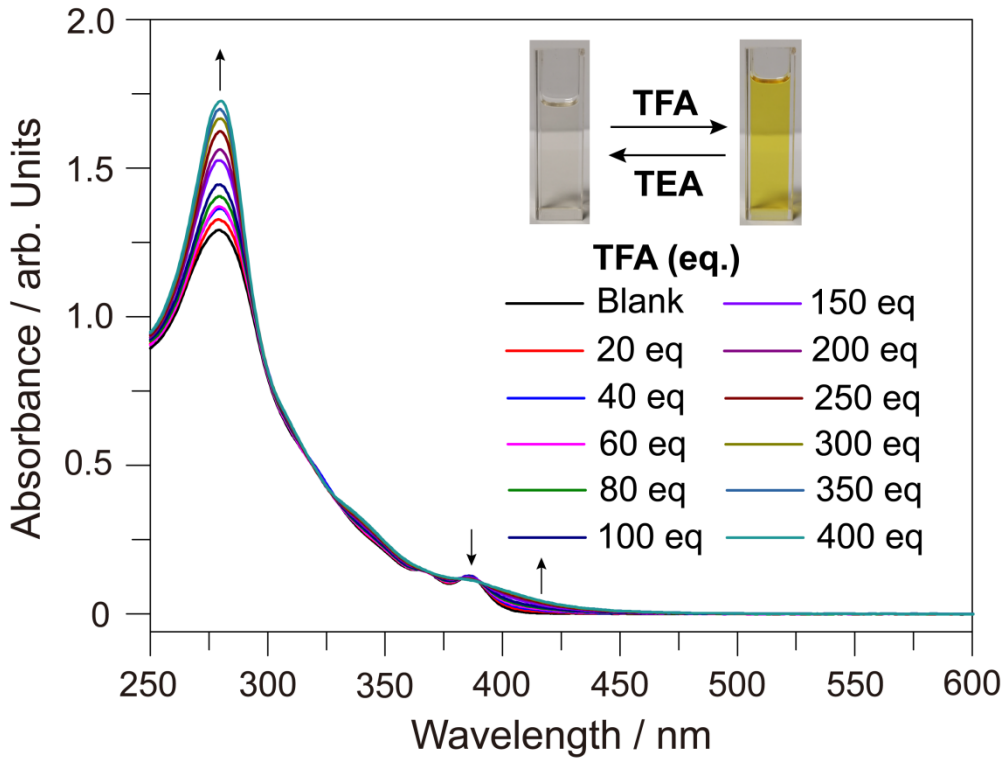

Fig. S23 UV-Vis absorption spectra of **2** in CH_2Cl_2 upon titration with TFA.

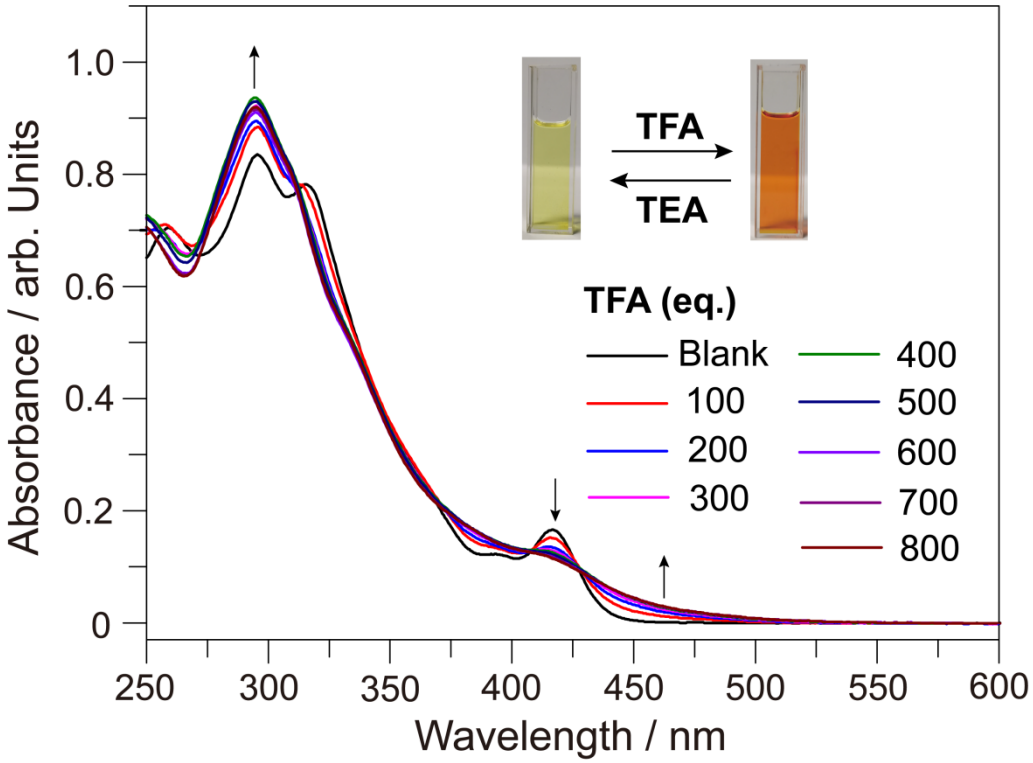

Fig. S24 UV-Vis absorption spectra of **9** in CH_2Cl_2 upon titration with TFA.

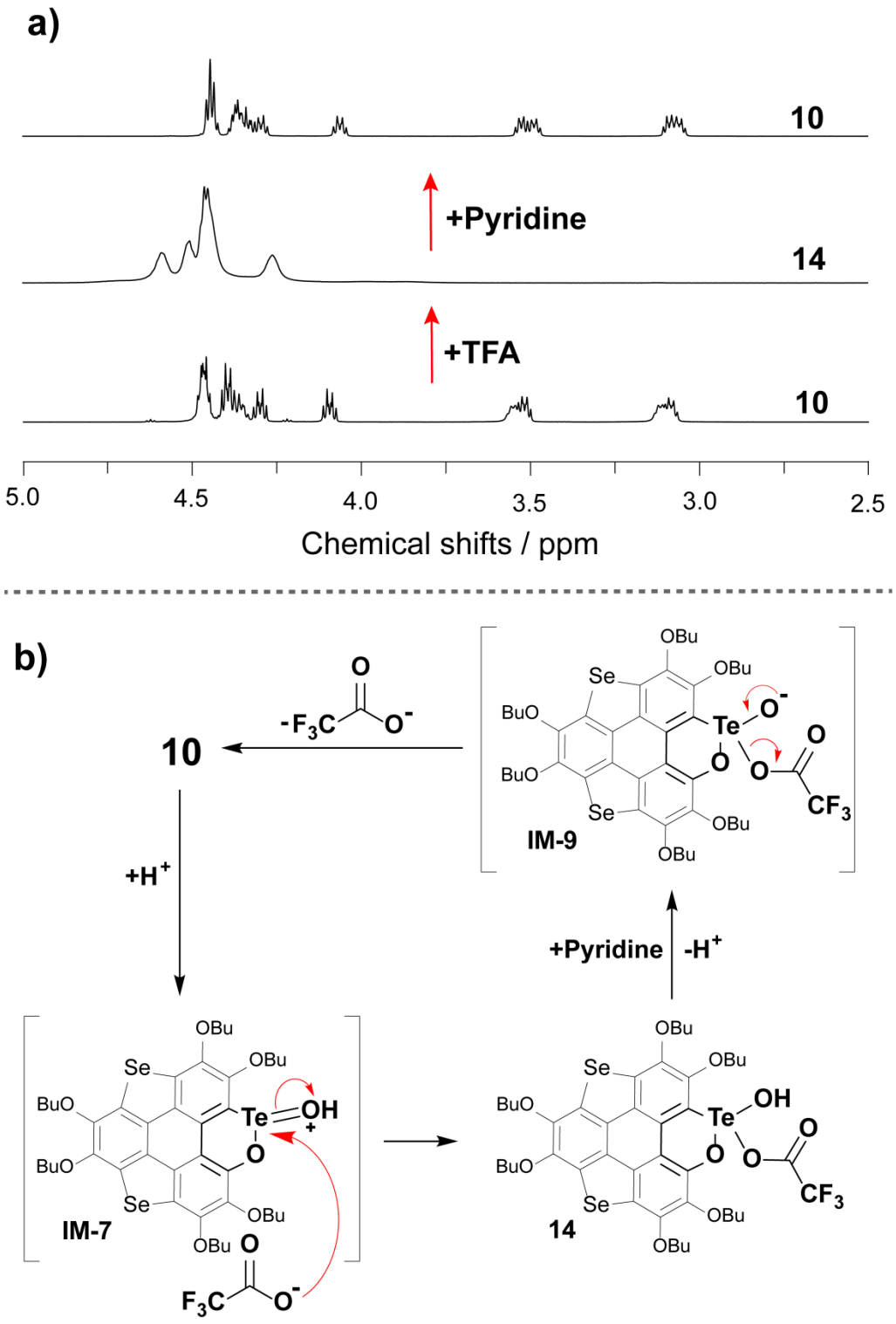

Fig. S25 a) The ^{1}H NMR spectra of **10** in the presence of acid and neutralization with base; b) The reaction mechanism.

6.3 Emission spectra

The excitation and emission spectra of ***mono*-2**, **2**, ***mono*-9**, **9**, ***mono*-10**, and **10** at 77K are shown in **Figs. S26-S27**, and the numeric data are collected in **Table S10**.

Table S10 The emission and excitation properties.[a]

Compound	Concentration	λ_{ex}/nm	λ_{em}/nm	τ_1	τ_2
mono-**2**	1×10^{-6} mol L^{-1}	289	466	0.18μs	4.57μs
2	2×10^{-3} mol L^{-1}	420	570	4.66 ms	18.41 ms
mono-**9**	1×10^{-6} mol L^{-1}	287	466	0.27 μs	7.35μs
9	2×10^{-3} mol L^{-1}	382	564	3695.64μs	
mono-**10**	1×10^{-6} mol L^{-1}	289	465		
10	2×10^{-3} mol L^{-1}	375	537	0.51μs	9.94μs

[a] λ_{ex}: excitation wavelength; λ_{em}: maximum emission wavelength; τ: lifetime. These data were measured in 77K.

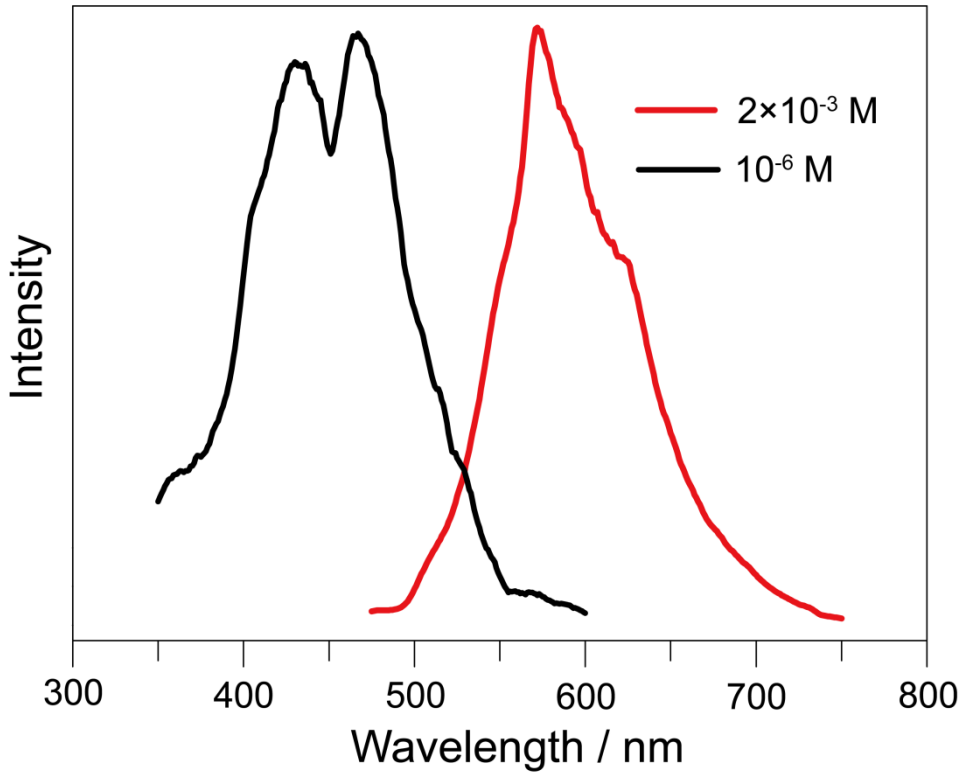

Fig. S26 Emission spectra of **2** in THF at 77K.

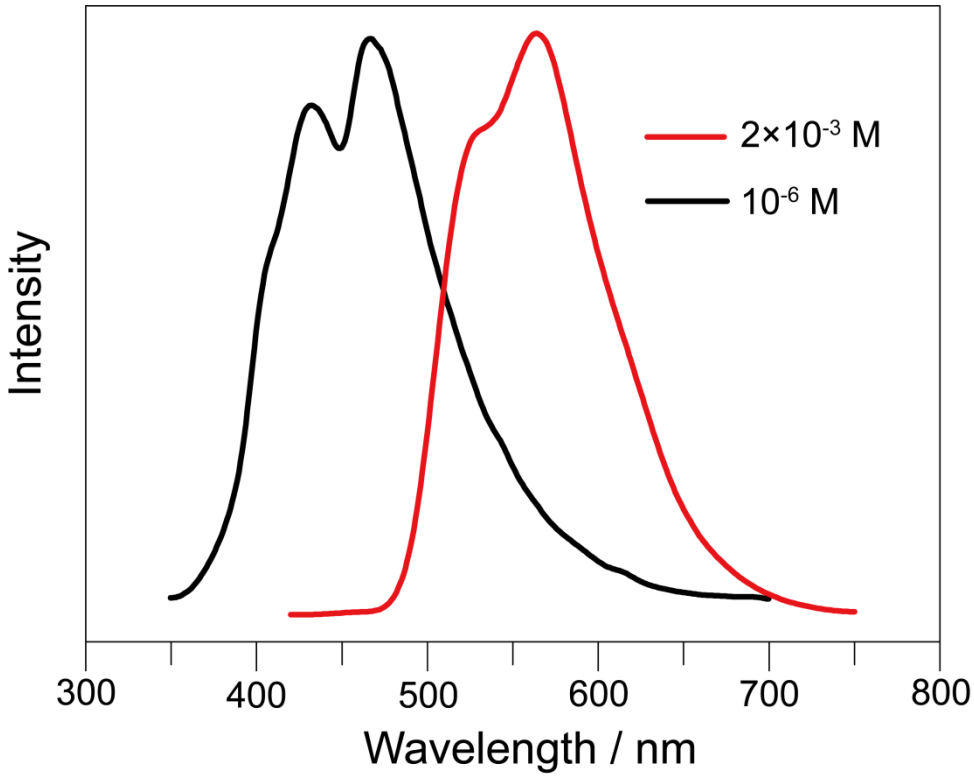

Fig. S27 Emission spectra of **9** at 77K.

7 Calculations

7.1. Computational Details

During the structure optimizations and frontier orbital calculations, the butyl groups on **1**, **2**, **7**, **8**, **9**, **10**, *mono*-**2,** *mono*-**9** and *mono*-**10** were replaced by methyl groups to give the corresponding **1'**, **2'**, **7'**, **8'**, **9'**, **10'**, *mono*-**2',** *mono*-**9'** and *mono*-**10'** (**Scheme S1**), because alkyl groups have almost no contribution on the HOMO and LUMO orbitals and the geometry of the conjugated framework.

All the calculations were performed with Gaussian 16 software package.[S6] Geometry optimizations were carried out using PBE0[S7]/Def2-SVP[S8]/IEFPCM(CH_2Cl_2)[S9] method. Molecular orbital energies and dipole moments were calculated at PBE0/Def2-SVP/IEFPCM(CH_2Cl_2) level of theory using optimized structures. Aromaticity of each ring was measured by nucleus independent chemical shift (NICS)[S10, S11], which was computed using the gauge invariant atomic orbital (GIAO)[S12] approach at the GIAO-PBE0/Def2-SVP[S8]/IEFPCM(CH_2Cl_2)[S9] level with optimized structures. The UV-Vis absorption spectra were calculated at TD-PBE0/Def2-SVP/IEFPCM(CH_2Cl_2) (nstates = 100, root = 1) level of theory using optimized structures.

The optimized structures and molecular orbitals are displayed using Chemcraft.[S13] The calculated UV-Vis absorption spectra were displayed using Multiwfn software[S14], Gaussian function was chosen as broadening function, full width at half maximum (FWHM) was set to 0.5 eV, and only the excited states (**ES**s) with oscillator strength higher than 0.05 were shown. Molecular orbital composition was analyzed using Multiwfn software.[S14, S15]

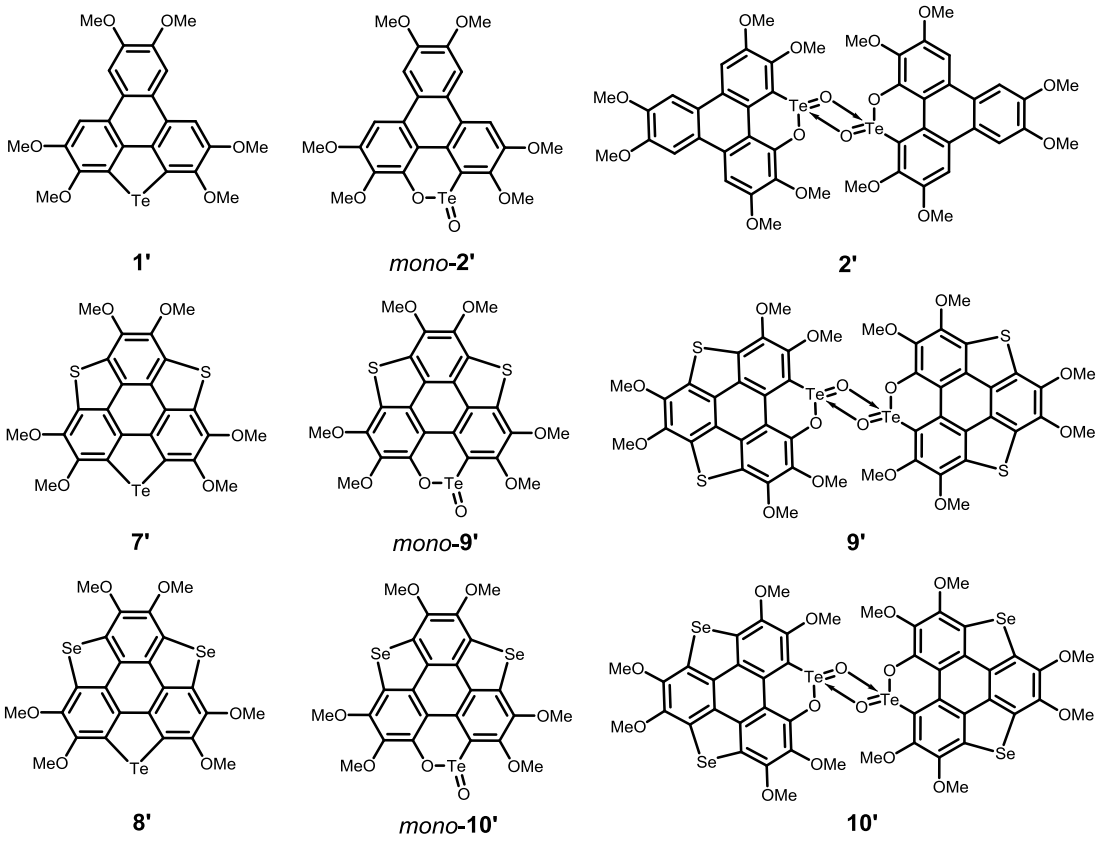

Scheme S1. The chemical structures of calculated molecules.

7.2 Optimized Structures, Molecular Orbitals and Corresponding Energies, Molecular Electrostatic Potential Surfaces and Dipole Moments

The optimized structures of **1'**, **2'**, **7'**, **8'**, **9'**, **10'**, *mono*-**2',** *mono*-**9'** and *mono*-**10'** are displayed in **Fig S28**, and their frontier molecular orbitals and energies levels are shown in **Fig S29-S37**. Molecular orbital energies from HOMO-10 to LUMO+10 are listed in **Table S12**. The molecular electrostatic potential surfaces and dipole moments are displayed in **Fig S39**.

The theoretical investigations give the following conclusions: (1) the HOMO-LUMO energy gaps are narrowed by transforming **1'**, **7'** and **8'** respectively into *mono*-**2'/2**, *mono*-**9'/9,** and *mono*-**10'/10**. The calculated HOMO energy gaps for **1'**, **7'**, **8'**, *mono*-**2'/2**, *mono*-**9'/9,** and *mono*-**10'/10** are summarized in **Table S11** and also depicted in **Fig S38**. (2) the molecular dipole moments are increased upon transformation of **1'**, **7'** and **8'** respectively into *mono*-**2'/2**, *mono*-**9'/9,** and *mono*-**10'/10**. This is because the Te=O groups on *mono*-**2'/2**, *mono*-**9'/9,** and *mono*-**10'/10** show the large contribution on the negative electrostatic potential.

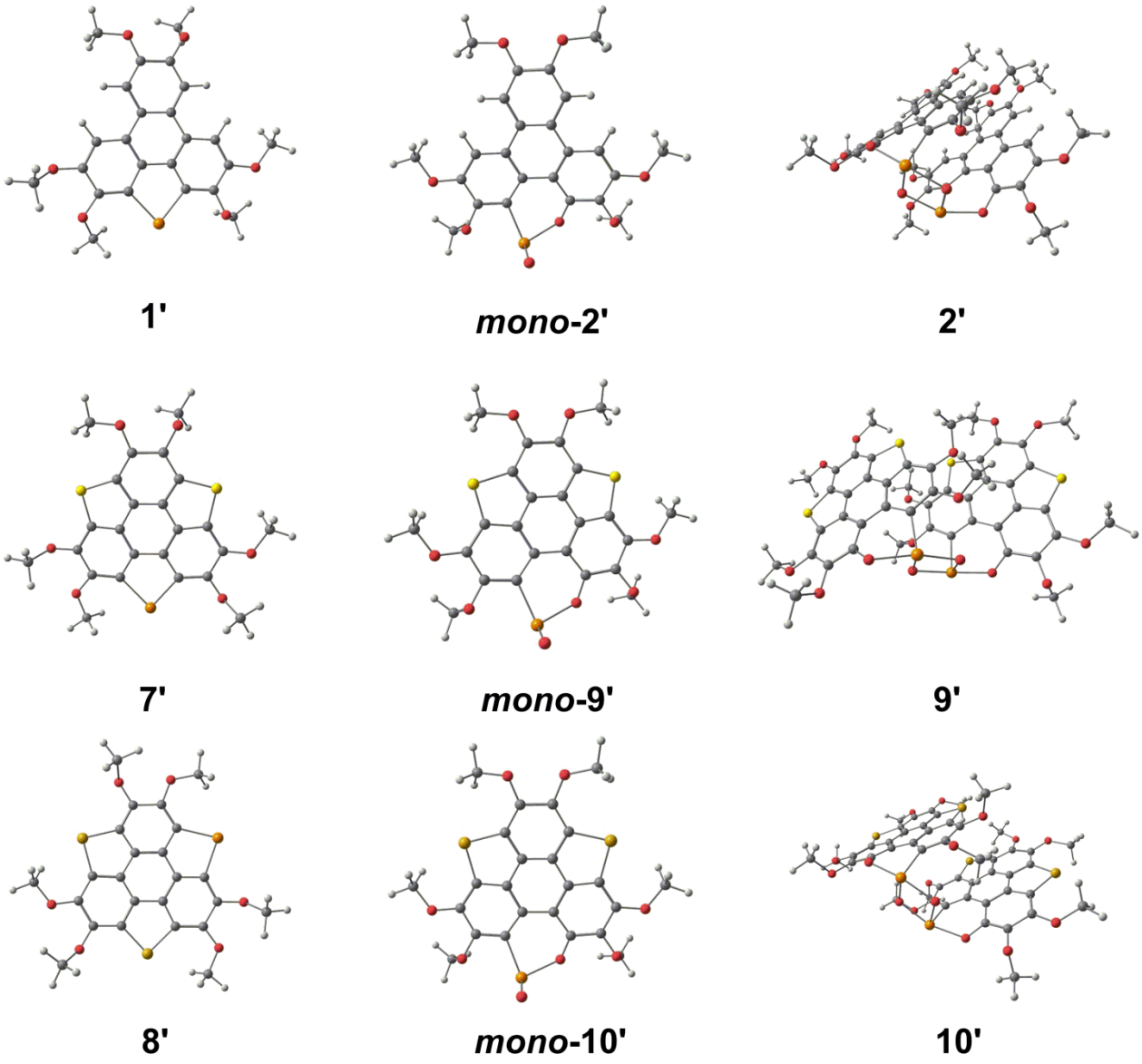

Fig. S28 Optimized molecular structures.

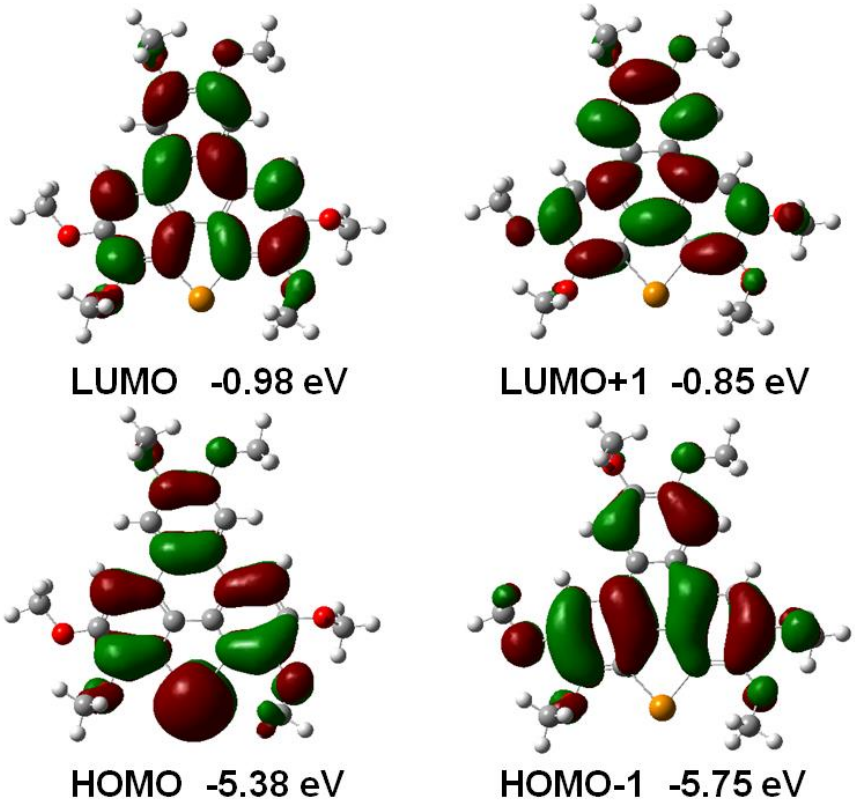

Fig. S29 Calculated molecular orbitals of compound **1'**.

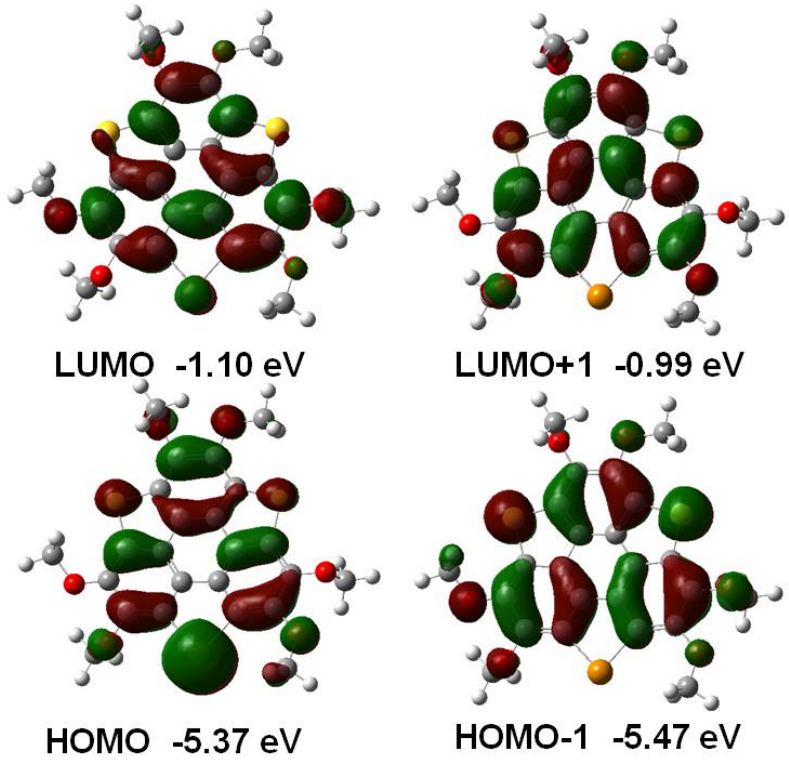

Fig. S30 Calculated molecular orbitals of compound **7'**.

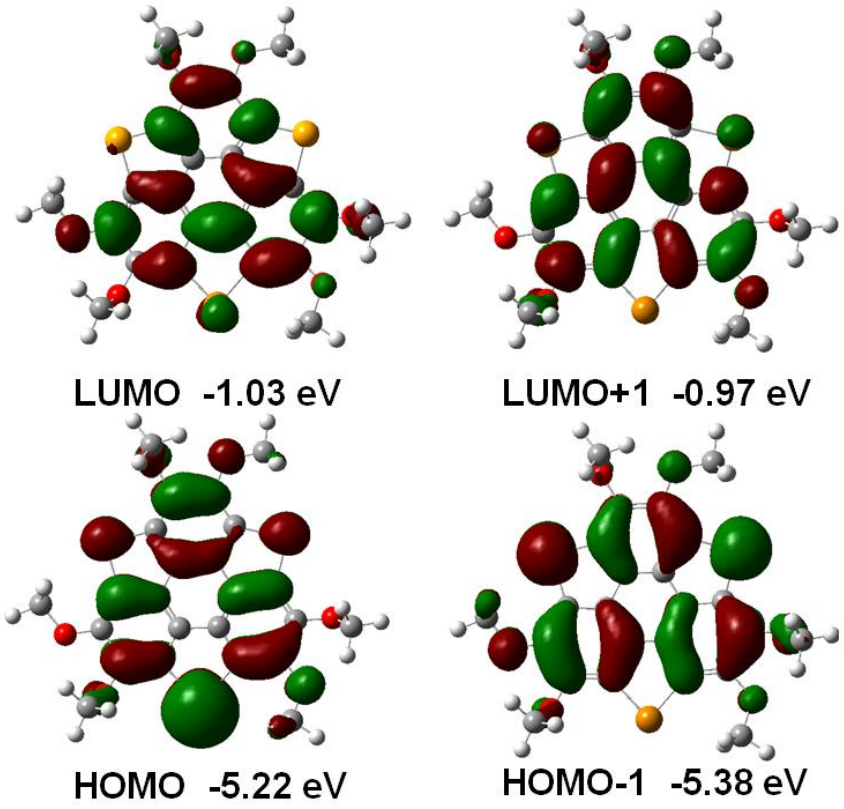

Fig. S31 Calculated molecular orbitals of compound **8'**.

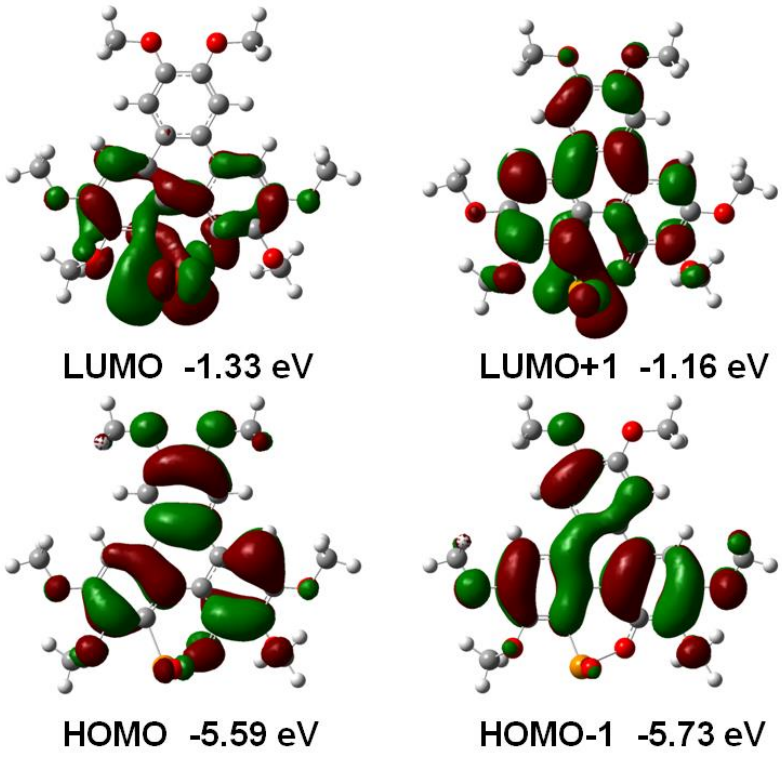

Fig. S32 Calculated molecular orbitals of compound *mono*-**2'**.

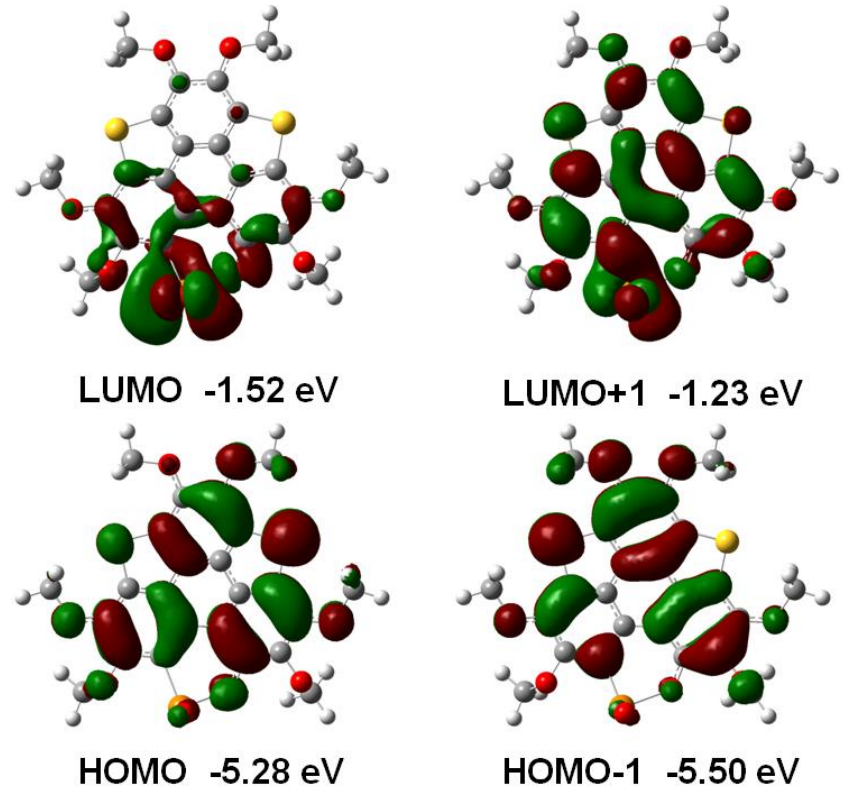

Fig S33. Calculated molecular orbitals of compound *mono*-**9'**.

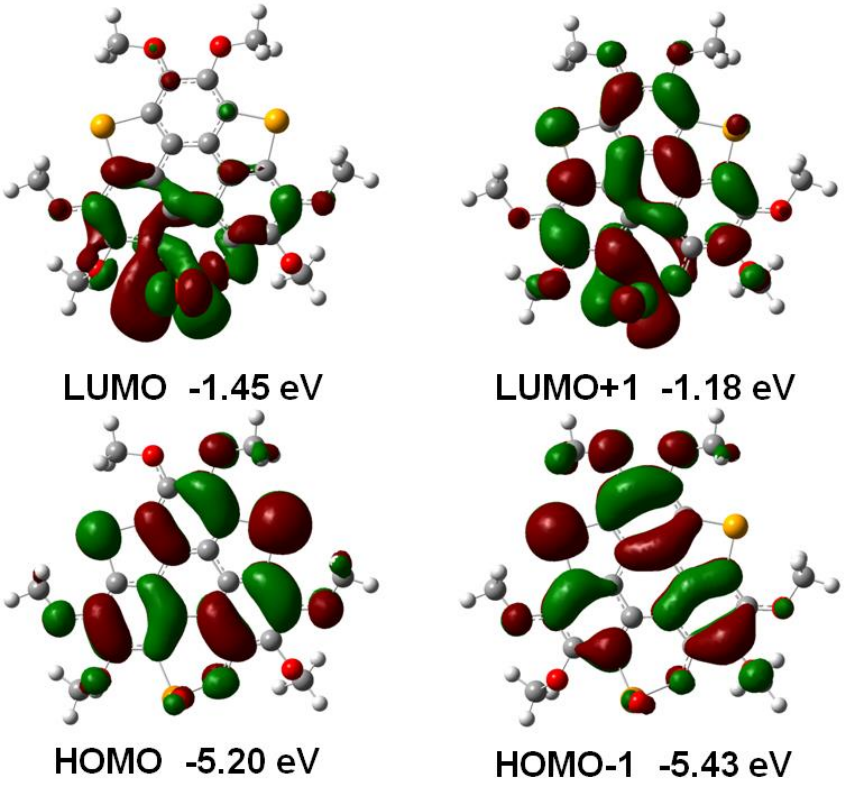

Fig. S34 Calculated molecular orbitals of compound *mono*-**10'**.

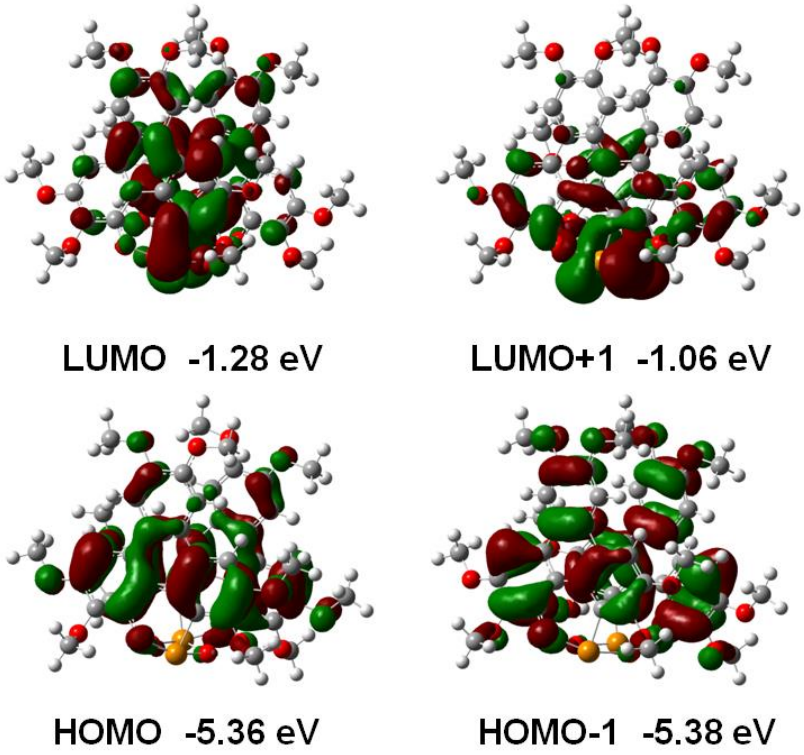

Fig. S35 Calculated molecular orbitals of compound **2'**.

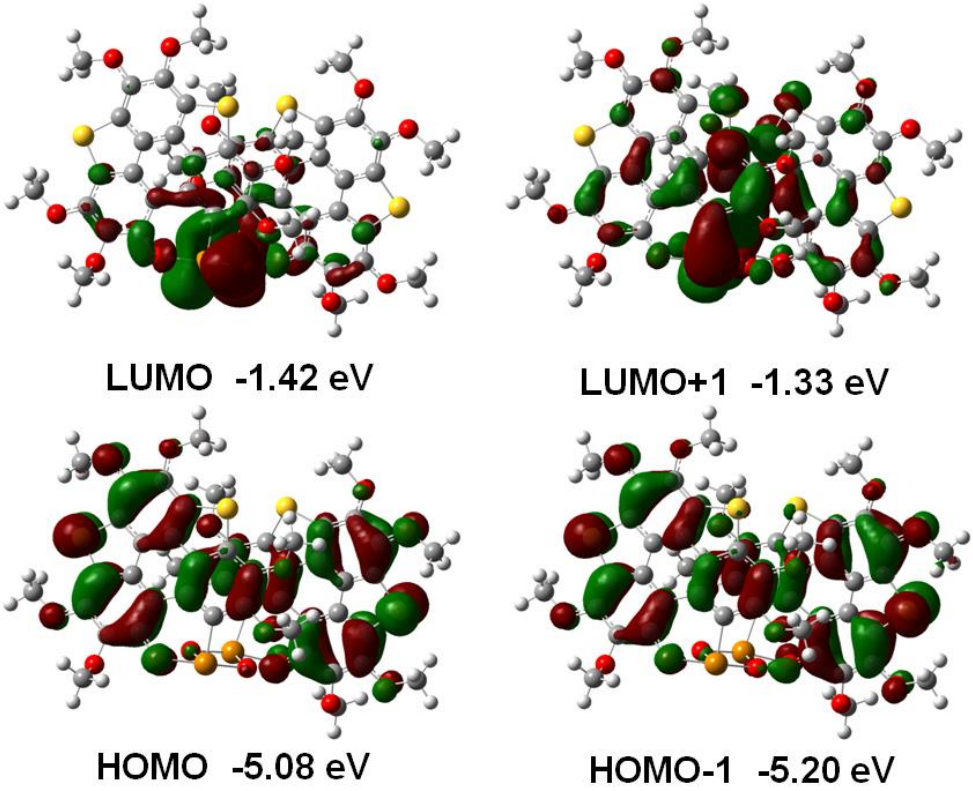

Fig. S36 Calculated molecular orbitals of compound **9'**.

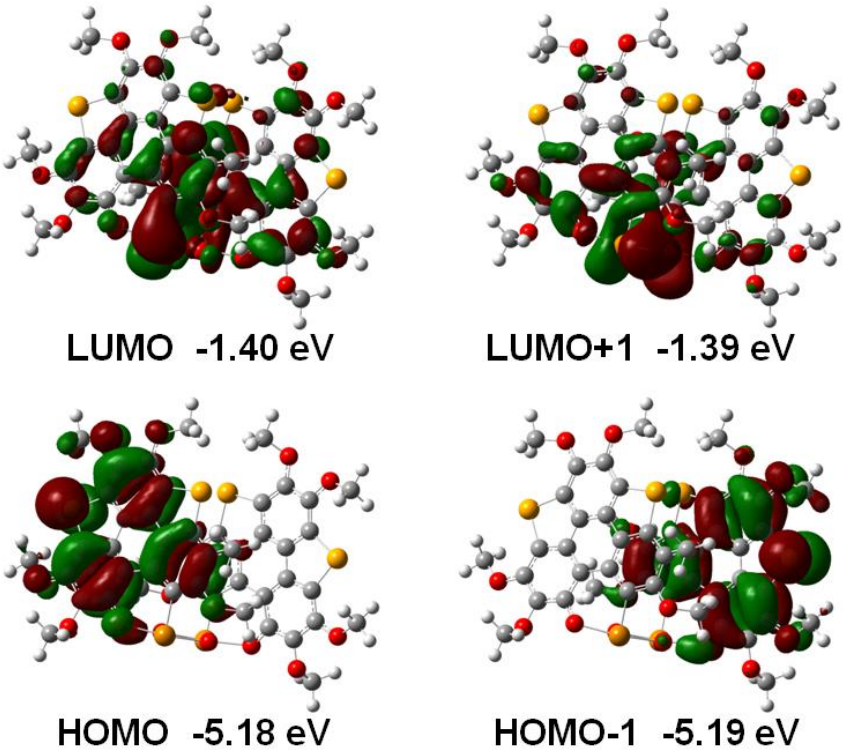

Fig. S37 Calculated molecular orbitals of compound **10'**.

Table S11 The calculated energy level for the frontier orbitals for compound **1'**, **2'**, **7', 8'**, **9'**, **10'**, *mono*-**2', *mono*-9'** and *mono*-**10'**.

compounds	Energy levels / eV				
	HOMO-1	HOMO	LUMO	LUMO+1	E_g[a]
1'	-5.74	-5.38	-0.98	-0.85	4.40
2'	-5.38	-5.36	-1.28	-1.06	4.08
7'	-5.47	-5.37	-1.10	-0.99	4.27
8'	-5.38	-5.22	-1.03	-0.97	4.19
9'	-5.20	-5.08	-1.42	-1.33	3.66
10'	-5.19	-5.18	-1.40	-1.39	3.78
***mono*-2'**	-5.73	-5.59	-1.33	-1.16	4.26
***mono*-9'**	-5.50	-5.28	-1.52	-1.23	3.76
***mono*-10'**	-5.43	-5.20	-1.45	-1.18	3.75

[a]$Eg = E_{LUMO} - E_{HOMO}$

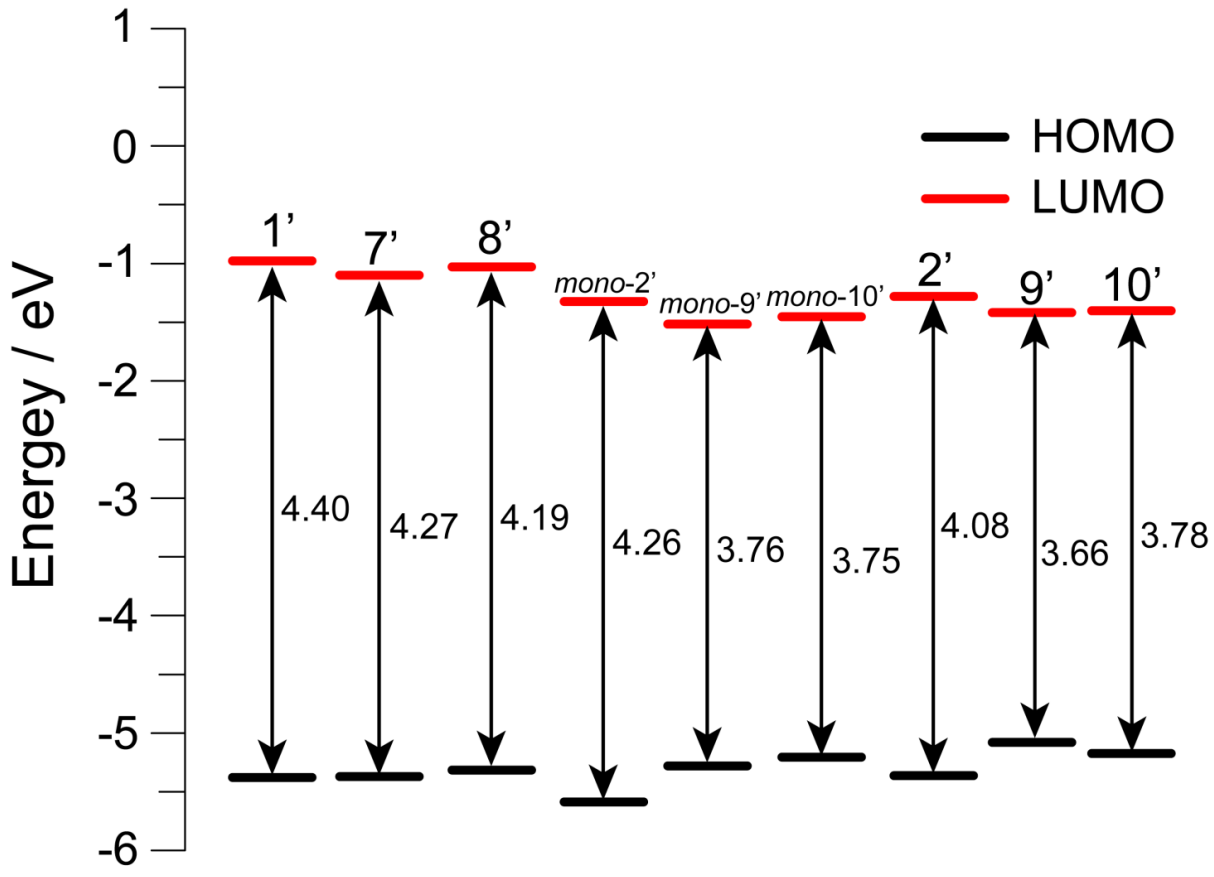

Fig. S38 Schematic plot of HOMO–LUMO levels.

Table S12 Calculated molecular orbital energies (in unit of eV).

Orbital	1’	2’	7’	8’	9’	10’	*mono*-2’	*mono*-9’	*mono*-10’
LUMO+10	2.51	0.77	1.37	1.25	0.43	0.30	1.99	1.28	1.25
LUMO+9	2.26	0.68	1.16	1.07	0.38	0.20	1.90	1.10	1.07
LUMO+8	2.22	0.43	0.82	0.64	0.36	0.14	1.71	0.90	0.76
LUMO+7	1.65	0.11	0.66	0.52	-0.24	-0.24	1.51	0.73	0.54
LUMO+6	1.11	-0.34	0.49	0.49	-0.28	-0.41	1.00	0.58	0.35
LUMO+5	0.83	-0.59	0.43	0.25	-0.53	-0.61	0.85	0.41	0.17
LUMO+4	0.73	-0.59	0.41	0.13	-0.71	-0.79	0.16	-0.02	0.01
LUMO+3	-0.52	-0.71	-0.38	-0.42	-0.86	-0.82	-0.52	-0.52	-0.52
LUMO+2	-0.56	-0.87	-0.73	-0.67	-1.15	-1.20	-0.79	-0.98	-0.92
LUMO+1	-0.85	-1.06	-0.99	-0.97	-1.33	-1.39	-1.16	-1.23	-1.18
LUMO	-0.98	-1.28	-1.10	-1.03	-1.42	-1.40	-1.33	-1.52	-1.45
HOMO	-5.38	-5.36	-5.37	-5.22	-5.08	-5.18	-5.59	-5.28	-5.20
HOMO-1	-5.75	-5.38	-5.47	-5.38	-5.20	-5.19	-5.73	-5.50	-5.43
HOMO-2	-6.28	-5.44	-6.38	-6.32	-5.32	-5.45	-6.39	-6.56	-6.48
HOMO-3	-6.70	-5.65	-6.72	-6.59	-5.51	-5.56	-6.90	-6.84	-6.72
HOMO-4	-7.17	-6.17	-6.92	-6.71	-6.38	-6.38	-6.96	-7.01	-6.80
HOMO-5	-7.52	-6.24	-7.31	-7.17	-6.40	-6.42	-7.23	-7.09	-7.04
HOMO-6	-7.71	-6.55	-7.90	-7.84	-6.45	-6.61	-7.53	-7.48	-7.34
HOMO-7	-7.90	-6.78	-7.92	-7.88	-6.64	-6.66	-7.56	-7.65	-7.60
HOMO-8	-7.99	-7.00	-7.95	-7.90	-6.71	-6.75	-7.83	-7.93	-7.88
HOMO-9	-8.07	-7.09	-8.12	-7.99	-6.94	-6.77	-8.45	-8.32	-8.13
HOMO-10	-8.73	-7.20	-8.61	-8.36	-7.20	-7.07	-8.63	-8.45	-8.24

Table S13. O-Te=O moiety contribution to molecular orbitals of molecules **2’**, **9’**, **10’,** *mono*-**2’,** and *mono*-**9’** *mono*-**10’**.

Molecular Orbital	*mono*-2’	*mono*-9’	*mono*-10’	2’	9’	10’
LUMO+1	16.37%	14.47%	18.97%	60.91%	27.84%	56.80%
LUMO	64.86%	62.44%	69.86%	19.22%	74.43%	27.33%
HOMO	5.78%	3.91%	4.09%	5.33%	6.34%	5.47%
HOMO-1	0.83%	1.24%	2.01%	0.25%	5.81%	5.46%

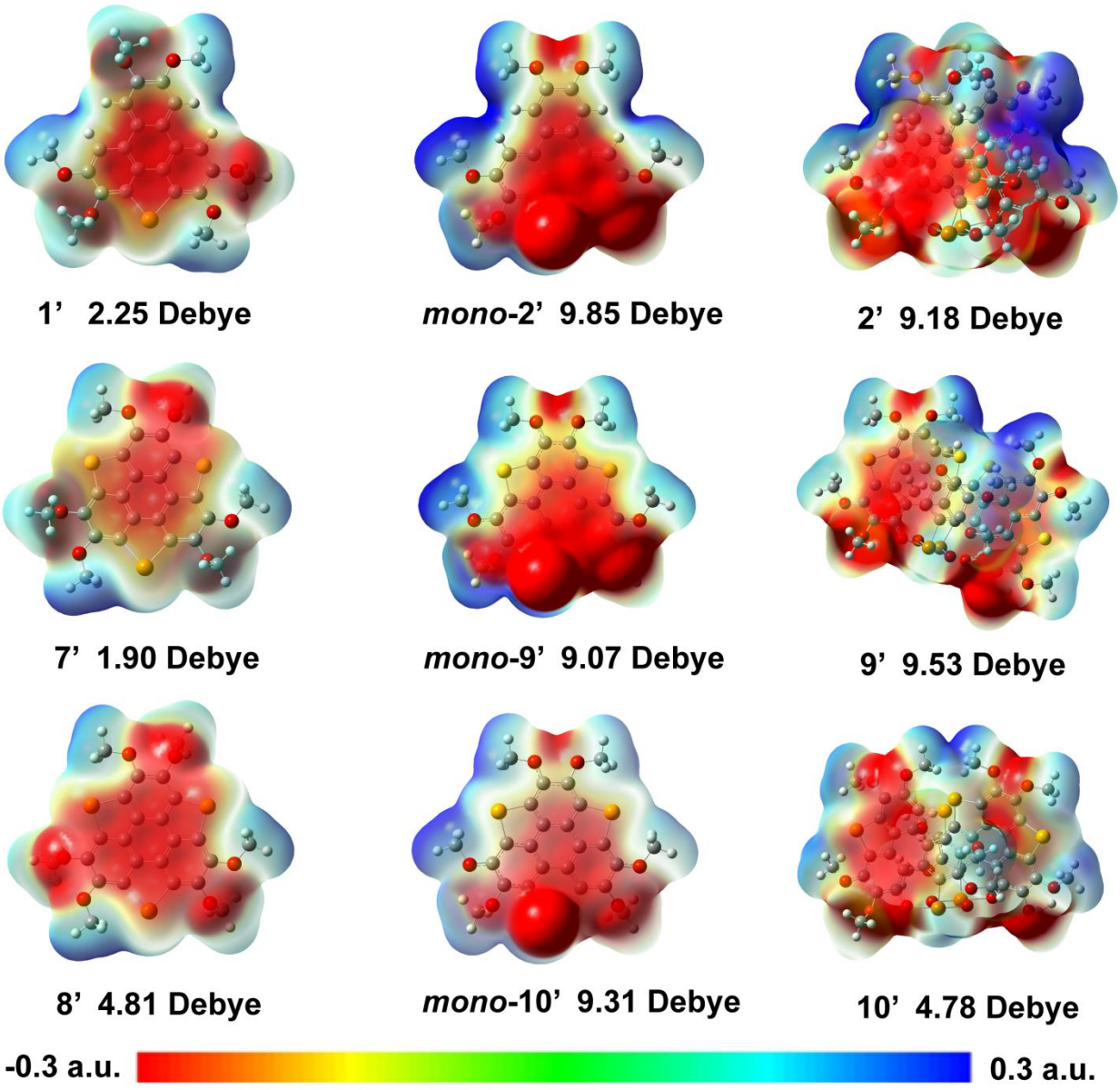

Fig. S39 Calculated electrostatic potential surfaces and dipole moments**.**

7.3. NICS Calculations

Table S14 shows the aromaticity of each ring in **1-7 and 1'-7'**. The aromaticity of **ring 2** in **1'**, **2'**, **7'**, **8'**, **9'**, **10'**, *mono*-**2',** *mono*-**9'** and *mono*-**10'** is strikingly low aromaticity.

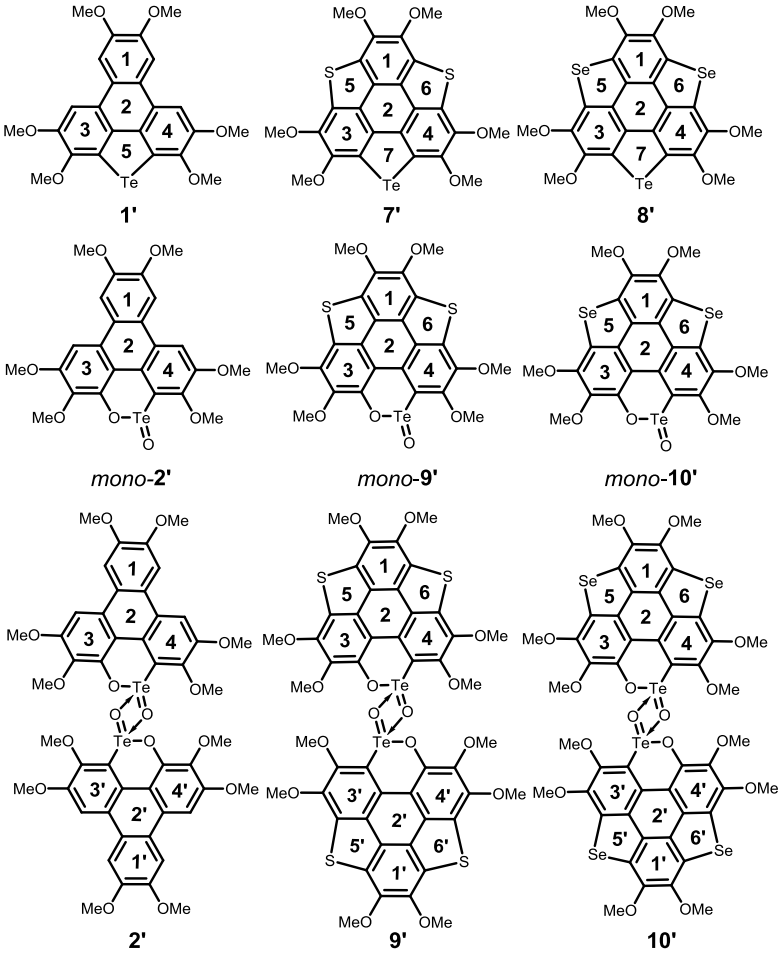

Scheme S2 The chemical structures of **1'**, **2'**, **7'**, **8'**, **9'**, **10'**, *mono*-**2',** *mono*-**9'** and *mono*-**10'**.

Table S14 The calculated NICS values for **1'**, **2'**, **7'**, **8'**, **9'**, **10'**, *mono*-**2',** *mono*-**9'** and *mono*-**10'**.

Comp.	1 ring	2 ring	3 ring	4 ring	5 ring	6 ring	7 ring	1' ring	2' ring	3' ring	4' ring	5' ring	6' ring
1'	-9.5872	-2.5417	-10.598	-10.5809	-4.5772								
2'	-9.547	-4.286	-10.8906	-11.7996				-9.5506	-4.2296	-10.8519	-11.8169		
7'	-12.6048	-2.0634	-11.69	-11.5522	-6.5933	-6.5197	-4.3003						
8'	-11.31	-1.8869	-11.8305	-11.2286	-5.5293	-4.4021	-4.4021						
9'	-12.2151	-1.7005	-11.9082	-12.274	-6.31	-6.8648		-12.222	-1.7154	-11.9525	-12.3507	-6.3295	-6.8707
10'	-11.8635	-2.2587	-11.7126	-12.1363	-5.5812	-6.5793		-11.9125	-1.876	-11.8727	-12.3459	-5.5912	-6.6302
***mono*-2'**	-9.111	-3.1866	-10.5785	-10.4872									
***mono*-9'**	-12.5409	-1.6372	-12.2602	-11.2476	-6.4442	-6.5719							
***mono*-10'**	-11.7111	-1.5496	-11.7924	-10.8579	-5.5187	-5.6245							

7.4. UV-Vis absorption spectra calculation

The calculated UV-Vis absorption spectra for *mono*-**2'**, *mono*-**9'**, *mono*-**10'**, **2'**, **9'**, and **10'** are displayed in **Fig. S40-S45**. The excited states (**ES**s) with oscillator strength (*f*) higher than 0.06 are listed in **Table S15-S20**. The computational results reveal that each molecule has two absorption peaks (denoted as λ and λ', respectively), and each absorption peak consisted of different excited states ($\mathbf{S_n}$). The λ for *mono*-**2'**/**2'** is at 250–310 nm, and the λ' is at 330–450 nm. The λ for *mono*-**9'**/**9'** and *mono*-**10'**/**10'** is at 300–330 nm, and the λ' is at 350–450 nm.

We proposed that the origin of UV-Vis absorption spectra difference can be attributed to different molecular orbital energy gaps (denoted as $\boldsymbol{E_{gap}}$s). In order to simplify the investigation, we choose some "critical excited states" and "critical transition types" to investigate. The "critical excited states" had high oscillator strengths and made important contributions to absorption peaks, and the "critical transition types" had dominant contribution to "critical excited states". Some absorption peaks have multiple critical transition types, we calculated average value of their $\boldsymbol{E_{gap}}$s in one absorption peak for convenience of comparison, denoted as $\boldsymbol{E_{gap}(A)}$. The calculated critical excitation states, critical transition types, contributions, corresponding $\boldsymbol{E_{gap}}$s, and $\boldsymbol{E_{gap}(A)}$s of molecules *mono*-**2'**, *mono*-**9'**, *mono*-**10'**, **2'**, **9'** and **10'** are summarized in **Table S21**.

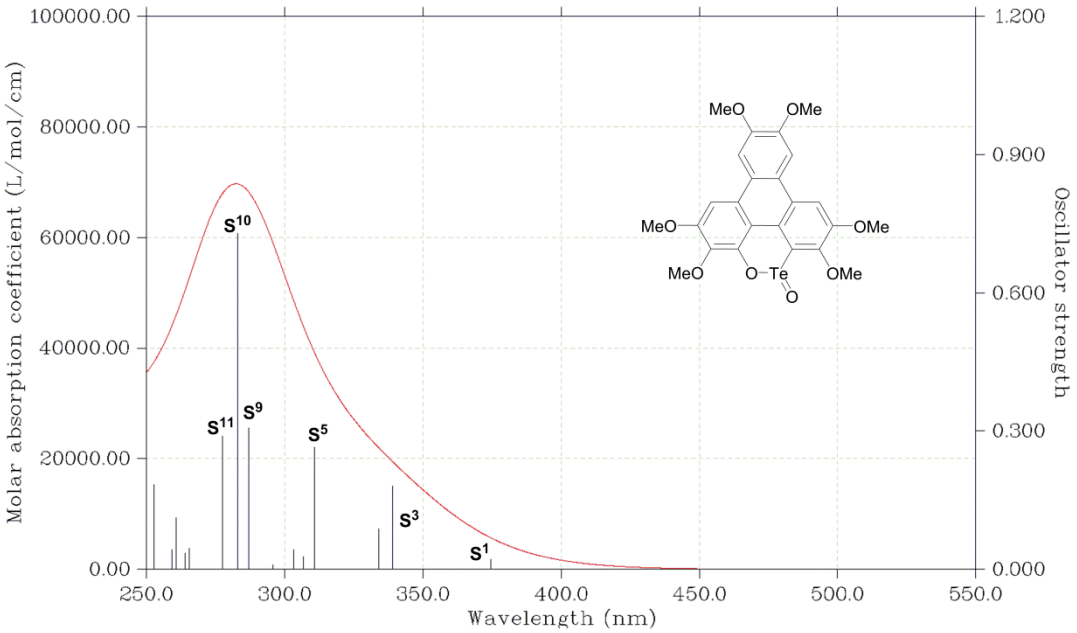

Fig. S40 Calculated UV-Vis absorption spectra and corresponding excitation states of *mono*-**2'**.

Table S15. Calculated excitation energy, excitation wavelength, oscillator strength, transition type and corresponding contribution of each excited state (**ES**) of *mono* -**2'**.

	Excitation Energy/eV	Excitation Wavelength/nm	Oscillator Strengths	Transition Type	Contribution
S^1	3.3135	374.18	0.0214	HOMO-2 → LUMO	2.19%
				HOMO-1 → LUMO	8.07%
				HOMO-1 → LUMO+1	2.07%
				HOMO → LUMO	85.47%
S^3	3.6603	338.73	0.1815	HOMO-1 → LUMO	14.25%
				HOMO-1 → LUMO+1	31.90%
				HOMO-1 → LUMO+2	4.07%
				HOMO → LUMO	5.17%
				HOMO → LUMO+1	33.06%
				HOMO → LUMO+2	7.56%
S^5	3.9942	310.41	0.2642	HOMO-2 → LUMO	4.50%
				HOMO-1 → LUMO+1	15.33%
				HOMO-1 → LUMO+3	14.44%
				HOMO → LUMO+2	52.79%
				HOMO → LUMO+3	6.72%
S^9	4.3226	286.83	0.3076	HOMO-2 → LUMO	2.75%
				HOMO-2 → LUMO+1	6.61%
				HOMO-1 → LUMO+2	22.16%
				HOMO-1 → LUMO+3	17.23%
				HOMO → LUMO+2	4.66%
				HOMO → LUMO+3	35.91%
S^{10}	4.3859	282.69	0.7284	HOMO-2 → LUMO	4.16%
				HOMO-2 → LUMO+1	3.67%
				HOMO-1 → LUMO+2	16.29%
				HOMO-1 → LUMO+3	46.06%
				HOMO → LUMO+1	4.43%
				HOMO → LUMO+2	9.26%
				HOMO → LUMO+3	8.38%
				HOMO → LUMO+4	2.63%
S^{11}	4.4727	277.20	0.2891	HOMO-2 → LUMO+1	75.98%
				HOMO-1 → LUMO+2	5.94%
				HOMO-1 → LUMO+3	7.92%
				HOMO → LUMO+2	2.90%

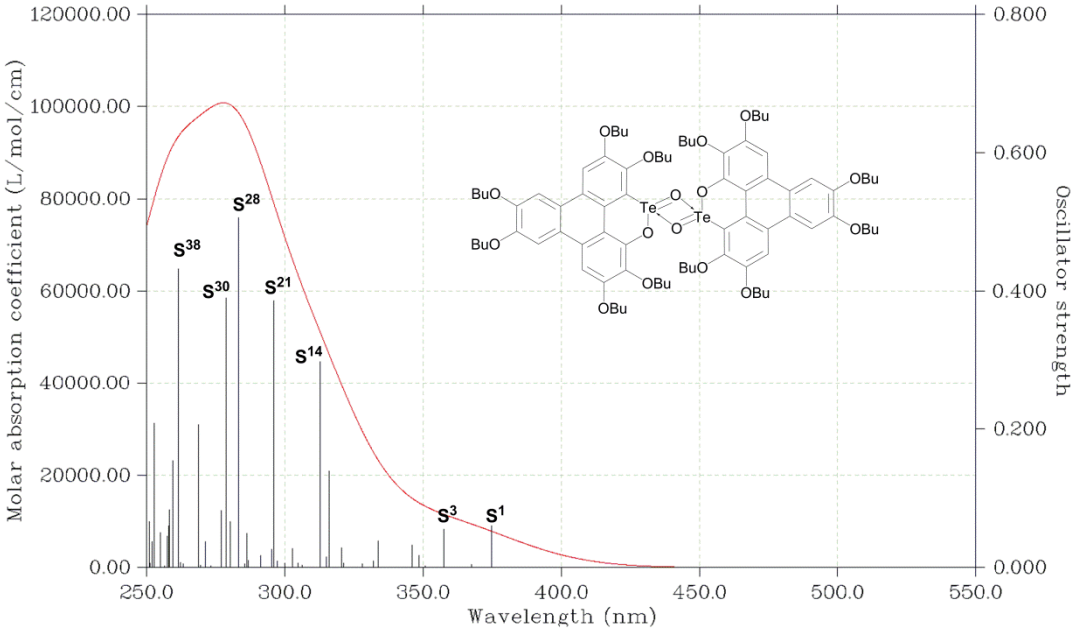

Fig. S41 Calculated UV-Vis absorption spectra and corresponding excitation states of **2'**.

Table S16. Calculated excitation energy, excitation wavelength, oscillator strength, transition type and corresponding contribution of each excited state (**ES**) of **2'**.

	Excitation Energey/ev	Excitation Wavelength/nm	Oscillator Strengths	Transition Type	Contribution
S^1	3.3108	374.48	0.0603	HOMO-2 → LUMO	7.23%
				HOMO → LUMO	84.84%
S^3	3.4693	357.38	0.0554	HOMO-2 → LUMO	86.79%
				HOMO → LUMO	8.21%
S^{14}	3.9687	312.40	0.2972	HOMO-3 → LUMO	4.84%
				HOMO-3 → LUMO+5	6.52%
				HOMO-2 → LUMO+2	6.18%
				HOMO-2 → LUMO+6	3.66%
				HOMO-1 → LUMO+3	44.80%
				HOMO-1 → LUMO+5	4.43%
				HOMO → LUMO+2	3.92%
				HOMO → LUMO+4	12.69%
				HOMO → LUMO+6	4.59%
S^{21}	4.1919	295.77	0.3858	HOMO-4 → LUMO+1	5.99%
				HOMO-3 → LUMO+2	4.68%
				HOMO-3 → LUMO+4	11.34%
				HOMO-2 → LUMO+3	16.60%
				HOMO-2 → LUMO+5	35.91%
				HOMO → LUMO+3	3.24%
				HOMO → LUMO+5	12.69%
S^{28}	4.3800	283.07	0.5061	HOMO-5 → LUMO+1	9.80%
				HOMO-4 → LUMO	2.82%
				HOMO-4 → LUMO+3	2.72%
				HOMO-3 → LUMO+3	3.66%
				HOMO-3 → LUMO+5	26.09%
				HOMO-2 → LUMO+4	3.77%
				HOMO-2 → LUMO+6	15.42%
				HOMO-1 → LUMO+3	3.04%
				HOMO-1 → LUMO+7	2.43%
				HOMO → LUMO+6	19.87%
S^{30}	4.4523	278.47	0.3898	HOMO-5 → LUMO	8.59%
				HOMO-4 → LUMO+1	13.67%
				HOMO-4 → LUMO+2	5.53%
				HOMO-3 → LUMO+2	2.13%
				HOMO-3 → LUMO+4	27.40%
				HOMO-1 → LUMO+6	29.42%
S^{38}	4.7449	261.30	0.4323	HOMO-9 → LUMO	6.20%
				HOMO-7 → LUMO	9.00%
				HOMO-6 → LUMO+1	3.24%
				HOMO-5 → LUMO+2	7.30%
				HOMO-4 → LUMO+3	38.02%
				HOMO-4 → LUMO+5	11.73%
				HOMO-1 → LUMO+7	10.10%

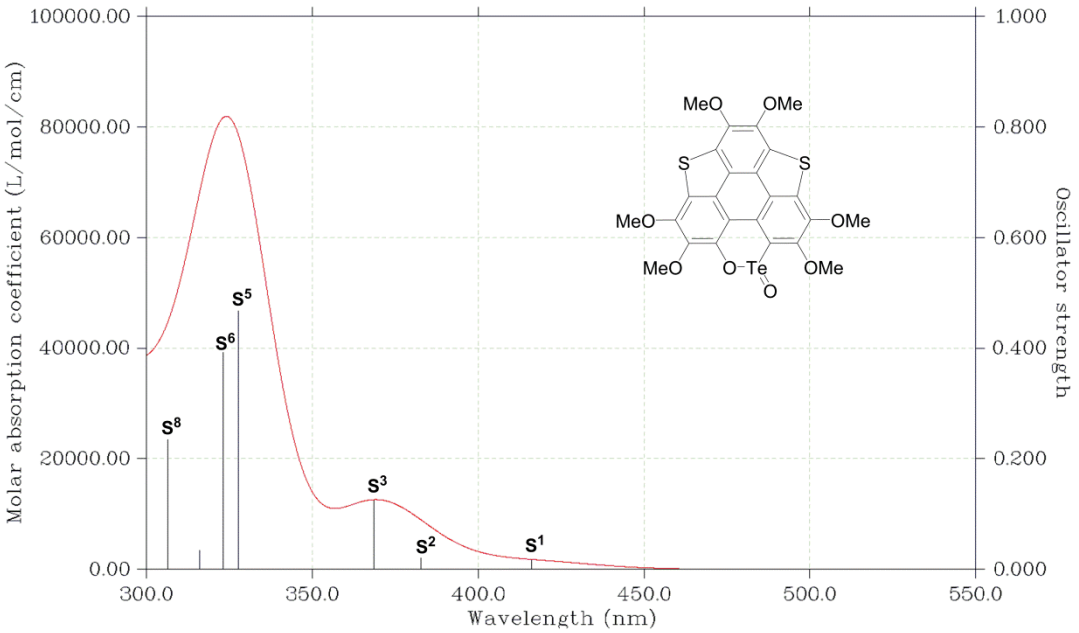

Fig. S42 Calculated UV-Vis absorption spectra and corresponding excitation states of *mono*-**9'**.

Table S17. Calculated excitation energy, excitation wavelength, oscillator strength, transition type and corresponding contribution of each excited state (**ES**) of *mono*-**9'**.

	Excitation Energy/eV	Excitation Wavelength/nm	Oscillator Strengths	Transition Type	Contribution
S^1	2.9818	415.80	0.0162	HOMO → LUMO	95.86%
S^2	3.2417	382.47	0.0207	HOMO-1 → LUMO	47.32%
				HOMO-1 → LUMO+2	6.31%
				HOMO → LUMO+1	43.80%
S^3	3.3670	368.24	0.1244	HOMO-1 → LUMO	48.81%
				HOMO-1 → LUMO+2	9.82%
				HOMO → LUMO+1	37.76%
S^5	3.7853	327.54	0.4667	HOMO-1 → LUMO+1	46.17%
				HOMO-1 → LUMO+3	3.51%
				HOMO → LUMO+2	41.19%
S^6	3.8394	322.92	0.3921	HOMO-1 → LUMO+2	53.45%
				HOMO → LUMO+1	12.64%
				HOMO → LUMO+2	2.39%
				HOMO → LUMO+3	24.97%
S^8	4.0492	306.19	0.2350	HOMO-2 → LUMO	7.63%
				HOMO-1 → LUMO+2	19.92%
				HOMO → LUMO+1	2.22%
				HOMO → LUMO+3	61.02%

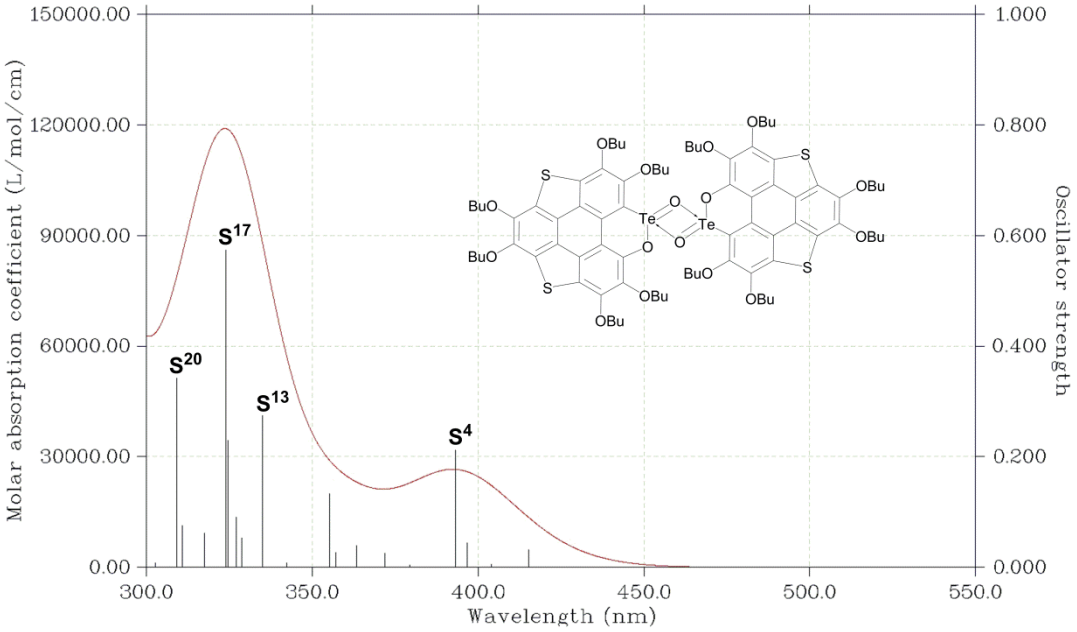

Fig. S43 Calculated UV-Vis absorption spectra and corresponding excitation states of **9'**.

Table S18 Calculated excitation energy, excitation wavelength, oscillator strength, transition type and corresponding contribution of each excited state (**ES**) of **9'**.

	Excitation Energy/eV	Excitation Wavelength/nm	Oscillator Strengths	Transition Type	Contribution
S^4	3.1560	392.85	0.2125	HOMO-3 → LUMO	4.75%
				HOMO-2 → LUMO+3	5.34%
				HOMO-1 → LUMO+1	55.19%
				HOMO → LUMO+2	27.69%
S^{13}	3.7040	334.73	0.2749	HOMO-3 → LUMO+1	8.00%
				HOMO-2 → LUMO+2	12.46%
				HOMO-2 → LUMO+4	3.40%
				HOMO-1 → LUMO+2	3.58%
				HOMO-1 → LUMO+4	2.52%
				HOMO → LUMO+3	60.61%
				HOMO → LUMO+5	4.77%
S^{17}	3.8311	323.62	0.5736	HOMO-3 → LUMO+2	32.54%
				HOMO-2 → LUMO+3	14.10%
				HOMO-1 → LUMO+5	2.83%
				HOMO → LUMO+4	40.30%
				HOMO → LUMO+6	2.44%
S^{20}	4.0136	308.91	0.3420	HOMO-3 → LUMO+4	3.41%
				HOMO-2 → LUMO+3	18.75%
				HOMO-1 → LUMO+3	2.69%
				HOMO-1 → LUMO+5	44.58%
				HOMO → LUMO+6	18.81%

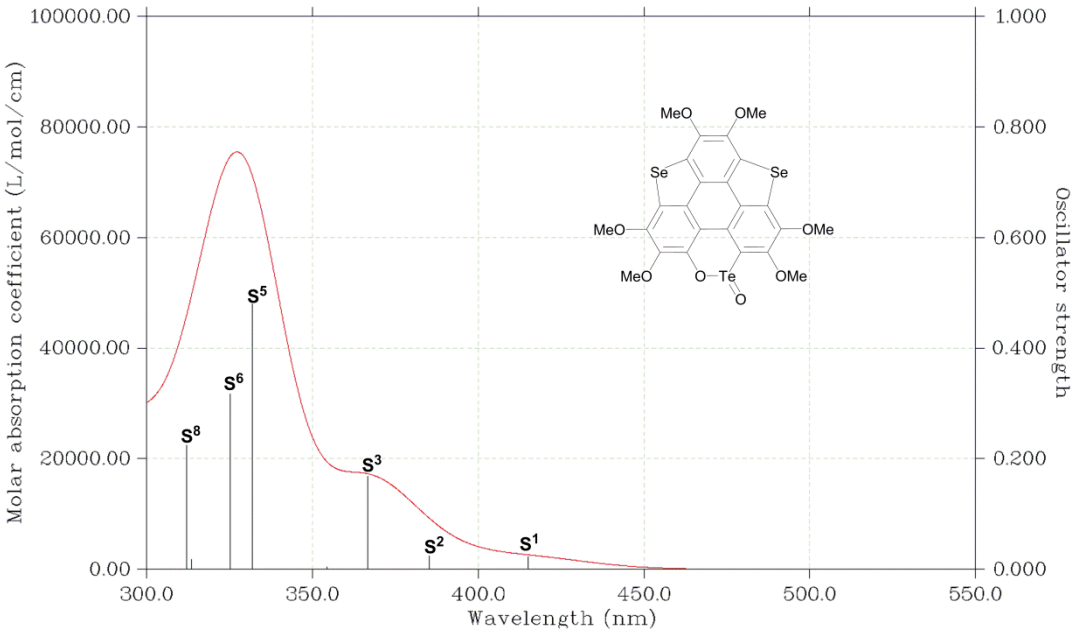

Fig. S44 Calculated UV-Vis absorption spectra and corresponding excitation states of *mono*-**10'**.

Table S19 Calculated excitation energy, excitation wavelength, oscillator strength, transition type and corresponding contribution of each excited state (**ES**) of *mono*-**10'**.

	Excitation energy/eV	Excitation wavelength/nm	Oscillator Strengths	Transition Type	Contribution
S^1	2.9894	414.75	0.0234	HOMO → LUMO	96.07%
S^2	3.2209	384.93	0.0241	HOMO-1 → LUMO	38.16%
				HOMO-1 → LUMO+2	6.00%
				HOMO → LUMO+1	53.26%
S^3	3.3842	366.36	0.1682	HOMO-1 → LUMO	57.46%
				HOMO-1 → LUMO+2	7.04%
				HOMO → LUMO+1	30.34%
S^5	3.7382	331.67	0.4796	HOMO-1 → LUMO+1	49.50%
				HOMO-1 → LUMO+3	2.82%
				HOMO → LUMO+2	39.30%
S^6	3.8160	324.90	0.3169	HOMO-1 → LUMO+2	54.59%
				HOMO → LUMO+1	10.74%
				HOMO → LUMO+3	28.38%
S^8	3.9752	311.89	0.2245	HOMO-5 → LUMO	19.35%
				HOMO-1 → LUMO+2	21.07%
				HOMO → LUMO+3	48.58%

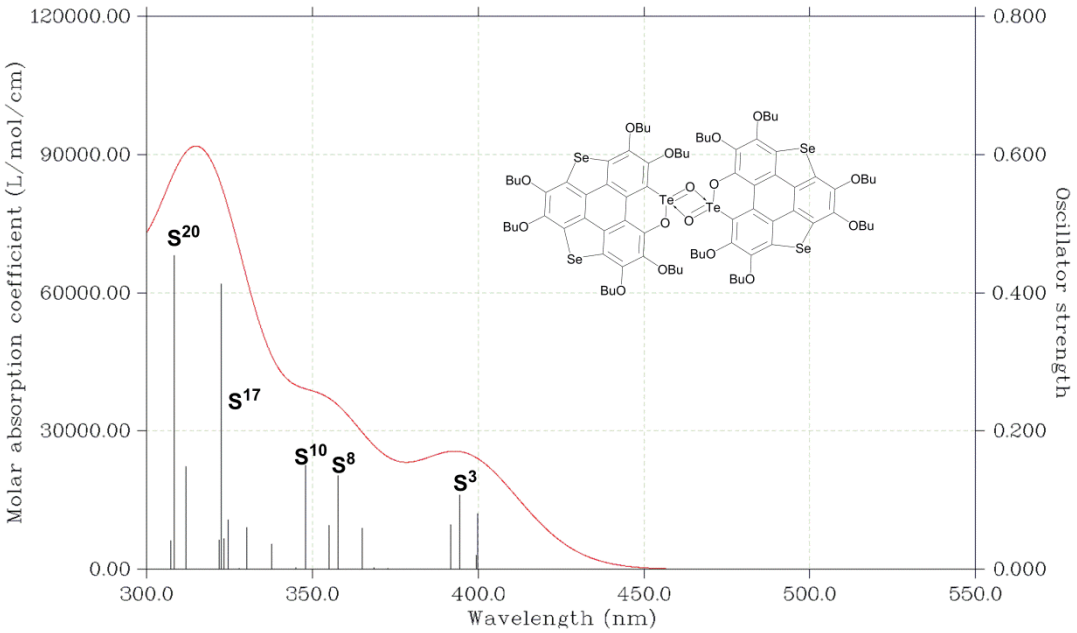

Fig. S45 Calculated UV-Vis absorption spectra and corresponding excitation states of **10'**.

Table S20 Calculated excitation energy, excitation wavelength, oscillator strength, transition type and corresponding contribution of each excited state (**ES**) of **10'**.

	Excitation Energey/ev	Excitation Wavelength /nm	Oscillator Strengths	Transition Type	Contribution
S^3	3.1457	394.14	0.1079	HOMO-2 → LUMO+1	3.51%
				HOMO-1 → LUMO	6.17%
				HOMO → LUMO	41.86%
				HOMO → LUMO+1	40.54%
S^8	3.4696	357.35	0.1352	HOMO-2 → LUMO	4.57%
				HOMO-2 → LUMO+1	66.36%
				HOMO → LUMO+2	21.93%
S^{10}	3.5667	347.61	0.1510	HOMO-3 → LUMO	7.77%
				HOMO-3 → LUMO+1	76.35%
				HOMO-1 → LUMO+2	9.53%
S^{17}	3.8464	322.34	0.4130	HOMO-3 → LUMO+2	25.84%
				HOMO-2 → LUMO+2	7.30%
				HOMO-2 → LUMO+4	3.11%
				HOMO-1 → LUMO+3	14.80%
				HOMO-1 → LUMO+4	12.58%
				HOMO-1 → LUMO+5	2.34%
				HOMO → LUMO+3	4.27%
				HOMO → LUMO+4	15.50%
				HOMO → LUMO+5	2.19%
S^{20}	4.0245	308.07	0.4543	HOMO-5 → LUMO	2.69%
				HOMO-3 → LUMO+3	29.61%
				HOMO-2 → LUMO+3	31.59%
				HOMO-2 → LUMO+4	8.34%
				HOMO-1 → LUMO+5	5.52%
				HOMO → LUMO+5	4.94%

Table S21 Calculated critical excitation states (**ES**s), critical transition types, contributions, corresponding molecular orbital energy gaps (E_{gap}s), and average value of molecular orbital energy gaps (E_{gap}**(A)**s) of molecules **2', 9', 10',** *mono*-**2',** *mono*-**9',** and *mono*-**10'**.

	Absorption Peak	Critical **ES**	Oscillator Strength	Critical Transition Type	Contri-bution	E_{gap} /eV	E_{gap}**(A)**/ eV
mono-**2'**	λ = 282 nm	9	0.3076	HOMO-1→LUMO+2	22.16%	4.94	5.11
				HOMO→LUMO+3	35.91%	5.07	
		10	0.7284	HOMO-1→LUMO+3	46.06%	5.21	
		11	0.2891	HOMO-2→LUMO+1	75.98%	5.23	
	λ' = 374 nm	1	0.0214	HOMO→LUMO	85.47%	4.26	4.26
mono-**9'**	λ' = 322 nm	5	0.4667	HOMO-1→LUMO+1	46.17%	4.27	4.36
				HOMO →LUMO+2	41.19%	4.3	
		6	0.3921	HOMO-1→LUMO+2	53.45%	4.52	
	λ' = 416 nm	1	0.0162	HOMO→LUMO	95.86%	4.26	4.26
mono-**10'**	λ = 324nm	5	0.4796	HOMO-1→LUMO+1	49.50%	4.25	4.35
				HOMO→LUMO+2	39.30%	4.28	
		6	0.3169	HOMO-1→LUMO+2	54.59%	4.51	
	λ' = 414 nm	1	0.0214	HOMO→LUMO	85.47%	3.75	3.75
2'	λ = 282 nm	28	0.5061	HOMO-3→LUMO+5	26.09%	4.97	4.99
		30	0.3898	HOMO-3→LUMO+4	27.40%	4.97	
				HOMO-1→LUMO+6	29.42%	5.04	
	λ' = 374 nm	1	0.0603	HOMO → LUMO	84.84%	4.08	4.08
9'	λ = 323 nm	17	0.5736	HOMO→LUMO+4	40.30%	4.37	4.36
				HOMO-3→LUMO+2	32.54%	4.36	
	λ' = 392nm	4	0.2125	HOMO-1→LUMO+1	55.19%	3.87	3.87
10'	λ = 320 nm	17	0.4130	HOMO-3→LUMO+2	25.84%	4.36	4.58
		20	0.4543	HOMO-3→LUMO+3	29.61%	4.74	
				HOMO-2→LUMO+3	31.59%	4.65	
	λ' = 394 nm	3	0.1079	HOMO → LUMO	41.86%	3.78	3.79
				HOMO→LUMO+1	40.54%	3.79	

8. References

[S1] W. L. F. Armarege and C. L. L. Chai., Purification of Laboratory Chemicals, 5th ed.

[S2] S. Wang, J. Shang, C. Yan, W. Wang, C. Yuan, H.-L. Zhang and X. Shao, *Org. Chem. Front.* 2019, **6**, 263.

[S3] Y. Xu, V. Kumar, M. J. Z. Bradshaw and D. L. Bryce, *Cryst. Growth Des.*, 2020, **20**, 7910.

[S4] M. C. Burla, R Caliandro., M. Camalli, B. Carrozzini, G. L. Cascarano, L. de Caro, C. Giacovazzo, G. Polidori and R. Spagna, *J. Appl. Cryst.*, 2005, **38**, 381.

[S5] G. M. Sheldrick, *SHELXL-97, A Program for Crystal Structure Refinement*, University of Göttingen, Göttingen, Germany, 1997.

[S6] M. J. Frisch, G. W. Trucks, H. B. Schlegel, G. E. Scuseria, M. A. Robb, J. R. Cheeseman, G. Scalmani, V. Barone, G. A. Petersson, H. Nakatsuji, X. Li, M. Caricato, A. V. Marenich, J. Bloino, B. G. Janesko, R. Gomperts, B. Mennucci, H. P. Hratchian, J. V. Ortiz, A. F. Izmaylov, J. L. Sonnenberg, D. Williams-Young, F. Ding, F. Lipparini, F. Egidi, J. Goings, B. Peng, A. Petrone, T. Henderson, D. Ranasinghe, V. G. Zakrzewski, J. Gao, N. Rega, G. Zheng, W. Liang, M. Hada, M. Ehara, K. Toyota, R. Fukuda, J. Hasegawa, M. Ishida, T. Nakajima, Y. Honda, O. Kitao, H. Nakai, T. Vreven, K. Throssell, J. A. Montgomery, Jr., J. E. Peralta, F. Ogliaro, M. J. Bearpark, J. J. Heyd, E. N. Brothers, K. N. Kudin, V. N. Staroverov, T. A. Keith, R. Kobayashi, J. Normand, K. Raghavachari, A. P. Rendell, J. C. Burant, S. S. Iyengar, J. Tomasi, M. Cossi, J. M. Millam, M. Klene, C. Adamo, R. Cammi, J. W. Ochterski, R. L. Martin, K. Morokuma, O. Farkas, J. B. Foresman, D. J. Fox, *Gaussian 16, Revision A.03*, Gaussian, Inc., Wallingford CT, 2016.

[S7] a) A. D. Becke, *J. Chem. Phys.* 1993, **98**, 5648; b) C. Lee, W. Yang and R. G. Parr, *Phys. Rev. B.* 1988, **37**, 785.

[S8] F. Weigend and R. Ahlrichs, *Phys. Chem. Chem. Phys.* 2005, **7**, 3297

[S9] J. Tomasi, B. Mennucci and R. Cammi, *Chem. Rev*. 2005, **105**, 2999.

[S10] P. V. R. Schleyer, C. Maerker, A. Dransfeld, H. Jiao and N. J. R. V. E. Hommes, *J. Am. Chem. Soc.* 1996, **118**, 6317.

[S11] Z. Chen, C. S. Wannere, C. Corminboeuf, R. Puchta and P. V. R Schleyer, *Chem. Rev*. 2005, **105**, 3842.

[S12] a) F. London, *J. Phys. Radium.* 1937, **8**, 397. b) H. F. Hameka, *Mol. Phys.* 1958, **1**, 203. c) R. Ditchfield, *Mol. Phys.* 1974, **27**, 789. d) K. Wolinski, J. F. Hinton and P. Pulay, *J. Am. Chem. Soc.* 1990, **112**, 8251.

[S13] G. A. Andrienko and Chemcraft, Version 1.8 (built 523b); http://www.chemcraftprog.com.

[S14] T. Lu and F. Chen, *J. Comput. Chem.* 2012, **33**, 580.

[S15] T. Lu and F. Chen, *Acta Chim. Sinica* 2011, **69**, 2393.

9. ^{125}Te NMR Spectra of Products

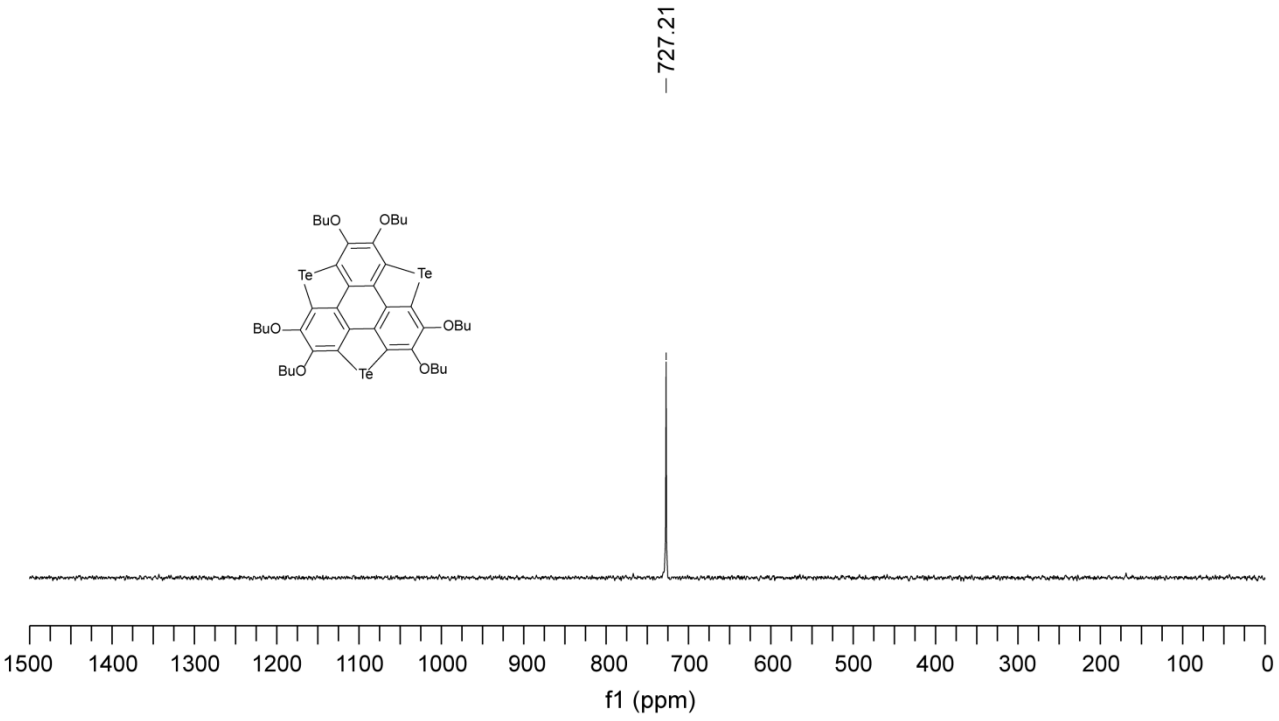

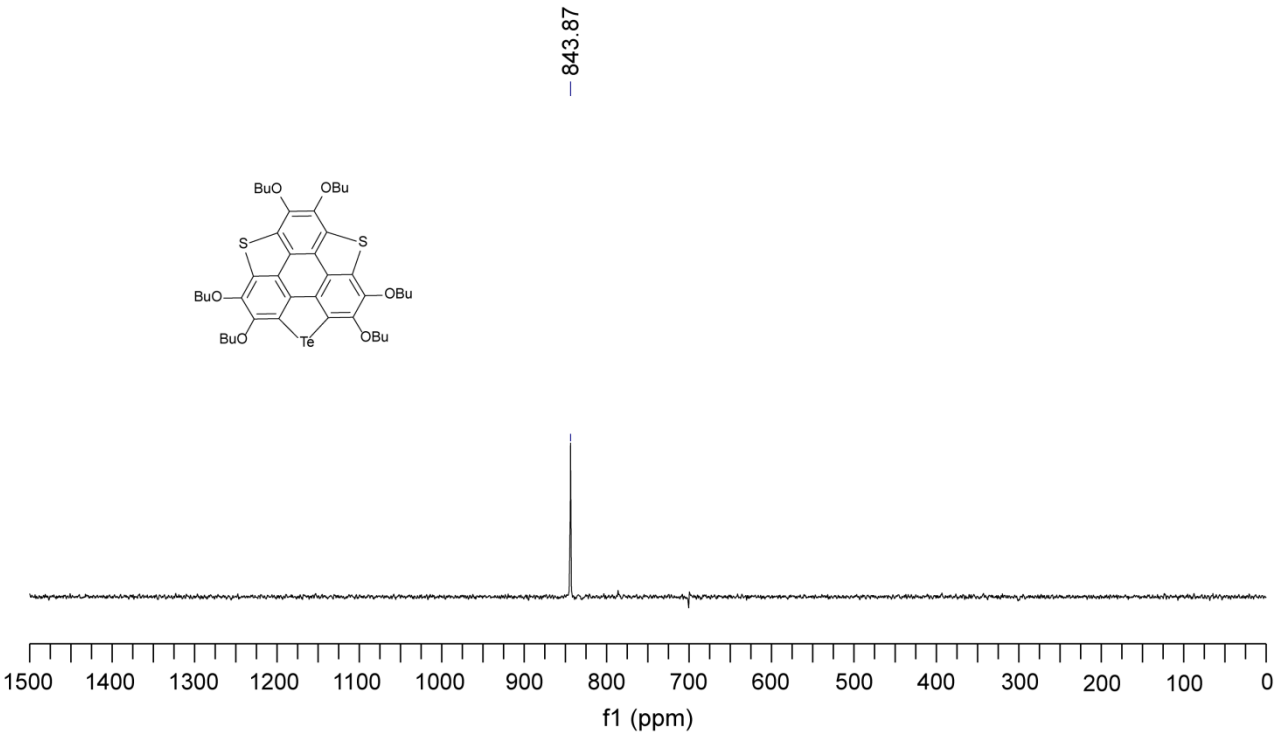

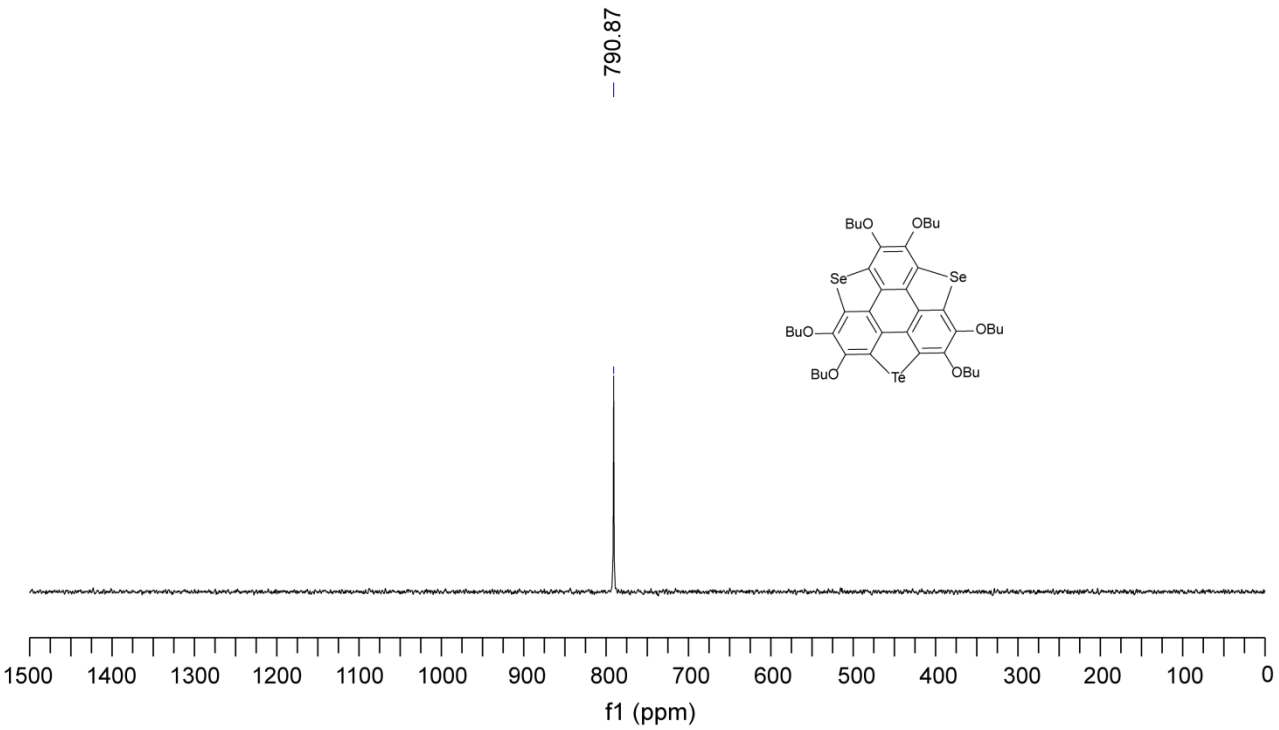
790.87
BuO
OBu
Se
Se
BuO
OBu
BuO
Te
OBu
1500 1400 1300 1200 1100 1000 900 800 700 600 500 400 300 200 100 0
f1 (ppm)

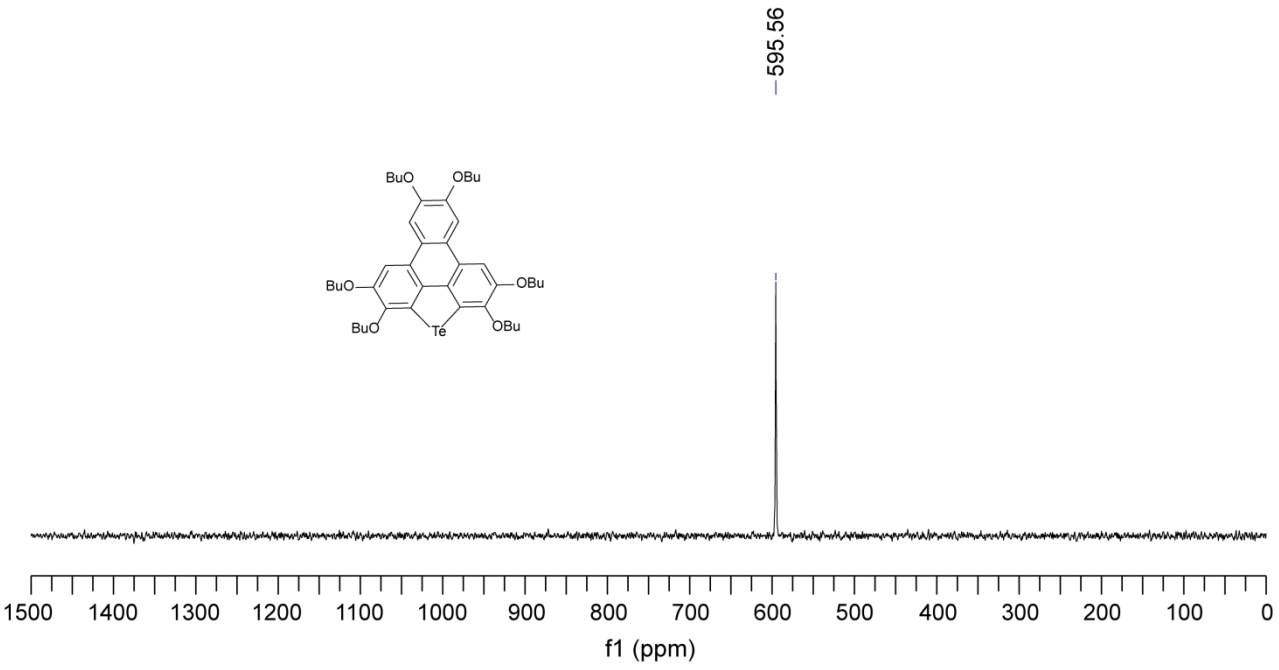
595.56
BuO
OBu
BuO
OBu
BuO
Te
OBu
1500 1400 1300 1200 1100 1000 900 800 700 600 500 400 300 200 100 0
f1 (ppm)

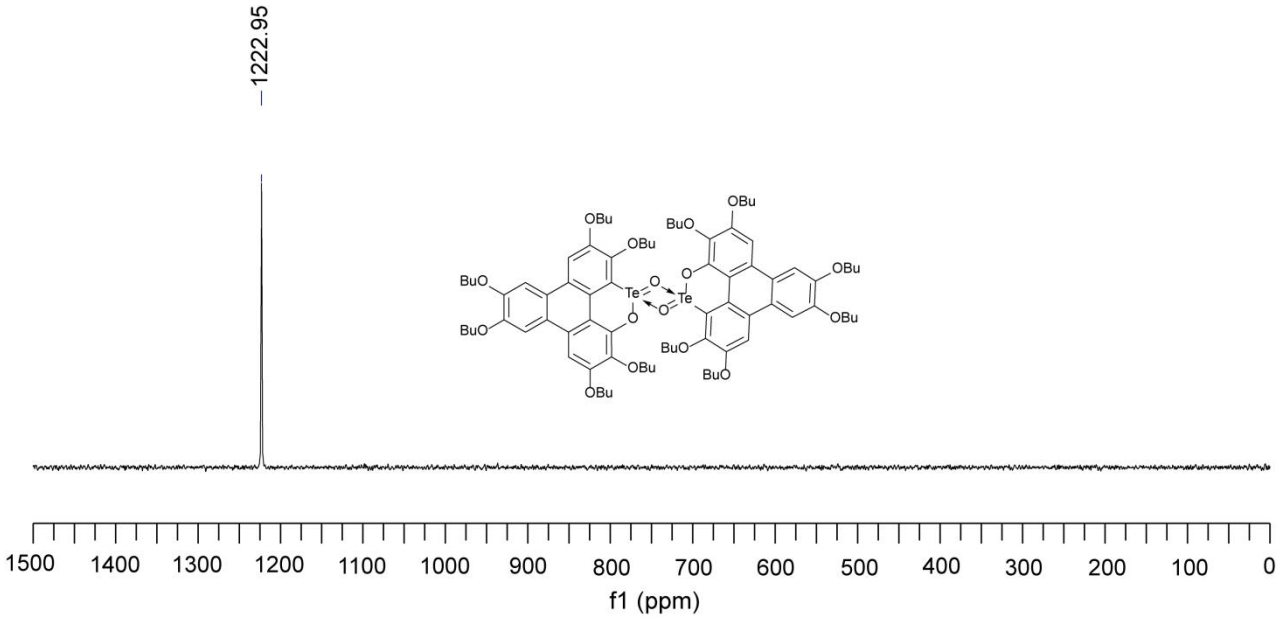
1222.95
OBu
BuO
Te
O
1500 1400 1300 1200 1100 1000 900 800 700 600 500 400 300 200 100 0
f1 (ppm)

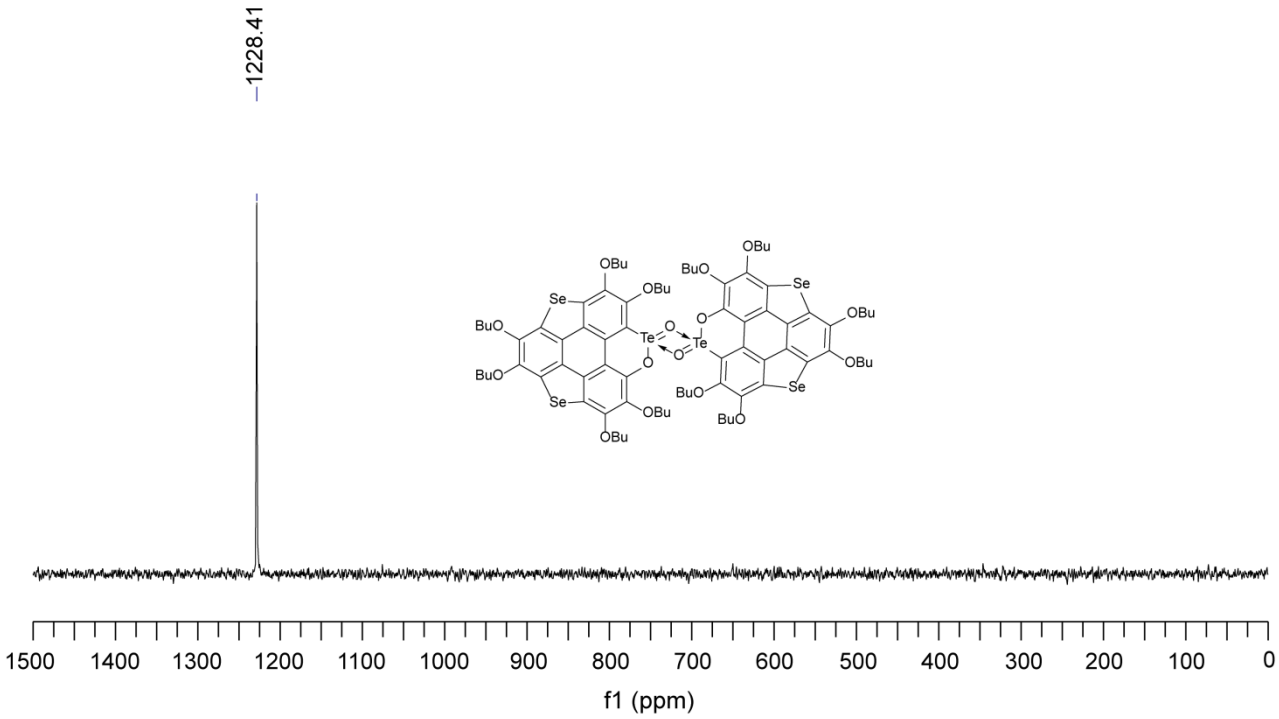
1228.41
OBu
BuO
Se
Te
O
1500 1400 1300 1200 1100 1000 900 800 700 600 500 400 300 200 100 0
f1 (ppm)

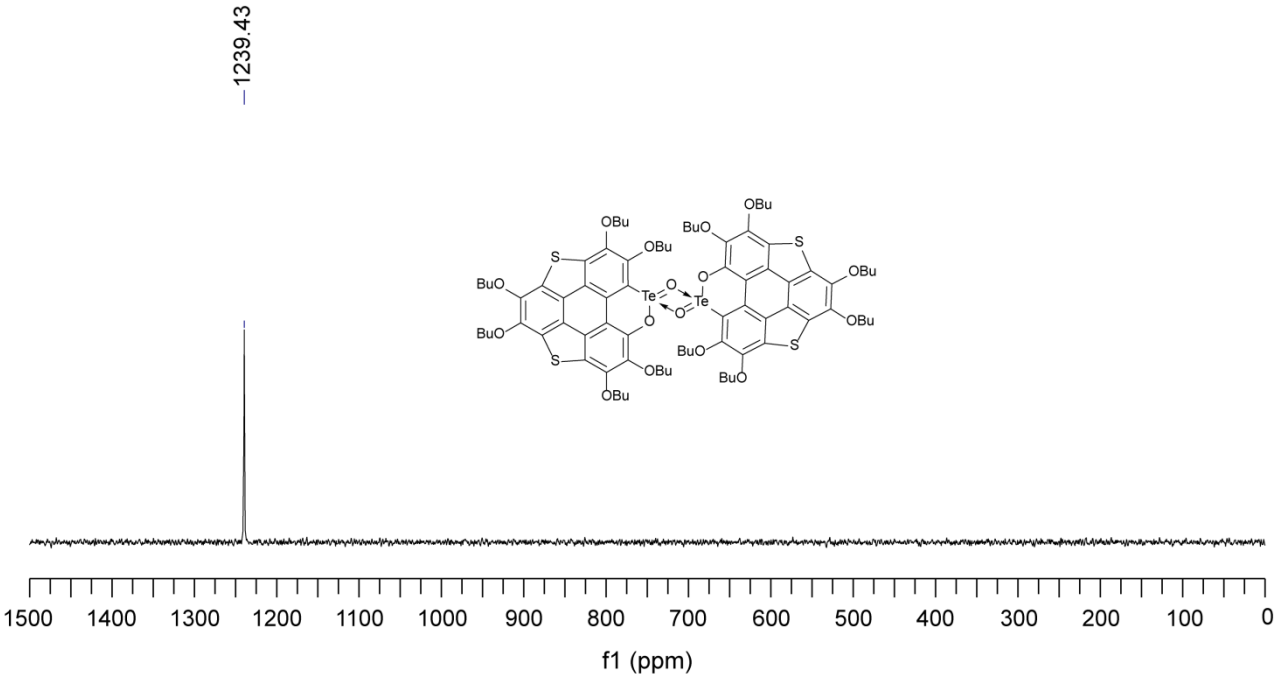
1239.43
OBu
BuO
S
Te
O
1500 1400 1300 1200 1100 1000 900 800 700 600 500 400 300 200 100 0
f1 (ppm)

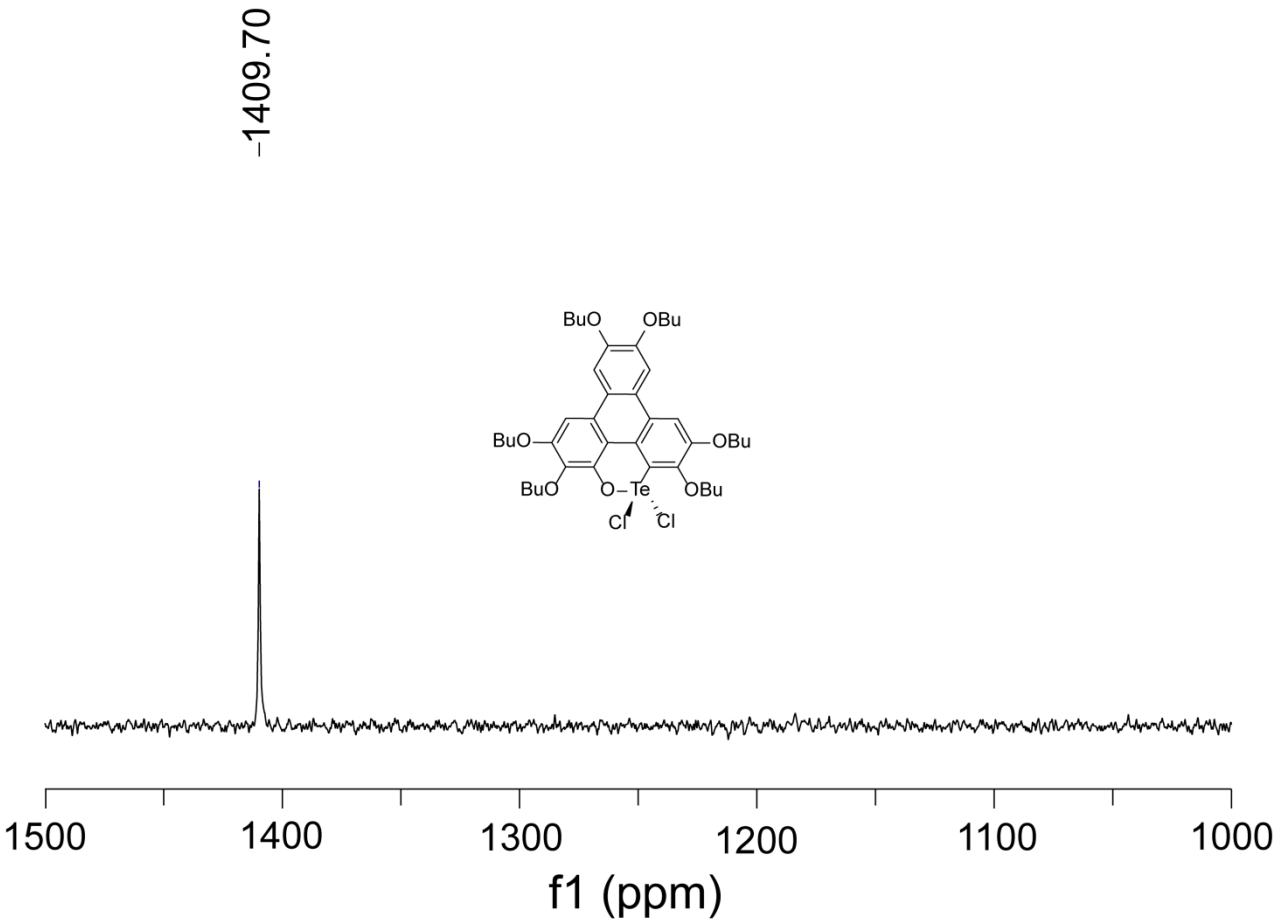
1409.70
BuO
OBu
O–Te
Cl
1500 1400 1300 1200 1100 1000
f1 (ppm)

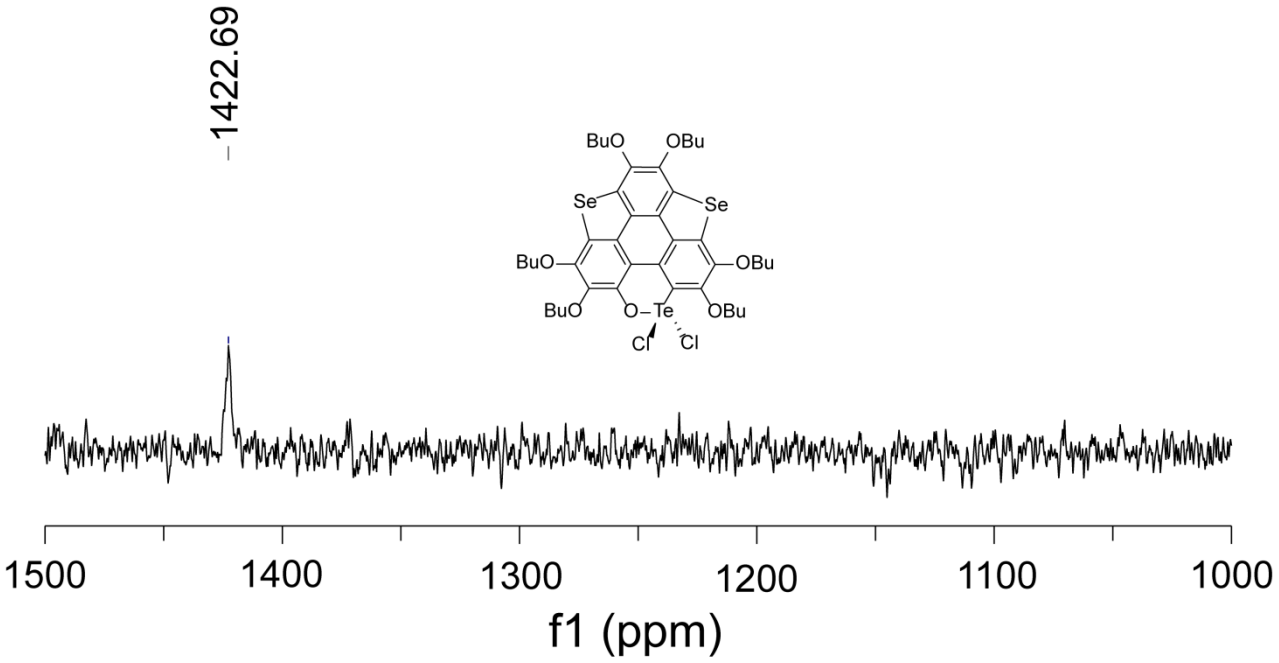
-1422.69
BuO
OBu
Se
Se
BuO
OBu
BuO
O–Te
OBu
Cl
Cl
1500
1400
1300
1200
1100
1000
f1 (ppm)

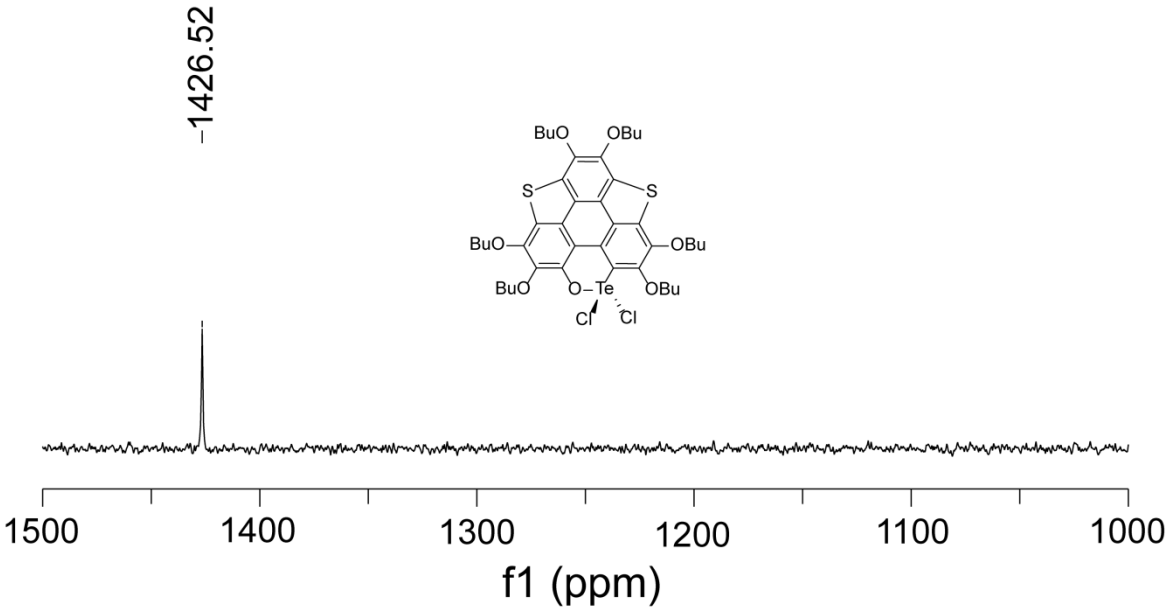
-1426.52
BuO
OBu
S
S
BuO
OBu
BuO
O–Te
OBu
Cl
Cl
1500
1400
1300
1200
1100
1000
f1 (ppm)

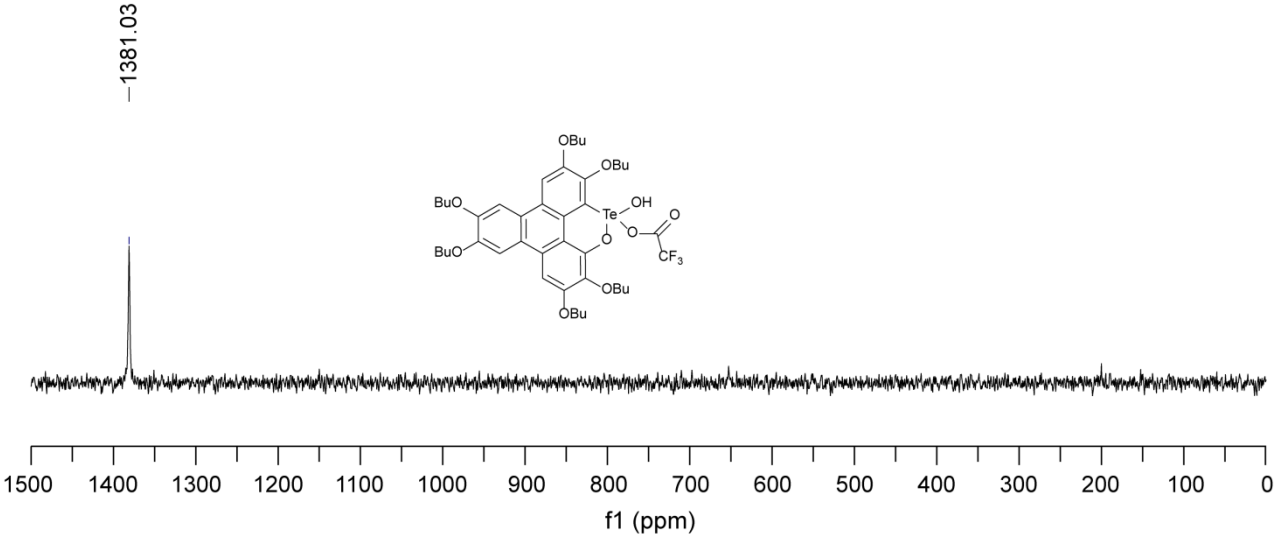
-1381.03
OBu
OBu
BuO
Te
OH
O
BuO
O
O
CF3
OBu
OBu
1500
1400
1300
1200
1100
1000
900
800
700
600
500
400
300
200
100
0
f1 (ppm)

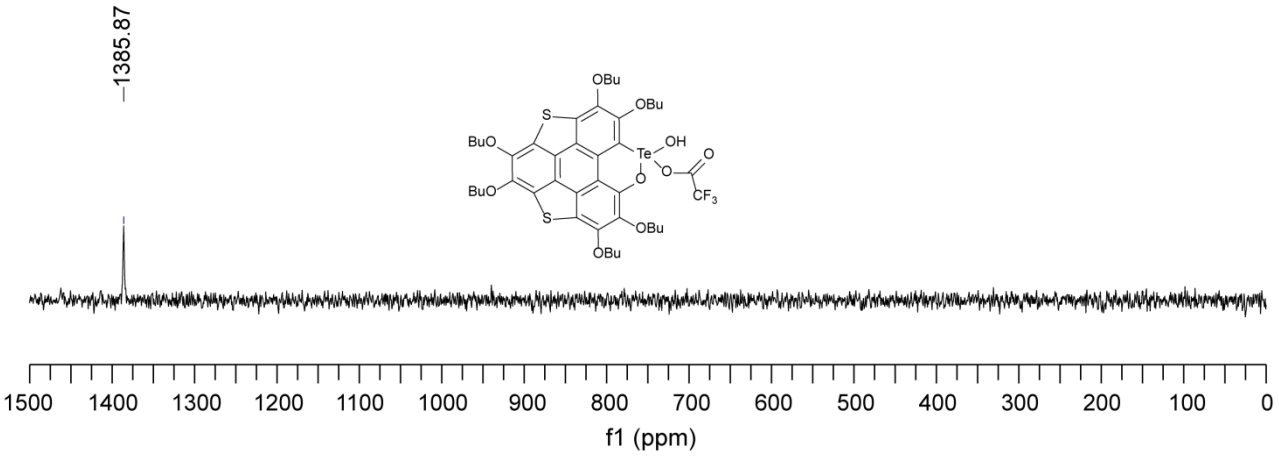
1385.87
OBu
OBu
S
BuO
Te
OH
O
O
BuO
CF3
S
OBu
OBu
1500 1400 1300 1200 1100 1000 900 800 700 600 500 400 300 200 100 0
f1 (ppm)

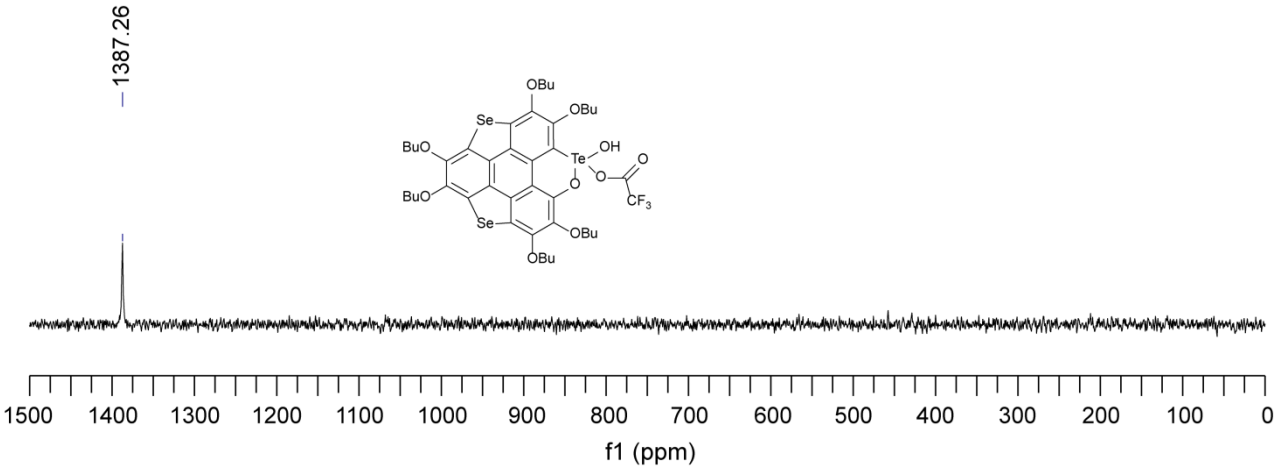
1387.26
OBu
OBu
Se
BuO
Te
OH
O
O
BuO
CF3
Se
OBu
OBu
1500 1400 1300 1200 1100 1000 900 800 700 600 500 400 300 200 100 0
f1 (ppm)

10. ^{1}H NMR, ^{13}C NMR, and IR Spectra of Products

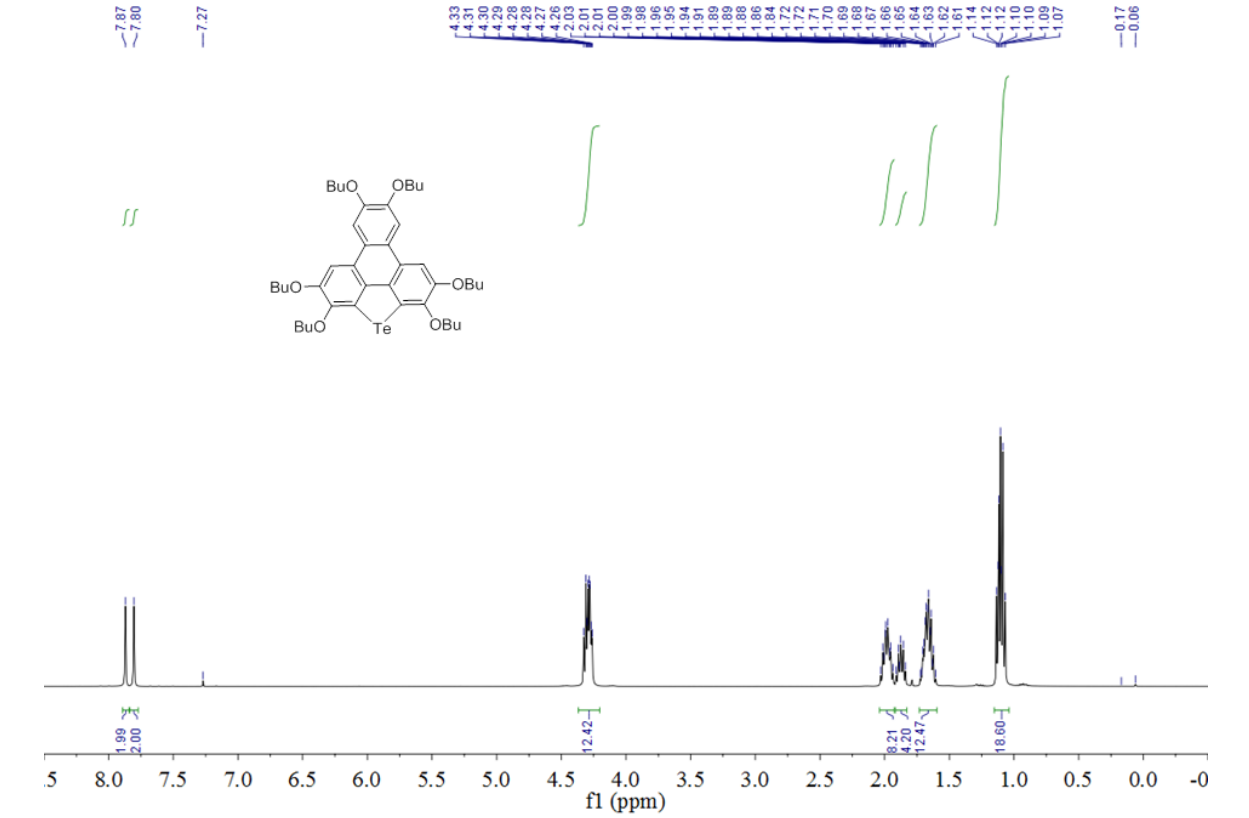

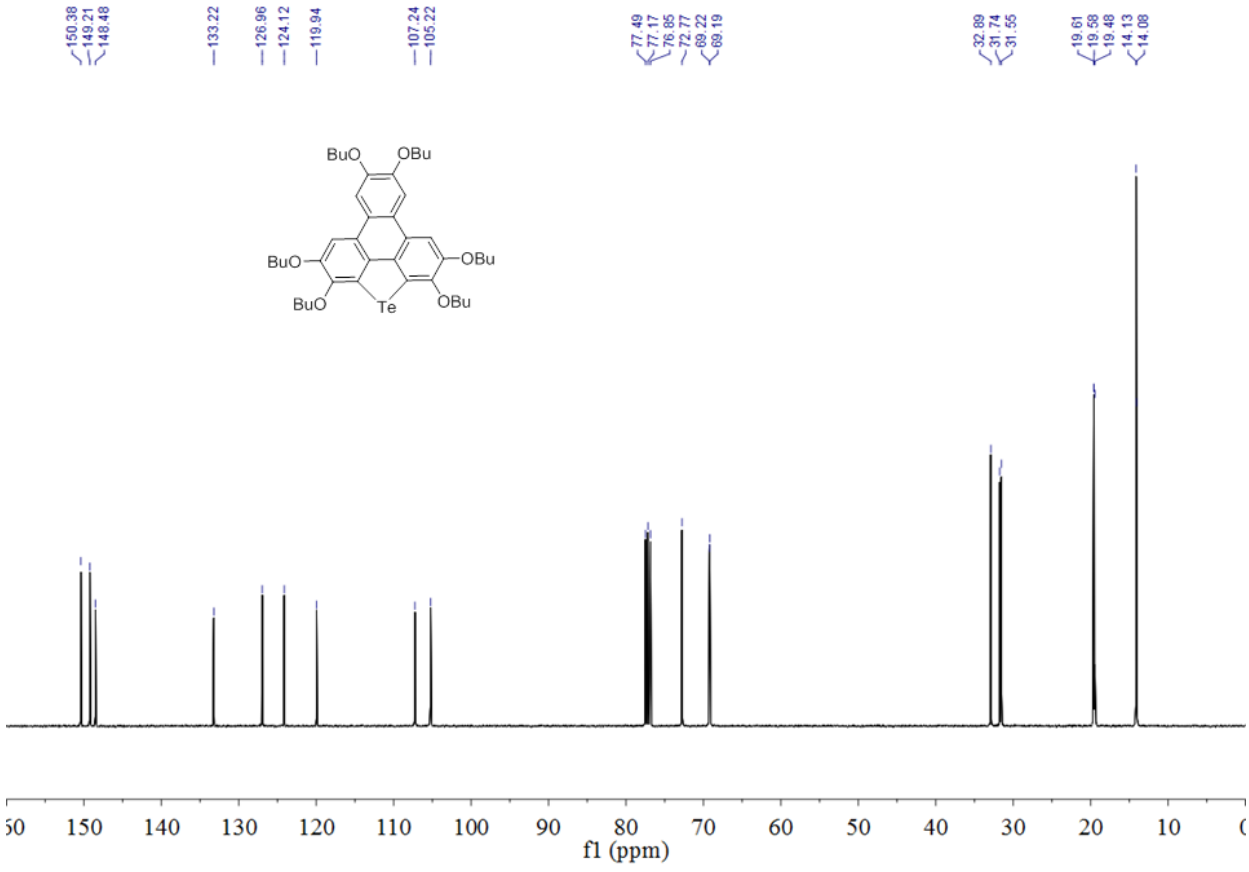

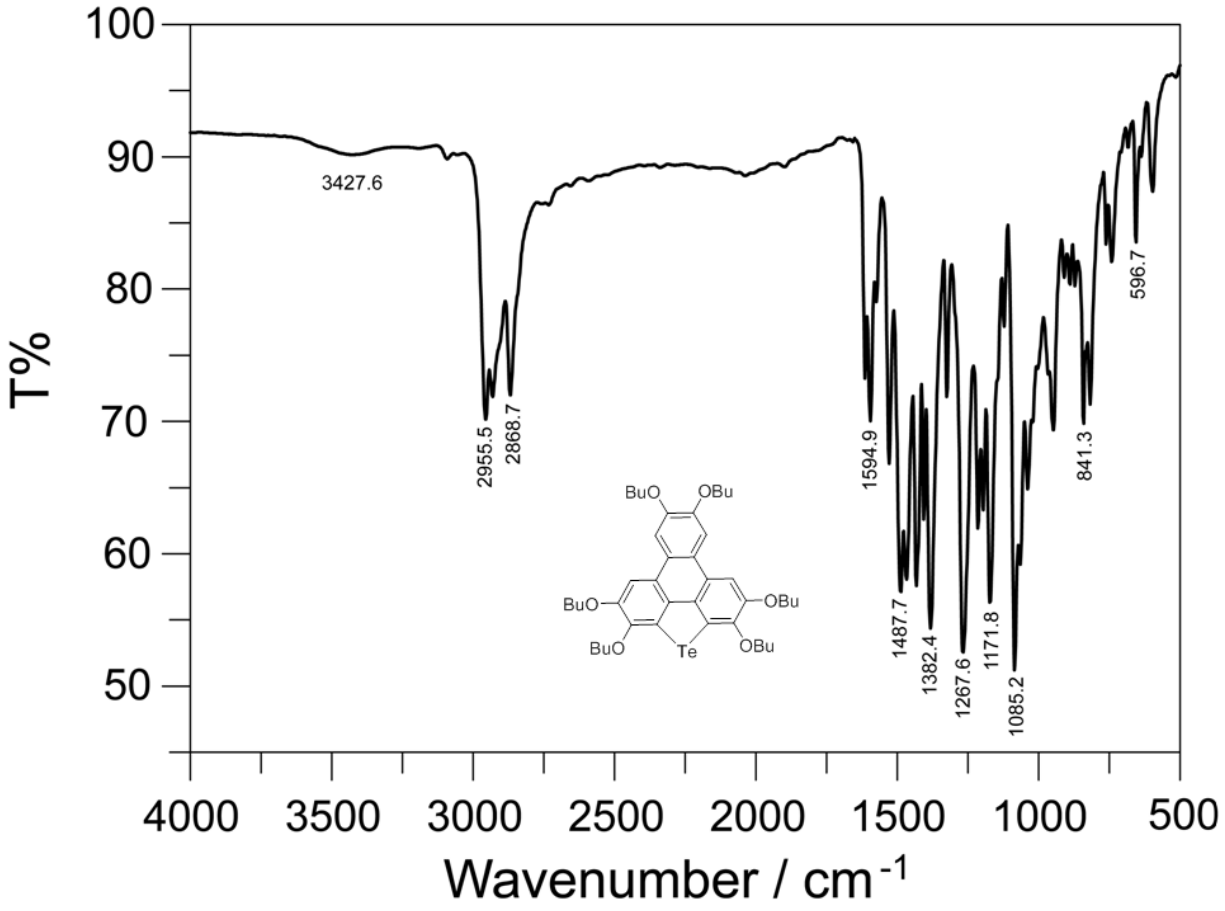
100
90
80
70
60
50
T%
3427.6
2955.5
2868.7
1594.9
1487.7
1382.4
1267.6
1171.8
1085.2
841.3
596.7
BuO
OBu
Te
4000
3500
3000
2500
2000
1500
1000
500
Wavenumber / cm-1

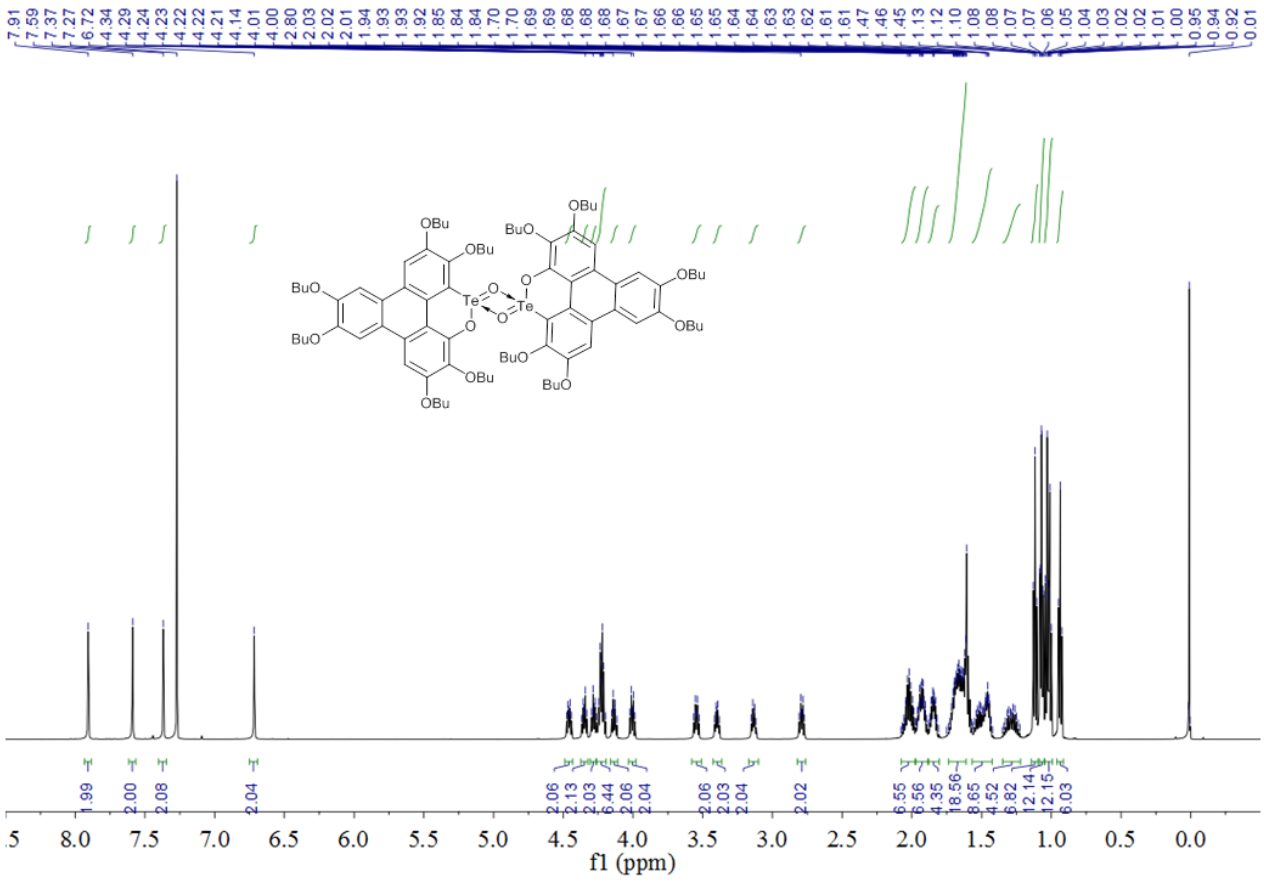
f1 (ppm)

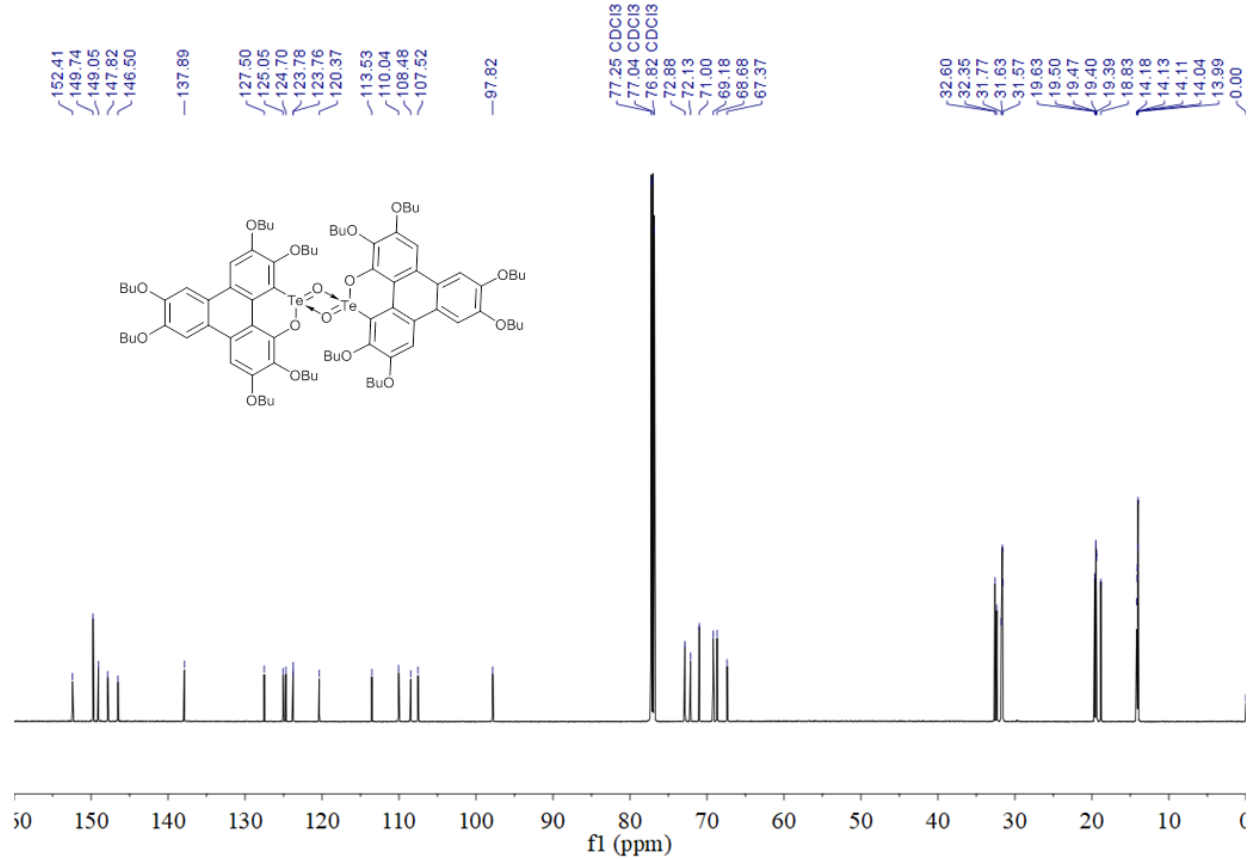
152.41
149.74
149.05
147.82
146.50
137.89
127.50
125.05
124.70
123.78
123.76
120.37
113.53
110.04
108.48
107.52
97.82
77.25 CDCl3
77.04 CDCl3
76.82 CDCl3
72.88
72.13
71.00
69.18
68.68
67.37
32.60
32.35
31.77
31.63
31.57
19.63
19.50
19.47
19.40
19.39
18.83
14.18
14.13
14.11
14.04
13.99
0.00
OBu
BuO
Te
O
f1 (ppm)

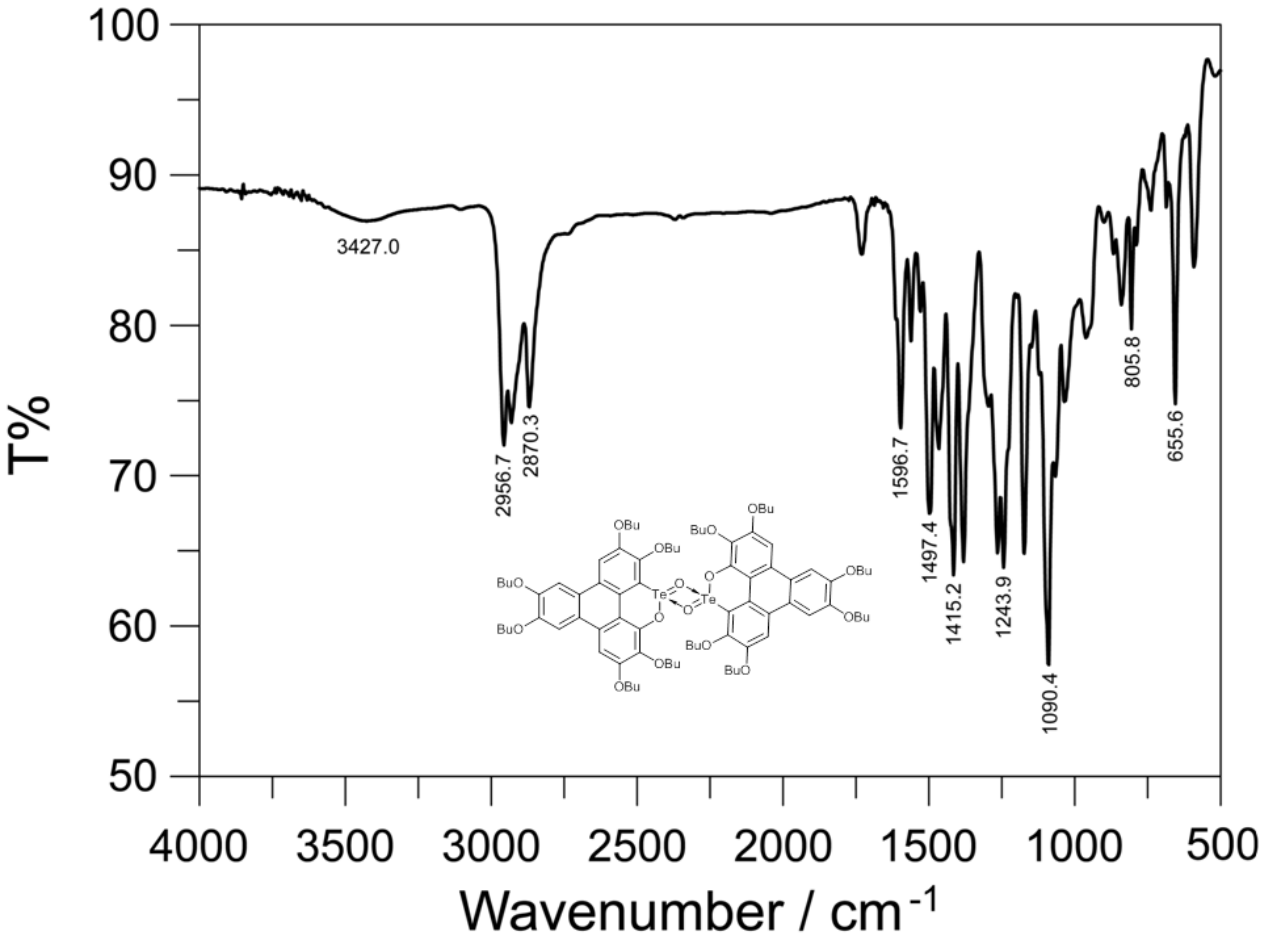
T%
Wavenumber / cm-1
3427.0
2956.7
2870.3
1596.7
1497.4
1415.2
1243.9
1090.4
805.8
655.6
OBu
BuO
Te
O

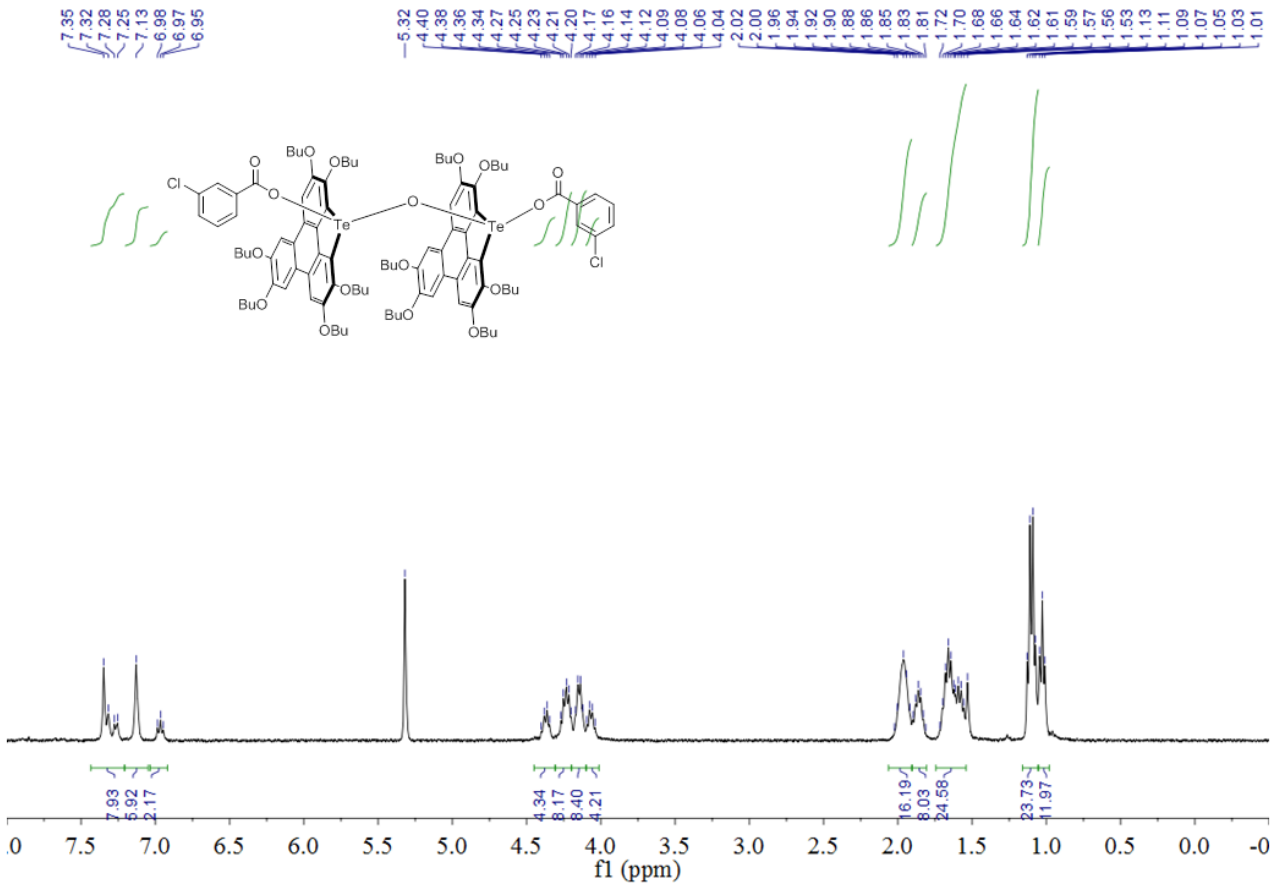
7.35
7.32
7.28
7.25
7.13
6.98
6.97
6.95
5.32
4.40
4.38
4.36
4.34
4.27
4.25
4.23
4.21
4.20
4.17
4.16
4.14
4.12
4.09
4.08
4.06
4.04
2.02
2.00
1.96
1.94
1.92
1.90
1.88
1.86
1.85
1.83
1.81
1.72
1.70
1.68
1.66
1.64
1.62
1.61
1.59
1.57
1.56
1.53
1.13
1.11
1.09
1.07
1.05
1.03
1.01
BuO
OBu
Cl
O
Te
7.93
5.92
2.17
4.34
8.17
8.40
4.21
16.19
8.03
24.58
23.73
11.97
f1 (ppm)

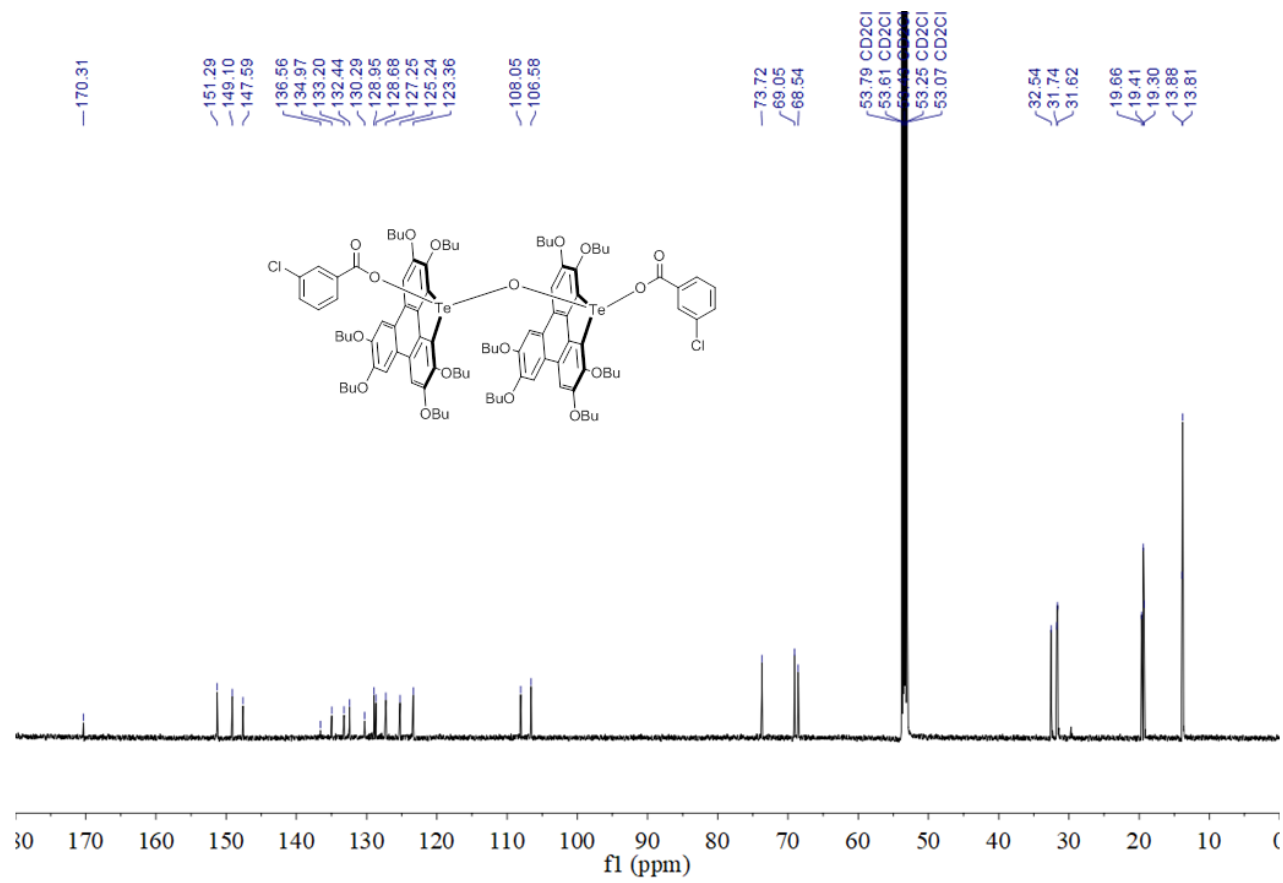
170.31
151.29
149.10
147.59
136.56
134.97
133.20
132.44
130.29
128.95
128.68
127.25
125.24
123.36
108.05
106.58
73.72
69.05
68.54
53.79 CD2Cl
53.61 CD2Cl
53.25 CD2Cl
53.07 CD2Cl
32.54
31.74
31.62
19.66
19.41
19.30
13.88
13.81
BuO
OBu
Cl
O
Te
f1 (ppm)

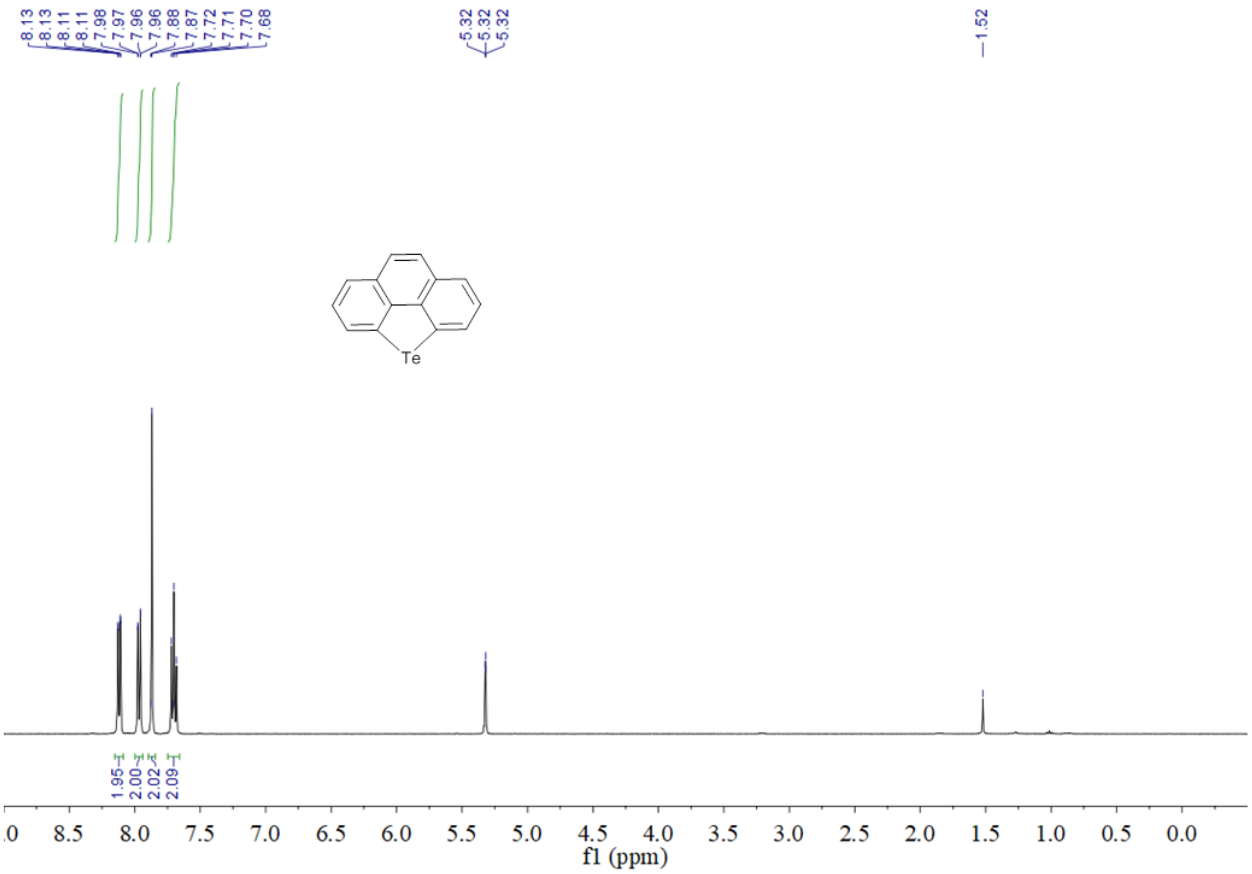
8.13
8.13
8.11
8.11
7.98
7.97
7.96
7.96
7.88
7.87
7.72
7.71
7.70
7.68
5.32
5.32
5.32
1.52
Te
1.95
2.00
2.02
2.09
f1 (ppm)

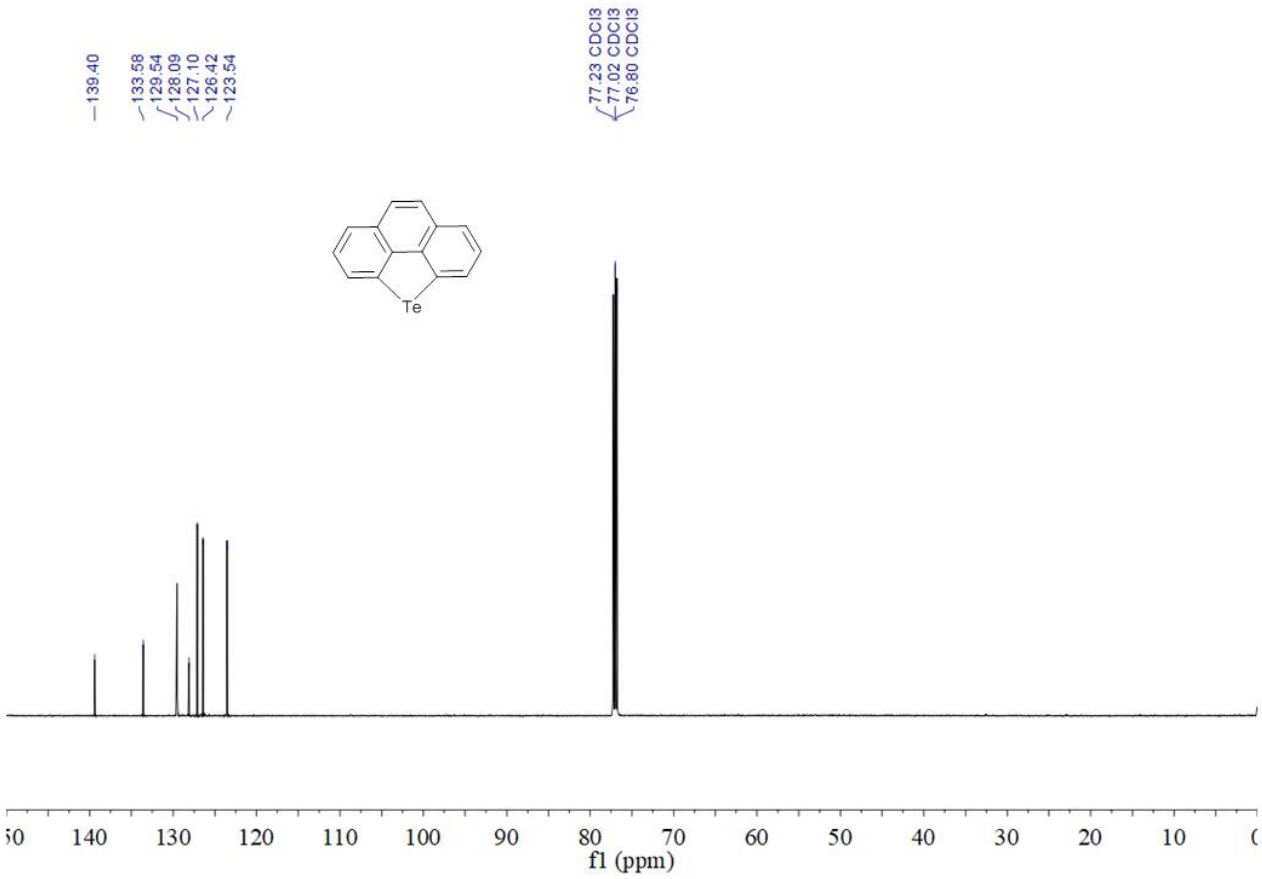
139.40
133.58
129.54
128.09
127.10
126.42
123.54
77.23 CDCl3
77.02 CDCl3
76.80 CDCl3
Te
f1 (ppm)

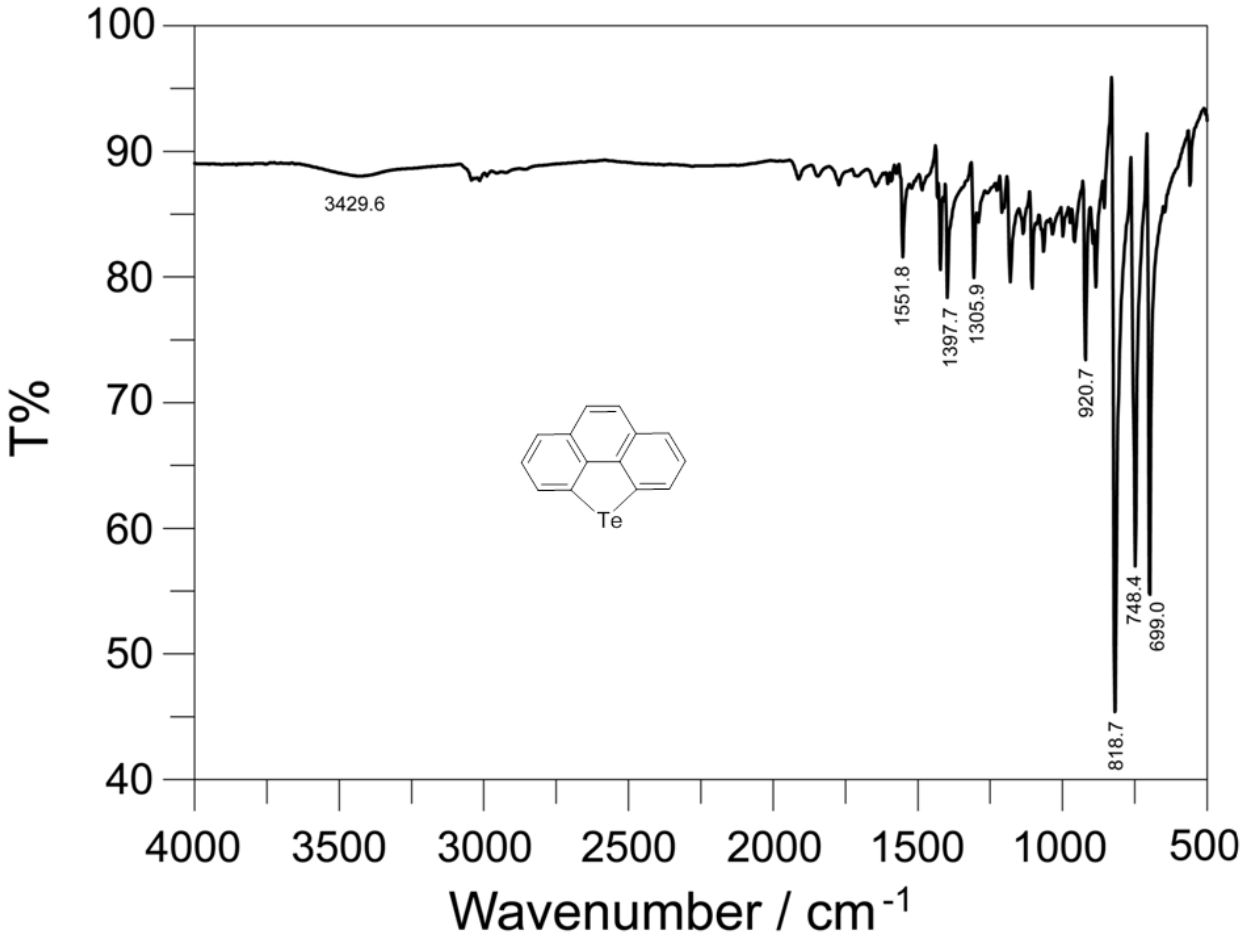
100
90
80
70
60
50
40
T%
3429.6
1551.8
1397.7
1305.9
920.7
818.7
748.4
699.0
Te
4000
3500
3000
2500
2000
1500
1000
500
Wavenumber / cm-1

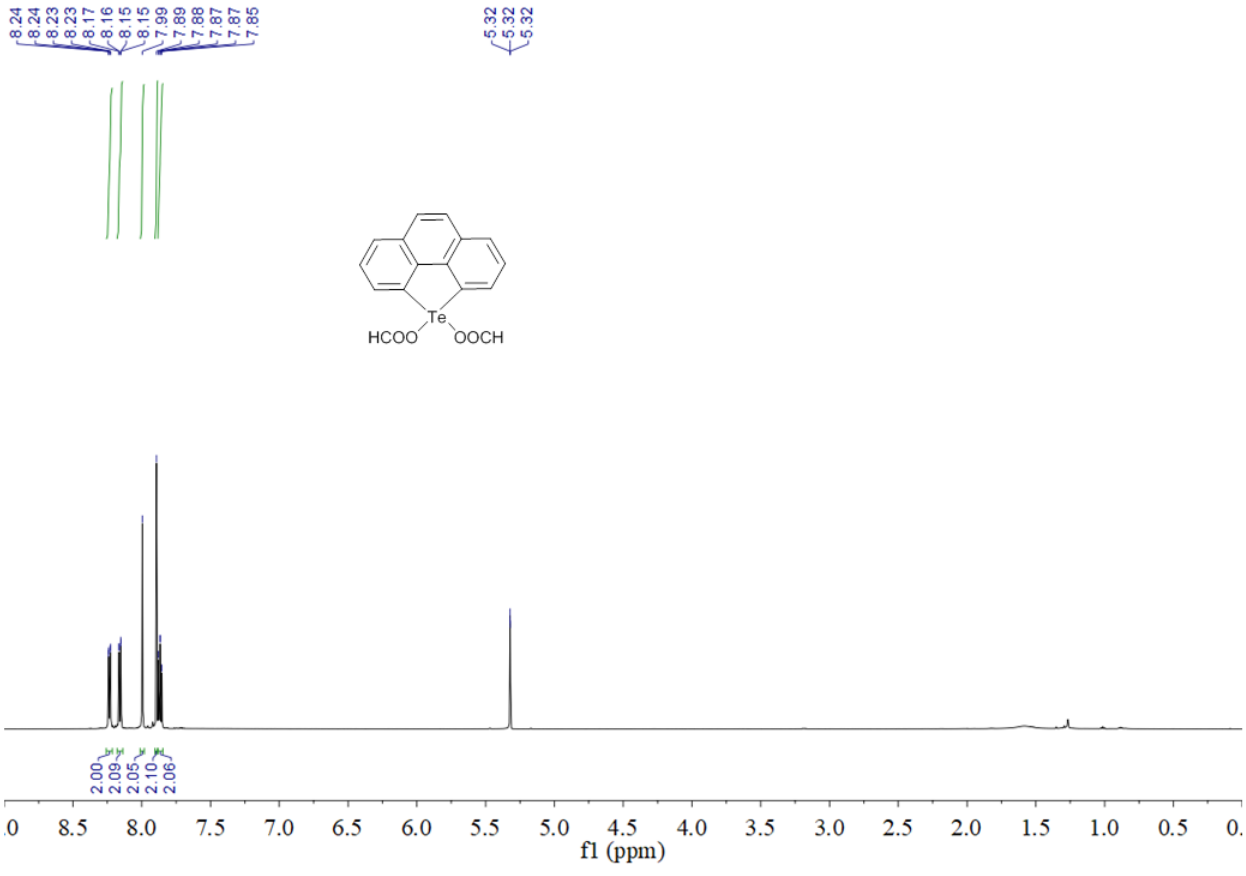
8.24
8.24
8.23
8.23
8.17
8.16
8.15
8.15
7.99
7.89
7.88
7.87
7.87
7.85
5.32
5.32
5.32
Te
HCOO
OOCH
2.00
2.09
2.05
2.10
2.06
f1 (ppm)

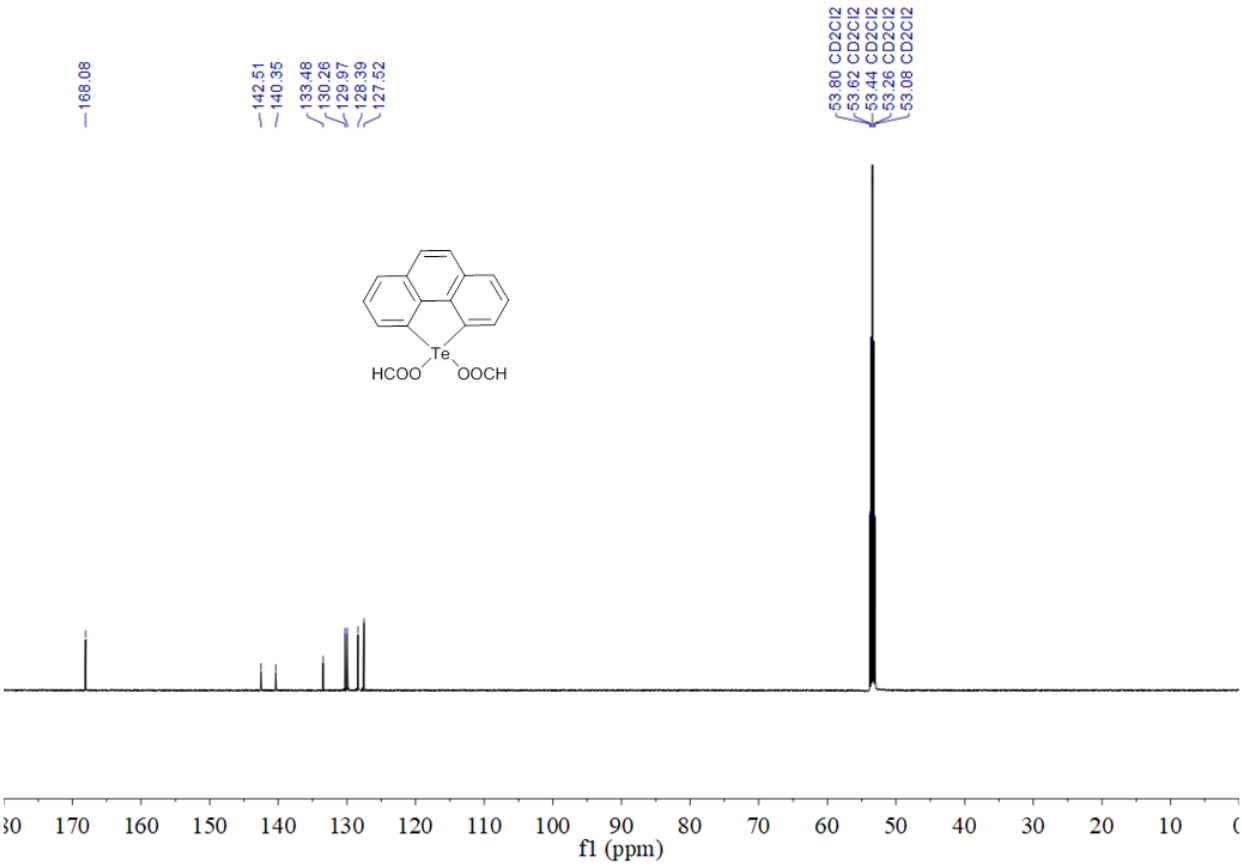
168.08
142.51
140.35
133.48
130.26
129.97
128.39
127.52
53.80 CD2Cl2
53.62 CD2Cl2
53.44 CD2Cl2
53.26 CD2Cl2
53.08 CD2Cl2
Te
HCOO
OOCH
f1 (ppm)

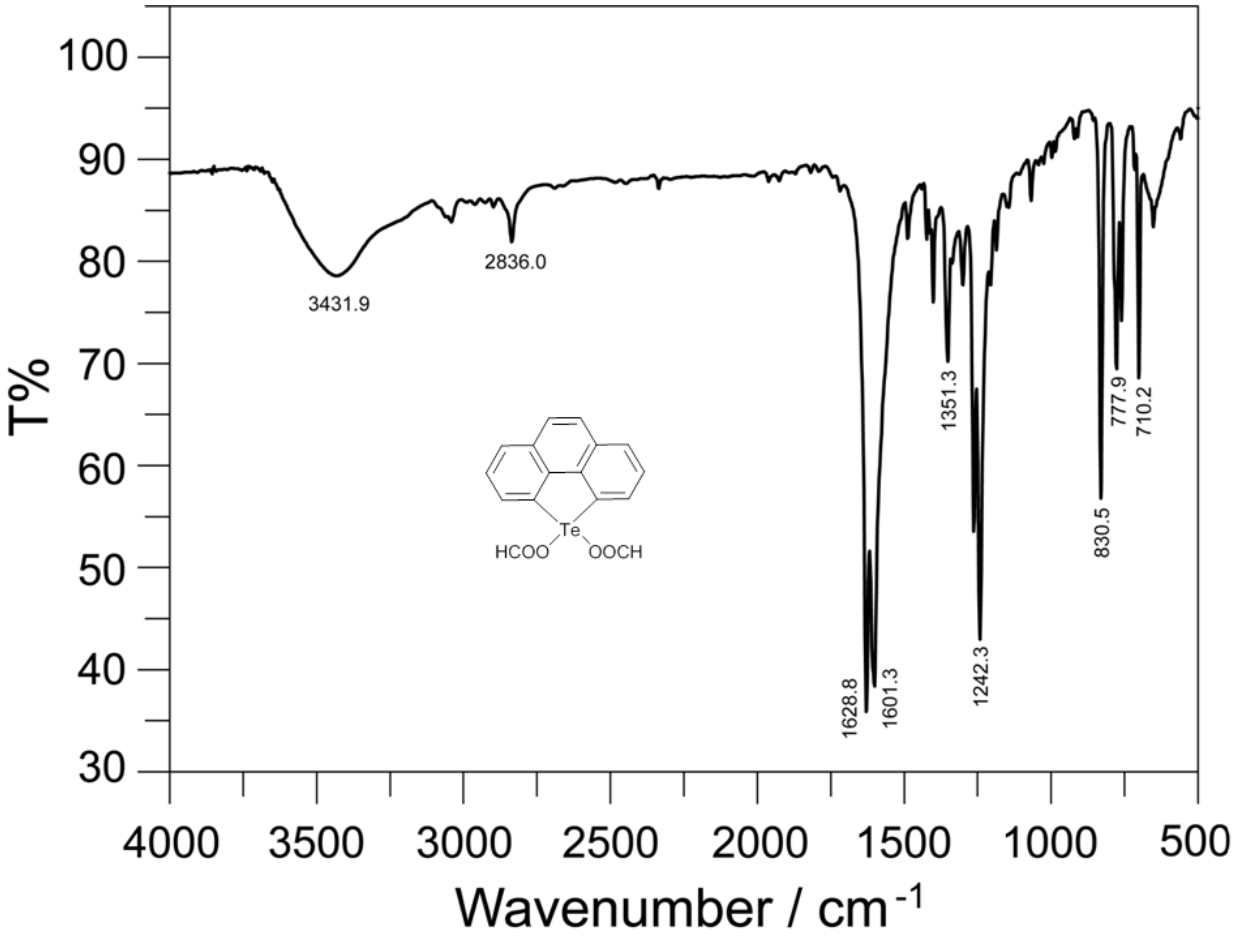
T%
Wavenumber / cm-1
3431.9
2836.0
1628.8
1601.3
1351.3
1242.3
830.5
777.9
710.2
Te
HCOO
OOCH

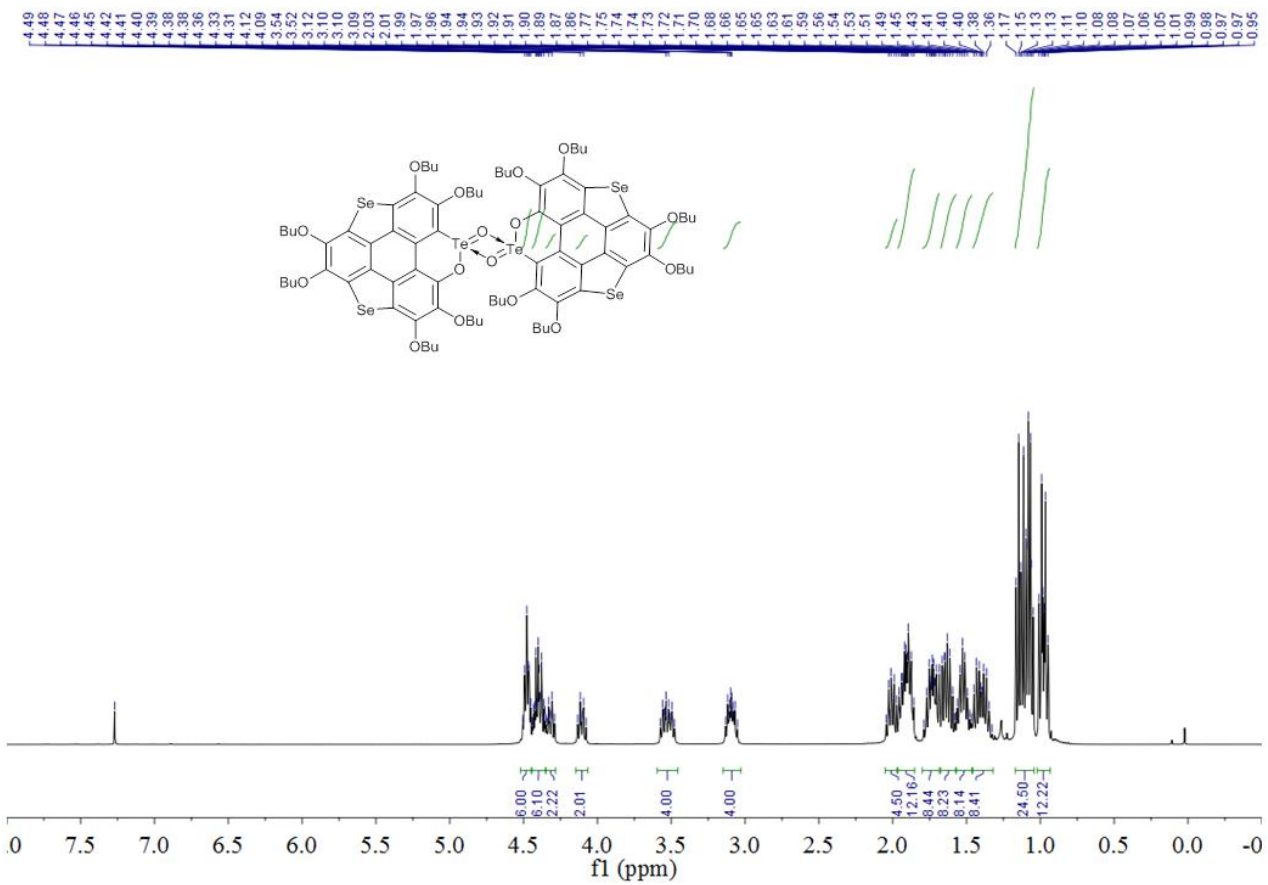
f1 (ppm)

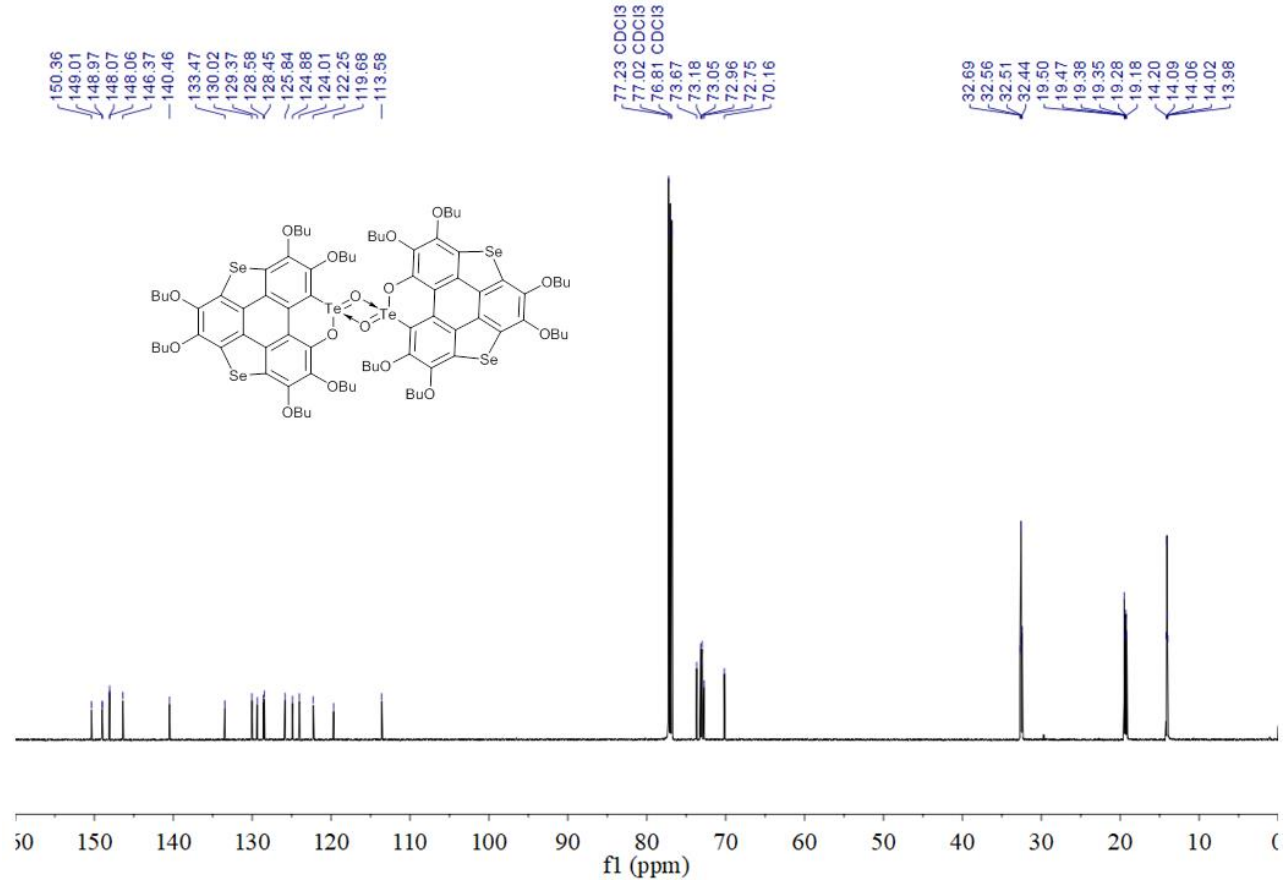
f1 (ppm)

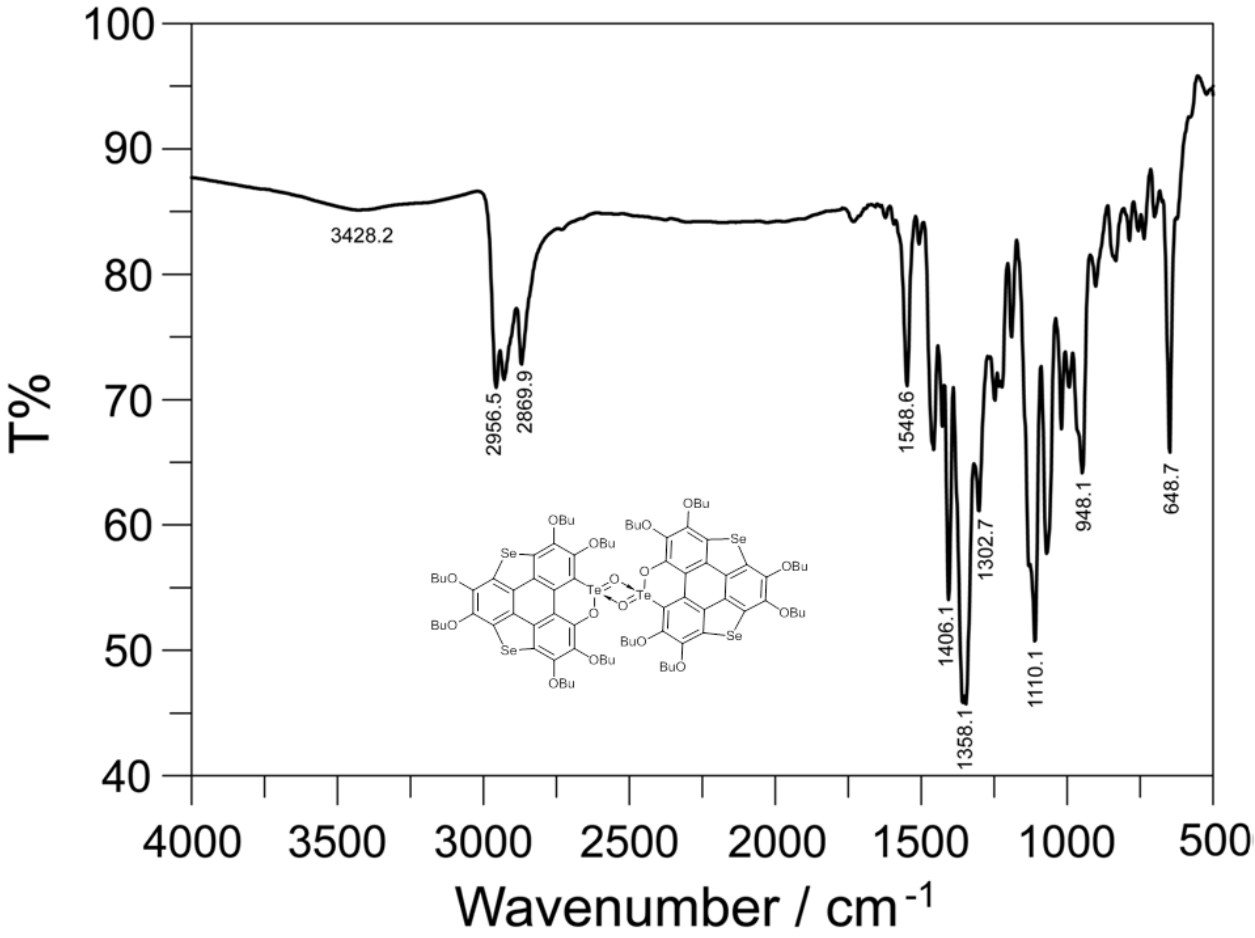
T%
Wavenumber / cm-1
3428.2
2956.5
2869.9
1548.6
1406.1
1358.1
1302.7
1110.1
948.1
648.7

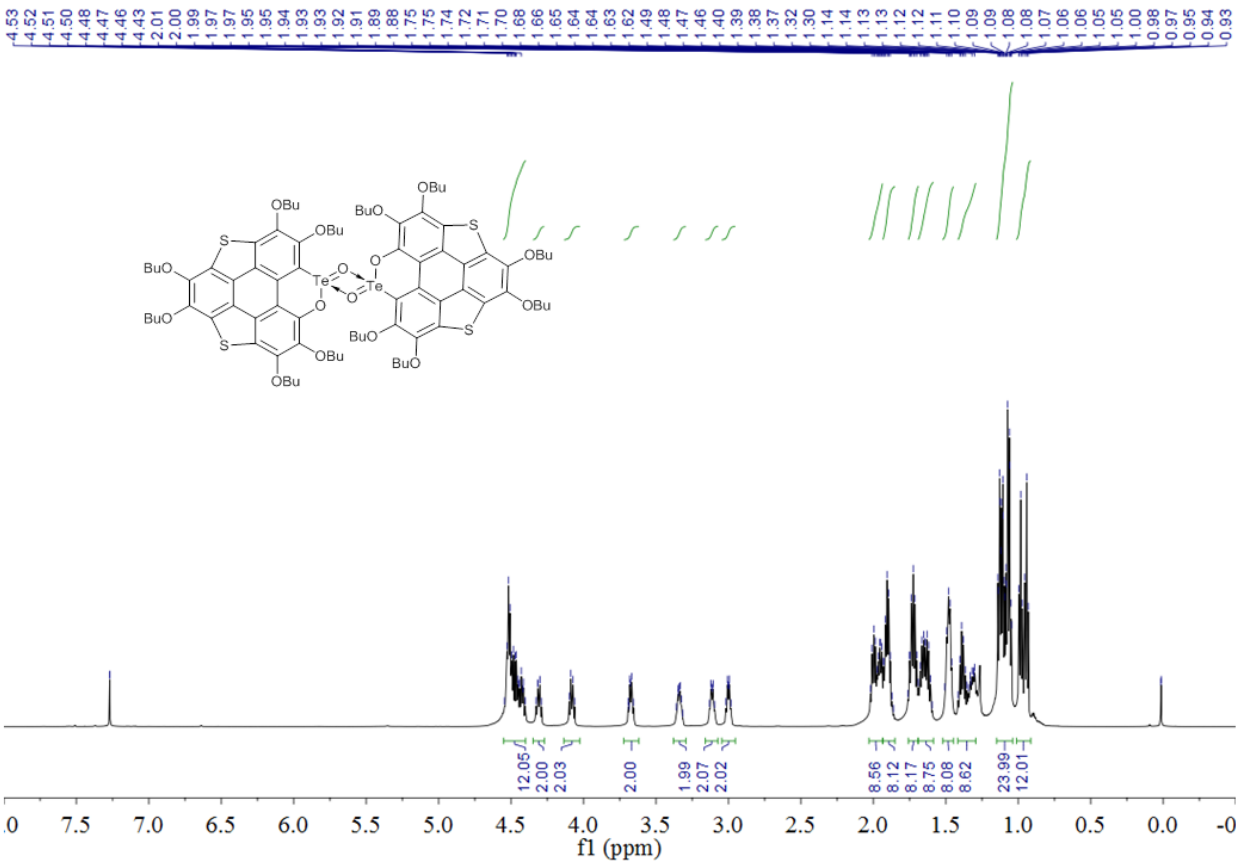
f1 (ppm)

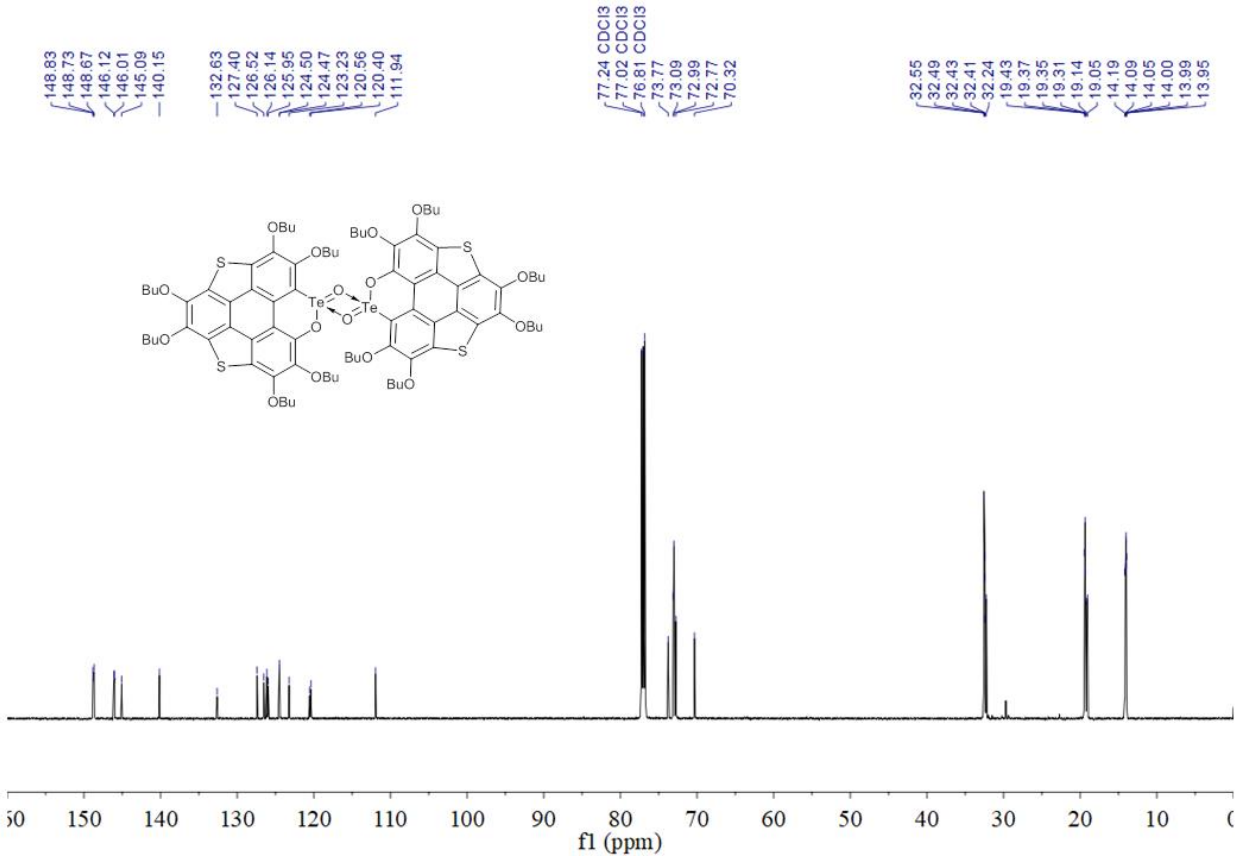
148.83
148.73
148.67
146.12
146.01
145.09
140.15
132.63
127.40
126.52
126.14
125.95
124.50
124.47
123.23
120.56
120.40
111.94
77.24 CDCl3
77.02 CDCl3
76.81 CDCl3
73.77
73.09
72.99
72.77
70.32
32.55
32.49
32.43
32.41
32.24
19.43
19.37
19.35
19.31
19.14
19.05
14.19
14.09
14.05
14.00
13.99
13.95
OBu
BuO
S
O
Te
f1 (ppm)

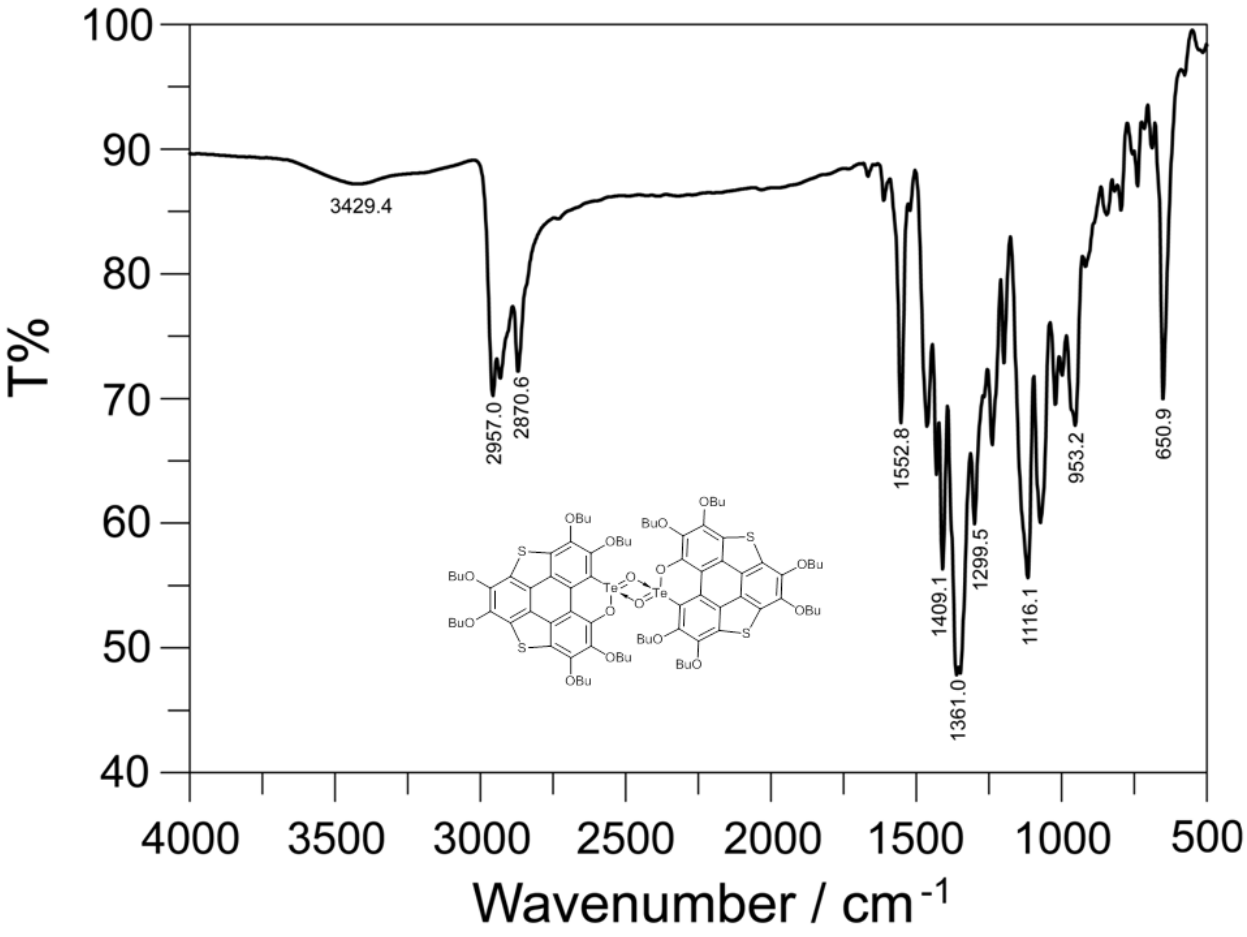
T%
3429.4
2957.0
2870.6
1552.8
1409.1
1361.0
1299.5
1116.1
953.2
650.9
Wavenumber / cm-1

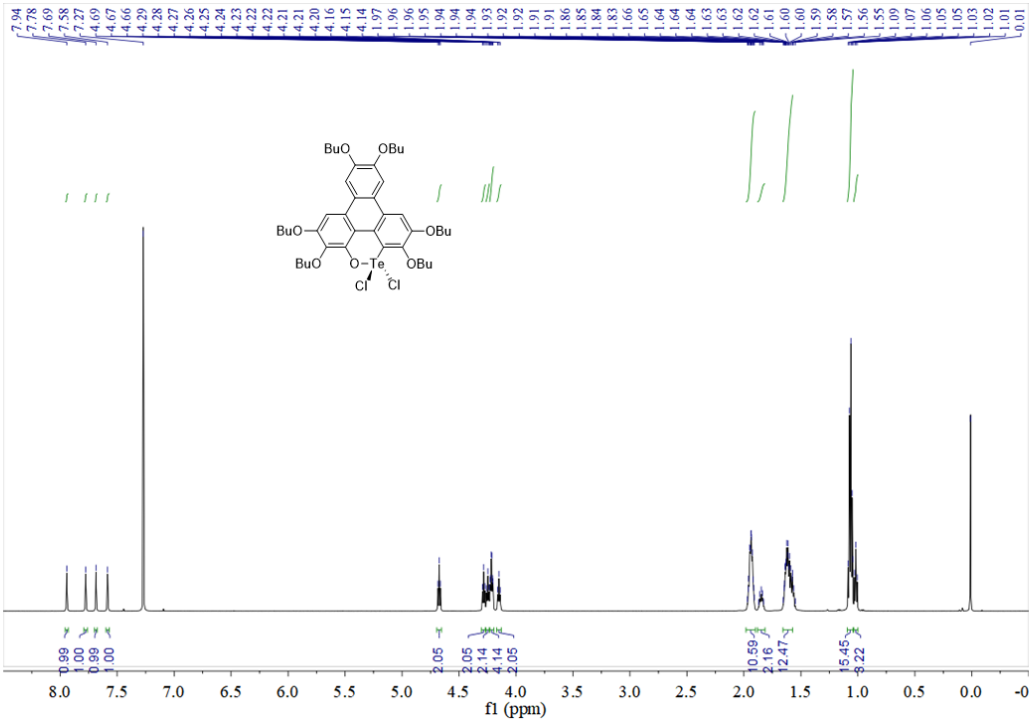
BuO
OBu
BuO
OBu
BuO
OBu
O
Te
Cl
Cl
f1 (ppm)

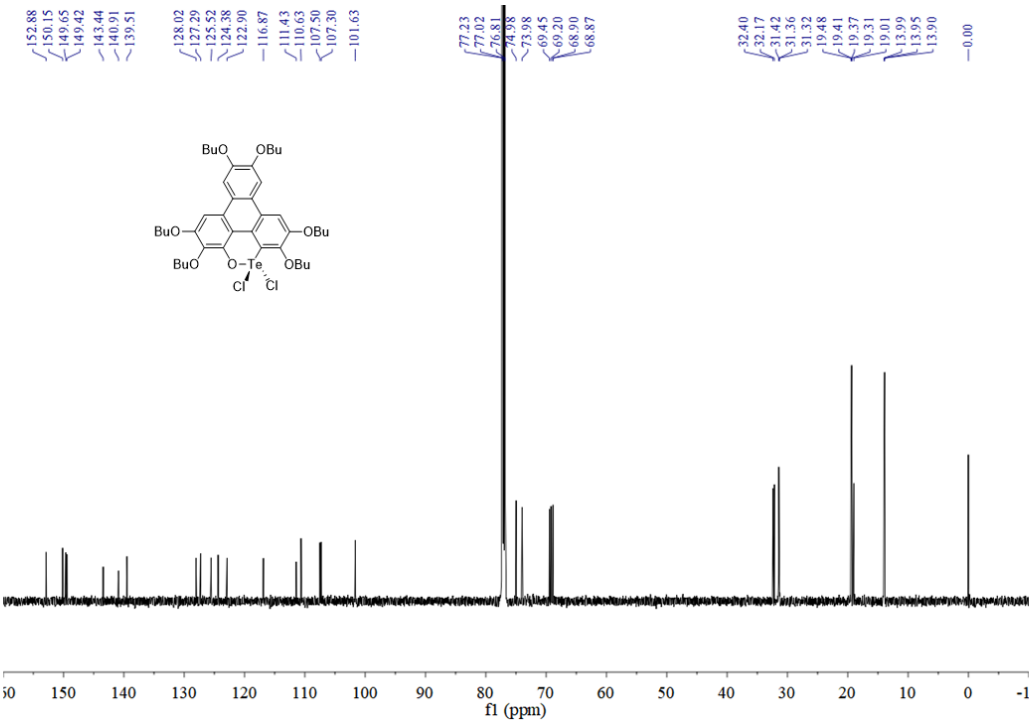
BuO
OBu
BuO
OBu
BuO
OBu
O
Te
Cl
Cl
f1 (ppm)

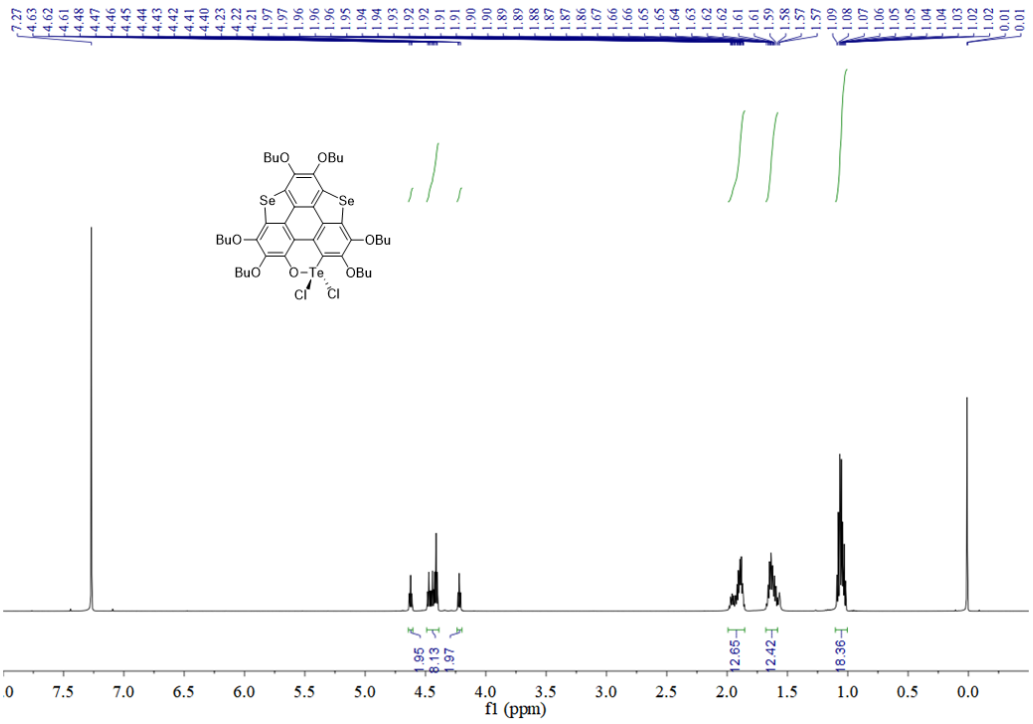
BuO
OBu
Se
Se
BuO
OBu
BuO
O–Te
OBu
Cl
Cl
1.95
6.13
1.97
12.65
12.42
18.36
f1 (ppm)

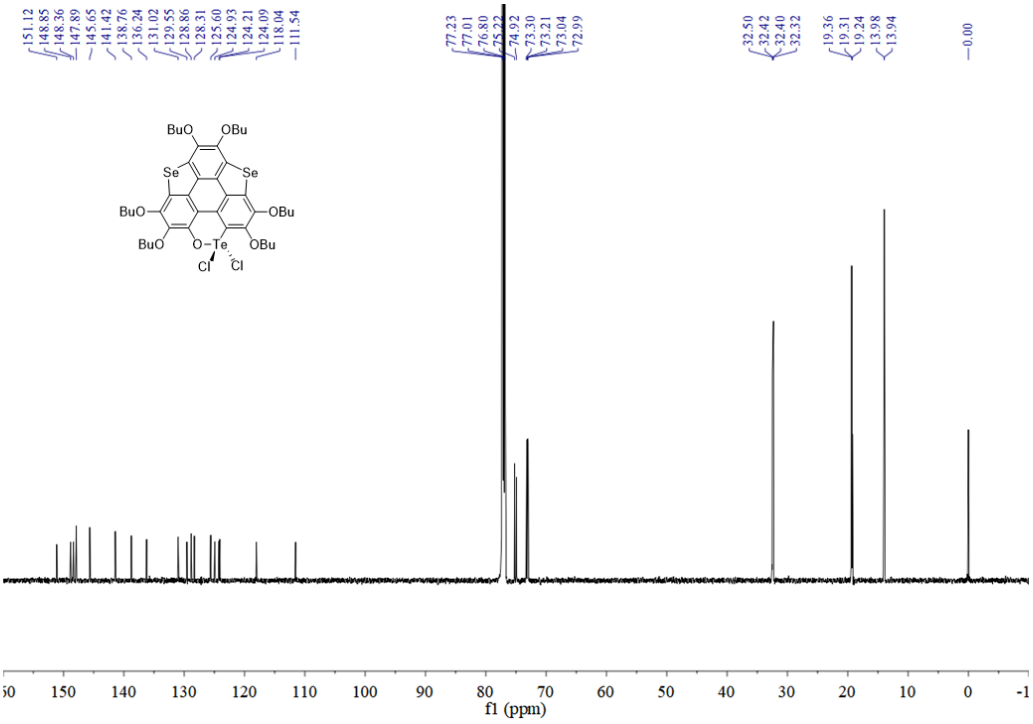
151.12
148.85
148.36
147.89
145.65
141.42
138.76
136.24
131.02
129.55
128.86
128.31
125.60
124.93
124.21
124.09
118.04
111.54
77.23
77.01
76.80
75.22
74.92
73.30
73.21
73.04
72.99
32.50
32.42
32.40
32.32
19.36
19.31
19.24
13.98
13.94
0.00
BuO
OBu
Se
Se
BuO
OBu
BuO
O–Te
OBu
Cl
Cl
f1 (ppm)

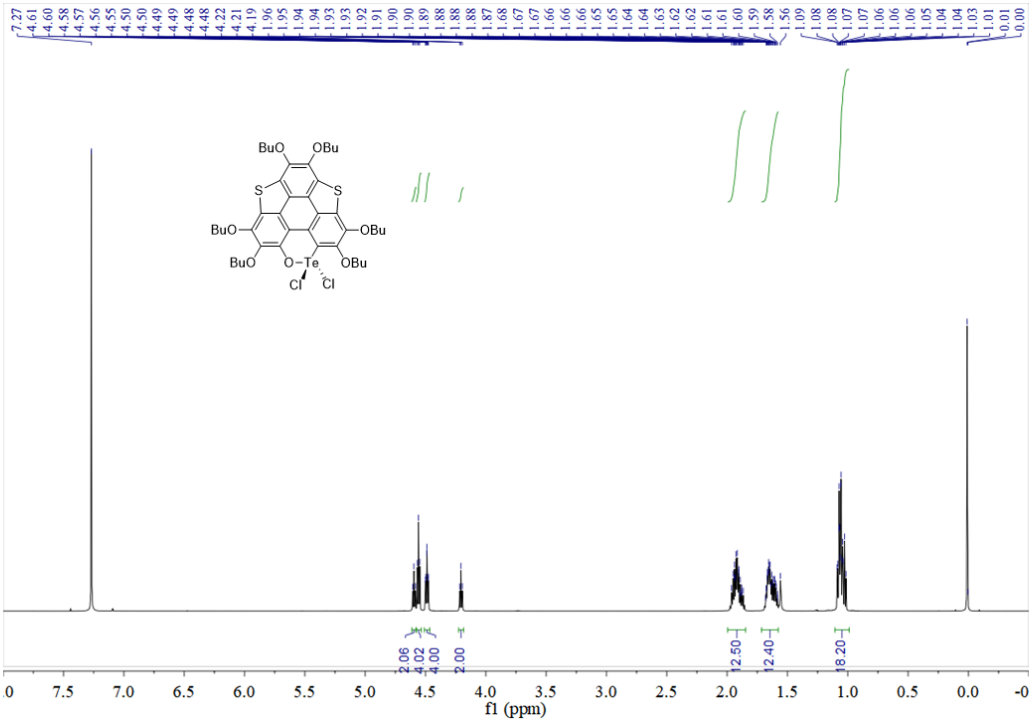
BuO
OBu
S
S
BuO
OBu
BuO
O–Te
OBu
Cl
Cl
2.06
4.02
4.00
2.00
12.50
12.40
18.20
f1 (ppm)

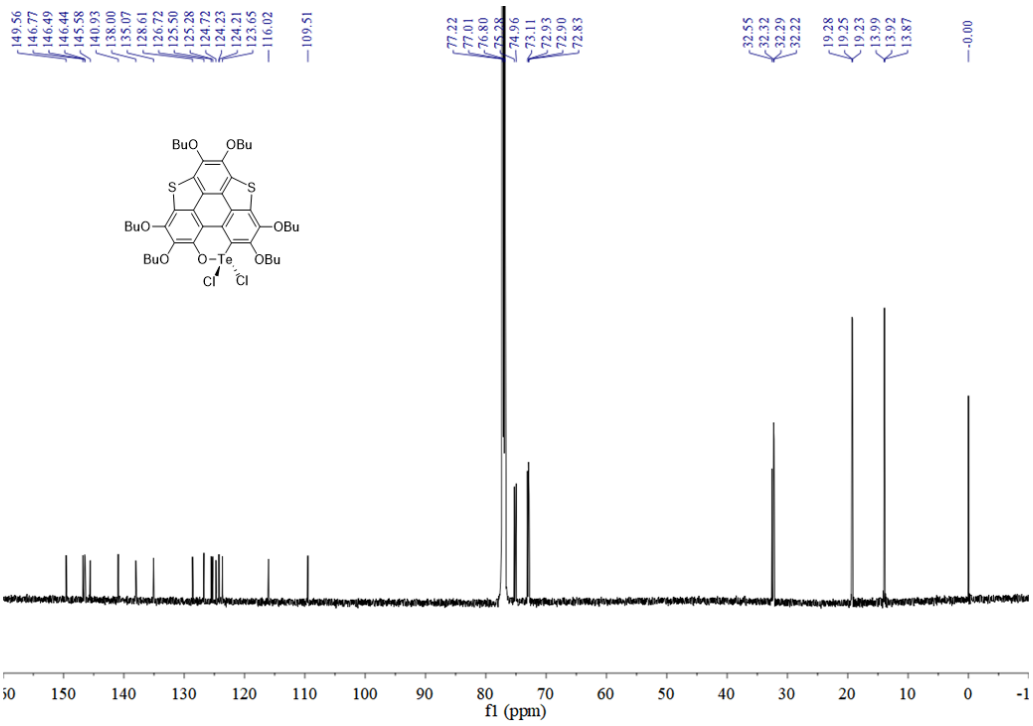
BuO
OBu
S
S
BuO
OBu
BuO
O–Te
OBu
Cl
Cl
f1 (ppm)

11. Cartesian Coordinates

1’

C	3.31254200	-1.34731400	-0.01163000
C	2.06704000	-0.68120200	-0.03155200
C	2.04891000	0.73751100	-0.09371500
C	3.28359500	1.42019000	-0.11677600
C	4.49574100	0.76232100	-0.09516500
C	4.51524800	-0.65862500	-0.04965100
C	0.81639200	-1.43671100	0.00838600
C	-0.40480700	-0.73061900	0.00298500
C	-0.40788200	0.70241900	-0.07695000
C	0.78020900	1.45691500	-0.12752900
C	0.74708900	-2.84019200	0.04319700
C	-0.46658000	-3.50346900	0.09574300
C	-1.69955400	-2.79209700	0.12209000
C	-1.65860000	-1.39882900	0.06230100
C	-1.65567500	1.35442900	-0.10448900
C	-1.76625100	2.72911900	-0.18668000
C	-0.57044200	3.49350000	-0.25291700
C	0.67122500	2.85966100	-0.21600500
Te	-3.25515300	0.00979500	-0.02667300
O	5.72995200	-1.23364100	-0.06247800
C	5.82048000	-2.63791400	-0.01701600
O	5.64592800	1.47757000	-0.17116600
C	6.46691000	1.46796900	0.98220800
O	-0.46828800	-4.85926500	0.18048600
C	-0.90360500	-5.55163800	-0.97410500
O	-2.79297500	-3.57742900	0.18425000
C	-3.98883400	-3.12277900	0.77066400
O	-2.99632900	3.29892600	-0.25429700

C	-3.37563500	4.10759900	0.84780100
O	-0.73995200	4.82365300	-0.36588000
C	0.39353500	5.65520100	-0.43886800
H	3.33238300	-2.43508300	0.02458500
H	3.32296400	2.50970800	-0.15763600
H	1.64189600	-3.46359800	0.04326600
H	1.57265600	3.46739800	-0.27025000
H	6.89060200	-2.88203800	-0.03487400
H	5.37580000	-3.04653300	0.90686800
H	5.33280600	-3.10629500	-0.88929600
H	7.32911800	2.11386000	0.76538200
H	5.92798200	1.87597000	1.85592500
H	6.82959300	0.45599800	1.22205200
H	-0.82307600	-6.62531100	-0.75341500
H	-1.95033200	-5.31609200	-1.22474000
H	-0.26246500	-5.31813900	-1.84301300
H	-4.58480700	-4.01796200	0.99723200
H	-3.80155100	-2.57720100	1.70995200
H	-4.58240600	-2.49800000	0.07974800
H	-4.41711100	4.41131500	0.67394700
H	-3.32224200	3.53919900	1.79267700
H	-2.74622900	5.00722800	0.92777000
H	0.01977300	6.68412100	-0.52137500
H	1.01978000	5.57374700	0.46635300
H	1.00981600	5.42718000	-1.32547000

7’

C	-2.82998600	-1.47081000	0.08074600
C	-1.67209800	-0.69848800	0.05599800
C	-1.66918200	0.67745800	0.07995500
C	-2.83347900	1.42590400	0.12004700
C	-4.03939100	0.70778400	0.14953100
C	-4.04463500	-0.73988100	0.13303200
C	-0.44933200	-1.38542300	-0.00632200
C	0.77191600	-0.71703900	-0.04851700
C	0.75544400	0.71208900	-0.02322800
C	-0.46049400	1.38912700	0.03988000
C	-0.57811500	-2.76872200	-0.03062800
C	0.60035300	-3.51563700	-0.10558500
C	1.87657200	-2.84216300	-0.15671300
C	1.97704600	-1.43082900	-0.12665800
C	1.93973000	1.44438100	-0.07299700
C	1.85451300	2.84049600	-0.06392600
C	0.58718400	3.52808200	-0.01025900
C	-0.60970000	2.77901800	0.04707400
Te	3.55130200	0.06083200	-0.18165000
S	-2.30764800	-3.20446900	0.02607900
S	-2.38533300	3.15050100	0.11771400
O	-5.27992800	-1.26300500	0.17676200
C	-5.44011900	-2.66228400	0.12462100
O	-5.22434100	1.36047300	0.22333800
C	-5.95950400	1.42916900	-0.98735400
O	0.55627600	-4.86722500	-0.17222600
C	0.91245700	-5.55319200	1.01666900
O	2.90313900	-3.70669100	-0.24236300
C	4.22522500	-3.24099600	-0.35620600

O	2.98925200	3.58175100	-0.15187400
C	3.41446000	4.19297600	1.05414300
O	0.69757100	4.86449900	-0.03042700
C	-0.46462100	5.66206200	-0.01236500
H	-6.52013800	-2.85523100	0.16420100
H	-5.04372500	-3.08104800	-0.81575300
H	-4.96590600	-3.15635000	0.98931800
H	-6.86956800	2.00762800	-0.77661400
H	-5.38151300	1.94459700	-1.77434500
H	-6.24662100	0.42722300	-1.34487200
H	0.79333400	-6.62642100	0.81370500
H	1.95819400	-5.35558700	1.30125400
H	0.24788600	-5.27088300	1.85194300
H	4.86392300	-4.13204300	-0.41953500
H	4.36972300	-2.64624500	-1.27411300
H	4.53308200	-2.66129600	0.53124800
H	4.35400500	4.71816300	0.83293300
H	2.67534600	4.92218600	1.42296700
H	3.60230000	3.43796200	1.83773700
H	-0.12697200	6.70623500	-0.04199200
H	-1.09716400	5.47430700	-0.89585200
H	-1.04741500	5.51013000	0.91158900

8’

C	-2.62149600	-1.44427200	0.10902100
C	-1.43763300	-0.69606200	0.09742500
C	-1.42653800	0.69122400	0.09430100
C	-2.60795200	1.42434300	0.09831900
C	-3.81644100	0.72439400	0.10899900
C	-3.83266600	-0.71599400	0.11843500
C	-0.20585600	-1.39377700	0.09566900
C	1.01818900	-0.72043500	0.08875100
C	1.00680600	0.70985800	0.08859800
C	-0.20497000	1.40564600	0.08935600
C	-0.28545700	-2.78408000	0.10225000
C	0.89981700	-3.51611300	0.10154800
C	2.16713800	-2.83629000	0.09718500
C	2.23531700	-1.42642500	0.08948800
C	2.20765300	1.42082500	0.08965800
C	2.16710800	2.81436800	0.09256900
C	0.91786800	3.52604900	0.09786400
C	-0.29493900	2.80612300	0.09317900
Te	3.81634500	0.04513800	0.11020400
Se	-2.11839500	-3.32259400	0.12316600
Se	-2.18182600	3.28531300	0.10378600
O	-5.07418800	-1.22777300	0.14749000
C	-5.26575900	-2.62233600	0.10119500
O	-4.99146800	1.40052100	0.14880100
C	-5.71608800	1.43941400	-1.06893900
O	0.86134300	-4.87081400	0.14389400
C	1.17492800	-5.53288100	-1.06977400
O	3.20862100	-3.68797100	0.11808100
C	4.52699600	-3.22170500	-0.03154400

O	3.32820000	3.51849600	0.13215000
C	3.70984500	4.13846300	-1.08391800
O	1.06490000	4.86035800	0.11673600
C	-0.06497200	5.70150500	0.10359800
H	-6.35115100	-2.78774200	0.10950400
H	-4.85250400	-3.05893500	-0.82365200
H	-4.83243500	-3.12157500	0.98421300
H	-6.61165600	2.04997900	-0.88866700
H	-5.11941300	1.90749600	-1.87143800
H	-6.02782000	0.43206400	-1.38831400
H	1.05342600	-6.60946400	-0.88664700
H	0.48729300	-5.22762700	-1.87785800
H	2.21295400	-5.33740500	-1.38258500
H	5.17009500	-4.11174600	-0.05262100
H	4.66208100	-2.67317000	-0.97903600
H	4.84045200	-2.59864200	0.82386200
H	4.67986400	4.62294800	-0.90540100
H	3.82538100	3.39353200	-1.89080900
H	2.98051500	4.90256900	-1.39687900
H	0.31420300	6.73182300	0.11388300
H	-0.66667400	5.56009300	-0.80991200
H	-0.69164100	5.55262400	0.99877200

mono-**2'**

C	-3.66577100	0.78381000	0.14594700
C	-2.31244100	0.37676000	0.04303800
C	-2.03454400	-1.00031200	-0.08765800
C	-3.11653200	-1.91262200	-0.14787200
C	-4.43208200	-1.50286300	-0.06119900
C	-4.71388300	-0.11440300	0.09979600
C	-1.22716000	1.35537200	0.03386100
C	0.11712300	0.91272100	-0.09170600
C	0.40542700	-0.51248200	-0.09464500
C	-0.65221100	-1.46190000	-0.11789800
C	-1.51076500	2.73389900	0.10694900
C	-0.50091100	3.68241900	0.04123600
C	0.83739000	3.26348000	-0.11159500
C	1.13513700	1.90454300	-0.23266300
C	1.71363900	-1.04375200	-0.02619400
C	1.99774500	-2.39429300	0.00191500
C	0.94525300	-3.33371100	-0.06311800
C	-0.35051400	-2.84230100	-0.11936900
O	1.82874100	4.18536600	-0.17316000
C	2.10415800	4.66608600	-1.47214200
O	3.30359300	-2.74233200	0.18043200
C	3.92278500	-3.51501400	-0.84294000
O	1.28178000	-4.63315100	-0.02065500
C	0.26001800	-5.60321200	-0.06270100
O	-5.50106600	-2.31239900	-0.11239200
C	-5.29397200	-3.69503900	-0.26265800
O	-6.01318700	0.20799800	0.18958800
C	-6.36399900	1.56044000	0.34845500
O	-0.68772700	5.01140200	0.10162800

C	-1.99521800	5.50621900	0.25912100
H	2.43782900	3.85237100	-2.13916300
H	1.22163800	5.15846600	-1.91707500
H	3.48936200	-4.52374400	-0.89398300
H	3.82253700	-3.01852000	-1.82294500
H	-0.41934500	-5.51441200	0.80226100
H	-0.32791200	-5.53441700	-0.99413400
H	-4.77414500	-3.93114800	-1.20797200
H	-4.71637800	-4.11643000	0.57904200
H	-5.94952500	1.98448300	1.27989000
H	-6.02714700	2.17423000	-0.50555400
H	-2.64435900	5.22807600	-0.58965500
H	-2.45709900	5.15037900	1.19647500
H	-7.46011900	1.59541200	0.39974800
H	-6.28802600	-4.16067500	-0.27882600
H	0.75786000	-6.58056800	-0.02603800
H	4.98622200	-3.58561800	-0.57895400
H	2.91294300	5.40556700	-1.38259900
H	-1.91262800	6.60034600	0.29783600
Te	3.48532700	0.08811400	0.21175300
O	3.50393600	0.39447300	2.00877800
O	2.41226200	1.63593100	-0.55113200
H	-1.16579000	-3.56191400	-0.12614800
H	-2.91771000	-2.97488700	-0.26813100
H	-3.90489600	1.83784800	0.26510700
H	-2.53903100	3.07187500	0.19917700

mono-**9'**

C	-3.34549900	0.51919300	0.03947900
C	-1.98918000	0.19384500	0.00794400
C	-1.54650100	-1.10874900	-0.03774300
C	-2.41281900	-2.20041900	-0.03726300
C	-3.79329100	-1.91993500	0.00031000
C	-4.26071600	-0.55304800	0.03645500
C	-1.06568000	1.26156100	0.00379200
C	0.32482200	1.03322500	-0.04131100
C	0.79050800	-0.34385100	-0.05290200
C	-0.16405400	-1.38100600	-0.06379300
C	-1.69709400	2.51379300	0.02717200
C	-0.86740800	3.64824700	0.00033600
C	0.54190600	3.45118400	-0.04167200
C	1.14477700	2.17708700	-0.10327600
C	2.11819400	-0.78181000	-0.03503100
C	2.44691700	-2.13577800	-0.03951500
C	1.46674800	-3.16777200	-0.05709000
C	0.11968700	-2.75955400	-0.07163700
O	1.33700200	4.55004600	-0.03722900
C	1.62653100	5.07152400	-1.31805800
O	3.77426400	-2.43173800	0.05039700
C	4.37361600	-3.05683100	-1.07787800
O	1.95581800	-4.41605000	-0.03081100
C	1.08951000	-5.53011400	-0.04723700
O	-4.79047700	-2.81893100	0.00855000
C	-4.49471800	-4.19169000	-0.08047100
O	-5.60019600	-0.45649300	0.05878600
C	-6.20967700	0.79392300	0.27322200
O	-1.23904000	4.93601100	0.00689000

C	-2.59907700	5.28317900	0.12943700
H	2.16379100	4.33465600	-1.94009200
H	0.70795800	5.38618300	-1.84331000
H	3.97884600	-4.07189000	-1.23007300
H	4.21233100	-2.45798600	-1.99061500
H	0.44840200	-5.55684300	0.84897700
H	0.47355400	-5.55182200	-0.96151500
H	-3.96478400	-4.43531400	-1.01712100
H	-3.91154500	-4.54260600	0.78799400
H	-5.88359200	1.24921200	1.22351500
H	-6.02466000	1.48961400	-0.56292400
H	-3.18778100	4.94112100	-0.73825400
H	-3.03577400	4.89254700	1.06350700
H	-7.29058700	0.60781700	0.32937000
H	-5.45794800	-4.71904800	-0.08192000
H	1.73189100	-6.42027400	-0.04035100
H	5.45019000	-3.11320000	-0.86850900
H	2.27057400	5.95089600	-1.17446000
H	-2.63800200	6.38010700	0.16079700
Te	3.73569900	0.56891800	0.18106500
O	3.88556600	0.66494600	1.99370000
O	2.47509600	2.13401100	-0.26406000
S	-1.41383000	-3.68079400	-0.06648400
S	-3.47794900	2.29713500	0.05712000

mono-**10’**

C	3.16510700	-0.20046600	0.05079900
C	1.77019700	-0.05886000	0.01037900
C	1.17661300	1.19530700	-0.04105600
C	1.93949300	2.37117400	-0.04197900
C	3.33793700	2.25852600	0.00358900
C	3.95508000	0.95950200	0.04856300
C	0.96972000	-1.23711800	-0.00534600
C	-0.44076600	-1.15706700	-0.05960300
C	-1.06049200	0.15755200	-0.06015500
C	-0.24059600	1.30903500	-0.06876100
C	1.69719300	-2.44185400	0.00824400
C	0.98243800	-3.64814600	-0.04018400
C	-0.43503900	-3.59024100	-0.09416600
C	-1.14565100	-2.37764600	-0.14832200
C	-2.43707600	0.41414800	-0.03076000
C	-2.95301200	1.70381900	-0.02827300
C	-2.12263600	2.85453800	-0.05520900
C	-0.73545900	2.63224600	-0.07417100
O	-1.12659600	-4.75645700	-0.11518700
C	-1.34228700	-5.28829400	-1.40591600
O	-4.30876000	1.80830200	0.08165600
C	-5.00684600	2.34003500	-1.03798000
O	-2.78452200	4.02184900	-0.02654900
C	-2.10701400	5.25798800	-0.06785100
O	4.22922300	3.26355500	0.01841200
C	3.82002700	4.59188600	-0.19370900
O	5.29798200	1.01502900	0.07052900
C	6.05623100	-0.11417300	0.43013900
O	1.46968500	-4.89844700	-0.04933400

C	2.84705100	-5.14622500	0.10416800
H	-1.93522400	-4.59815900	-2.03099600
H	-0.38882300	-5.50932900	-1.91649700
H	-4.75495000	3.39816200	-1.19934300
H	-4.78085600	1.76356700	-1.95138400
H	-1.47147100	5.40244700	0.82112800
H	-1.51125700	5.36600500	-0.98939600
H	3.28866400	4.70866900	-1.15345000
H	3.19705000	4.96893300	0.63573400
H	5.72884700	-0.53668300	1.39475500
H	6.03515500	-0.89316900	-0.35185600
H	3.43217900	-4.75627300	-0.74590600
H	3.23206300	-4.73817100	1.05339300
H	7.09456100	0.22929700	0.53388900
H	4.73607300	5.19689800	-0.22994000
H	-2.88386100	6.03389500	-0.06528800
H	-6.07742000	2.25130900	-0.80990000
H	-1.90302600	-6.22600000	-1.28324700
H	2.96393600	-6.23795600	0.12571500
Te	-3.88641400	-1.10381700	0.22906700
O	-3.92250800	-1.25419000	2.04480300
O	-2.47026800	-2.47201700	-0.33594500
Se	3.58258900	-2.06707900	0.05370700
Se	0.73731500	3.86237500	-0.06754900

2’

C	-3.16592600	3.05549500	-0.52667400
C	-2.03645200	2.32534000	-0.96757300
C	-2.23871500	1.03149000	-1.49471300
C	-3.56245200	0.54997900	-1.63538600
C	-4.65906900	1.28378100	-1.22846300
C	-4.45072500	2.55993600	-0.63212800
C	-0.69851900	2.91025000	-0.93642400
C	0.40202400	2.14709200	-1.39926200
C	0.21755800	0.74538500	-1.72694600
C	-1.08912200	0.20254800	-1.83598200
C	-0.49507800	4.23901800	-0.51553600
C	0.75713300	4.83438500	-0.60195800
C	1.84061400	4.11436500	-1.14732600
C	1.65801200	2.80063100	-1.58719400
C	1.29463400	-0.14978200	-1.92559300
C	1.12988900	-1.46411200	-2.33183500
C	-0.17731500	-1.97938700	-2.48975100
C	-1.25056900	-1.14428100	-2.22241500
O	3.05290500	4.71555000	-1.25182100
C	3.34041200	5.24149600	-2.52812200
O	2.23768800	-2.22369400	-2.51738800
C	2.46711300	-2.71660900	-3.82834500
O	-0.27689600	-3.26956600	-2.85938700
C	-1.55632800	-3.81911800	-3.05778200
O	-5.93924900	0.89019200	-1.32539400
C	-6.22550700	-0.35192200	-1.92134200
O	-5.55915200	3.19064300	-0.20227700
C	-5.42027700	4.44208800	0.42254500
O	1.03114100	6.09367300	-0.21352400

C	0.01642000	6.84467600	0.40176200
H	3.36104900	4.44928400	-3.29595800
H	2.60541000	6.01152800	-2.82539900
H	1.70567800	-3.45352800	-4.12258600
H	2.48353800	-1.89229700	-4.56277100
H	-2.15220500	-3.81007300	-2.12998300
H	-2.11204300	-3.28262100	-3.84676900
H	-5.84780100	-0.40118400	-2.95772800
H	-5.81680500	-1.19259300	-1.33853700
H	-4.79712800	4.37868600	1.33254600
H	-4.98405300	5.19390700	-0.25809200
H	-0.83489900	7.02769100	-0.27776500
H	-0.35543000	6.35381400	1.31851200
H	-6.43058500	4.76478900	0.70637400
H	-7.31956600	-0.44271700	-1.93764000
H	-1.40473700	-4.85893700	-3.37508900
H	3.45265400	-3.20105000	-3.81027100
H	4.33484300	5.70848600	-2.47394600
H	0.46160800	7.81099500	0.67405600
Te	3.31681300	0.34498100	-1.55415000
O	3.39018400	1.23371900	0.18610100
O	2.68622300	2.21788500	-2.20659300
H	-2.25304200	-1.56113900	-2.28609300
H	-3.73413100	-0.43820000	-2.05611700
H	-3.03097800	4.04459800	-0.09567800
H	-1.33046800	4.82769400	-0.14595700
C	-3.16660700	-3.05490800	0.52678900
C	-2.03696500	-2.32496100	0.96760600
C	-2.23895000	-1.03103100	1.49465200
C	-3.56258000	-0.54922300	1.63530500

C	-4.65936600	-1.28283000	1.22849100
C	-4.45130300	-2.55908800	0.63227900
C	-0.69915200	-2.91015000	0.93648300
C	0.40155000	-2.14719900	1.39929000
C	0.21738600	-0.74543400	1.72690300
C	-1.08918300	-0.20230700	1.83586200
C	-0.49599300	-4.23899100	0.51568300
C	0.75609900	-4.83460800	0.60213000
C	1.83973600	-4.11476600	1.14741200
C	1.65741300	-2.80097600	1.58722300
C	1.29463600	0.14953100	1.92551900
C	1.13015000	1.46394200	2.33159900
C	-0.17694200	1.97951700	2.48941200
C	-1.25036000	1.14460100	2.22213500
O	3.05190900	-4.71619400	1.25189100
C	3.33940000	-5.24207700	2.52822200
O	2.23808600	2.22334500	2.51707900
C	2.46750400	2.71638100	3.82799000
O	-0.27622800	3.26977200	2.85888100
C	-1.55551400	3.81966800	3.05727200
O	-5.93946300	-0.88896600	1.32544100
C	-6.22544400	0.35324400	1.92132700
O	-5.55989000	-3.18963200	0.20259600
C	-5.42134000	-4.44124300	-0.42196900
O	1.02985800	-6.09398100	0.21379100
C	0.01493200	-6.84491300	-0.40124200
H	3.36031200	-4.44978700	3.29597000
H	2.60422800	-6.01188800	2.82564900
H	1.70610100	3.45337800	4.12212700
H	2.48385400	1.89214600	4.56250400

H	-2.15140300	3.81071900	2.12948000
H	-2.11135900	3.28337700	3.84630200
H	-5.84772600	0.40248200	2.95771000
H	-5.81655400	1.19379700	1.33848200
H	-4.79827500	-4.37817500	-1.33204800
H	-4.98519900	-5.19300200	0.25878900
H	-0.83633200	-7.02767000	0.27842400
H	-0.35694800	-6.35414700	-1.31803000
H	-6.43174500	-4.76379500	-0.70562300
H	-7.31948200	0.44428400	1.93762200
H	-1.40364400	4.85946900	3.37450900
H	3.45307300	3.20076400	3.80989900
H	4.33370500	-5.70932800	2.47400200
H	0.45991800	-7.81135500	-0.67342700
Te	3.31670300	-0.34567500	1.55415000
O	3.38997500	-1.23443600	-0.18609300
O	2.68574700	-2.21843400	2.20661100
H	-2.25274700	1.56167400	2.28569200
H	-3.73403600	0.43903100	2.05594700
H	-3.03188600	-4.04406200	0.09584200
H	-1.33150000	-4.82752900	0.14615100

9’

C	5.49471900	1.85736500	0.19348800
C	4.37178000	1.17945100	-0.28173000
C	3.22077300	1.82950600	-0.65654900
C	3.07295200	3.21116100	-0.55360000
C	4.17093100	3.93691900	-0.05135600
C	5.39036700	3.25749000	0.31741600
C	4.46031200	-0.22239500	-0.41012400
C	3.37823600	-0.99132900	-0.88573900
C	2.12142700	-0.31715300	-1.19096500
C	2.10719500	1.09145600	-1.10688600
C	5.72903600	-0.70778300	-0.05829600
C	5.95991800	-2.08472200	-0.22905400
C	4.89906300	-2.88266700	-0.73637800
C	3.63977600	-2.35923400	-1.10675900
C	0.88754500	-0.89638300	-1.54278700
C	-0.23499000	-0.10804000	-1.85415700
C	-0.21048300	1.31161400	-1.74805000
C	0.99973600	1.91026700	-1.37103800
O	5.12125700	-4.21469900	-0.88431800
C	5.57578800	-4.59230200	-2.16616100
O	-1.35492400	-0.77684200	-2.18851400
C	-2.17421700	-0.34337100	-3.26065700
O	-1.37985000	1.94719800	-1.94542500
C	-1.39284400	3.20943500	-2.57445500
O	4.22581100	5.26625200	0.14326600
C	3.14994600	6.07621800	-0.26147900
O	6.34981800	4.09199300	0.75728000
C	7.50376800	3.56540500	1.36554500
O	7.09007300	-2.76211200	0.02516100

C	8.16438300	-2.12907400	0.67907200
H	4.83447100	-4.34374900	-2.94530200
H	6.53630600	-4.10685200	-2.41472500
H	-2.94045200	0.36847300	-2.92461400
H	-1.57675700	0.11592000	-4.06542800
H	-1.09191800	4.01487500	-1.88379600
H	-0.74334500	3.22265000	-3.46566700
H	2.94516500	5.97601400	-1.34108100
H	2.23404900	5.86381600	0.31655100
H	7.25455900	2.92222800	2.22649100
H	8.12936500	3.00711000	0.64807300
H	8.61575100	-1.33796800	0.05680800
H	7.85995200	-1.71483800	1.65488100
H	8.08548900	4.42374200	1.72797900
H	3.44732700	7.11432200	-0.06104900
H	-2.43039100	3.39570000	-2.88329900
H	-2.66566800	-1.24576500	-3.65136600
H	5.72469200	-5.68186200	-2.15358600
H	8.92369800	-2.90352400	0.85196000
Te	0.68013400	-3.00884800	-1.41459000
O	-1.19868700	-3.08241500	-0.48370400
O	2.76012600	-3.15869800	-1.69061200
S	1.40983200	3.61197500	-1.05917100
S	6.77565400	0.65060200	0.47495900
C	-5.43352900	1.92950400	-0.22022900
C	-4.33729800	1.22500700	0.27780900
C	-3.18060400	1.84814600	0.67971000
C	-2.99820000	3.22582500	0.58210800
C	-4.06704800	3.97728100	0.05604000
C	-5.29391000	3.32699400	-0.33937300

C	-4.45763900	-0.17568700	0.39288000
C	-3.40046900	-0.97130800	0.87985100
C	-2.13744700	-0.32512600	1.21571900
C	-2.09110400	1.08308800	1.14270600
C	-5.72903700	-0.63137500	0.01211100
C	-5.99164200	-2.00415200	0.16891300
C	-4.95851500	-2.82797500	0.69246900
C	-3.69468300	-2.33486900	1.08796100
C	-0.92502500	-0.93305800	1.58830600
C	0.20959000	-0.17347000	1.92874000
C	0.22509300	1.24551200	1.81031700
C	-0.96719100	1.87343600	1.42221800
O	-5.21171100	-4.15569300	0.83035800
C	-5.74335300	-4.52098100	2.08566400
O	1.29429900	-0.87755800	2.30143600
C	2.15026700	-0.42797800	3.33698300
O	1.40994600	1.85452100	2.00383800
C	1.45416000	3.11447100	2.63649000
O	-4.08295500	5.30721200	-0.14323000
C	-3.01623700	6.09494200	0.32480900
O	-6.22447800	4.18330600	-0.79939300
C	-7.36405500	3.68313700	-1.45511200
O	-7.12980500	-2.65675300	-0.11350100
C	-8.18264500	-1.99358400	-0.77245900
H	-5.04593100	-4.27521600	2.90536300
H	-6.71143200	-4.02447400	2.27591600
H	2.94423000	0.22664400	2.95260000
H	1.58919000	0.10137000	4.12457300
H	1.17118900	3.92846500	1.94805000
H	0.80731600	3.14086000	3.52936900

H	-2.86309400	5.97269400	1.41062400
H	-2.07696300	5.88005400	-0.21362100
H	-7.09427100	3.03972200	-2.30965700
H	-8.02795200	3.13295000	-0.76626200
H	-8.62400200	-1.19989500	-0.14635500
H	-7.85805800	-1.57508500	-1.73993100
H	-7.91476400	4.55475500	-1.83400300
H	-3.28979600	7.14046300	0.12882500
H	2.49664600	3.27535900	2.94321700
H	2.60359400	-1.33202700	3.76777000
H	-5.90252200	-5.60906300	2.07070200
H	-8.95628900	-2.74946400	-0.96298200
Te	-0.75729700	-3.04297900	1.41937300
O	1.12367300	-3.09542900	0.48665000
O	-2.84143000	-3.15678200	1.68060900
S	-1.33293300	3.58520500	1.11090100
S	-6.73466100	0.75289800	-0.53472300

10’

C	4.67636000	2.10845900	-0.17477000
C	3.67085900	1.21917000	-0.57431000
C	2.46129900	1.67433400	-1.07368000
C	2.18183500	3.03835800	-1.21340800
C	3.17253200	3.95289200	-0.82580200
C	4.42013100	3.48826500	-0.28505400
C	3.94023600	-0.17896800	-0.54942000
C	2.99268500	-1.11996600	-1.01923600
C	1.68756900	-0.64854900	-1.45297600
C	1.47809400	0.74609600	-1.49735900
C	5.22492400	-0.51521100	-0.08927600
C	5.60411800	-1.86804600	-0.11105800
C	4.68260300	-2.82119700	-0.61436900
C	3.41621700	-2.46424200	-1.11986900
C	0.58127800	-1.43438900	-1.83153600
C	-0.58778900	-0.86831200	-2.36995900
C	-0.72992900	0.53917500	-2.48117900
C	0.31051100	1.33191300	-2.00129200
O	5.04598800	-4.12853000	-0.61442000
C	5.64983700	-4.57064200	-1.81171400
O	-1.50939700	-1.72332200	-2.86631400
C	-2.86434200	-1.63573100	-2.42474900
O	-1.82806600	1.12205200	-3.02400100
C	-1.97755200	0.95107100	-4.42642300
O	3.07972900	5.29287500	-0.94844500
C	1.88098000	5.92206700	-0.56054100
O	5.26181000	4.48313900	0.04757000
C	6.37310000	4.22610800	0.87090100
O	6.77701800	-2.39073200	0.27987600

C	7.65435100	-1.65448500	1.09885600
H	4.96348700	-4.46745500	-2.66982000
H	6.58018200	-4.01501400	-2.02483600
H	-3.20515900	-0.59406400	-2.35804500
H	-3.46781900	-2.17248100	-3.16886100
H	-1.12137500	1.38928000	-4.96680600
H	-2.07145200	-0.11210000	-4.70092300
H	1.08188700	5.80916900	-1.31457300
H	1.52722300	5.53841800	0.41053900
H	6.08584000	3.68756300	1.78976400
H	7.16354600	3.66922300	0.33845700
H	8.16668500	-0.85265300	0.53979800
H	7.13502800	-1.23188400	1.97502500
H	6.78446000	5.20477900	1.15376400
H	2.10103900	6.99452500	-0.46381400
H	-2.89515100	1.48136100	-4.71419100
H	-2.95392000	-2.13387900	-1.45109500
H	5.89626000	-5.63427000	-1.68069700
H	8.41818600	-2.36081800	1.45155700
Te	0.59843000	-3.51649800	-1.47417500
O	-1.28420800	-3.47305700	-0.54174100
O	2.67823300	-3.40382800	-1.69489200
C	-4.52336700	2.28566800	0.21218000
C	-3.59420300	1.32163800	0.62520100
C	-2.34894600	1.68560200	1.11171600
C	-1.94581700	3.02427800	1.20982000
C	-2.85925900	4.01019100	0.80201100
C	-4.15424600	3.63795700	0.29503400
C	-3.96825700	-0.05177400	0.58634700
C	-3.09322400	-1.06449600	1.04327100

C	-1.76082600	-0.69210500	1.48473300
C	-1.44119300	0.68158500	1.53292300
C	-5.26873200	-0.28993500	0.10768800
C	-5.74468400	-1.61185100	0.10952200
C	-4.89182200	-2.63798300	0.59317700
C	-3.60202400	-2.38227100	1.09881000
C	-0.71532700	-1.56254200	1.84513600
C	0.50243100	-1.09649900	2.36708200
C	0.76853300	0.29067000	2.46132500
C	-0.21450000	1.16695200	2.00330000
O	-5.34788200	-3.91594800	0.56709200
C	-5.94618200	-4.34881000	1.77028700
O	1.35990100	-2.03731600	2.81289700
C	2.73539000	-1.97681000	2.45048600
O	1.93534100	0.76136700	2.97014900
C	2.02188700	0.71148300	4.38589000
O	-2.66709300	5.33975900	0.84803000
C	-1.35602900	5.84637800	0.88385400
O	-4.90347900	4.69383300	-0.07243900
C	-6.29444400	4.55622800	-0.22520100
O	-6.94860500	-2.04872600	-0.29169500
C	-7.82242200	-1.20688800	-1.00512700
H	-5.22925600	-4.32066800	2.60894300
H	-6.82707500	-3.73435800	2.02805300
H	2.86731600	-1.46655700	1.48952700
H	3.32690700	-1.46647800	3.22576200
H	1.24261900	1.33873400	4.85185600
H	1.92264900	-0.32075900	4.76226600
H	-0.89166700	5.72555700	1.87868600
H	-0.72972000	5.37093600	0.11346300

H	-6.55833700	3.96903400	-1.12243500
H	-6.76202800	4.10833700	0.66753000
H	-8.22993500	-0.40179700	-0.37013100
H	-7.33715300	-0.77797200	-1.89786400
H	-6.69511100	5.57039800	-0.35917300
H	-1.42595300	6.92238900	0.67238200
H	3.01100200	1.10194000	4.66094100
H	3.07698600	-3.01503400	2.35152800
H	-6.27324100	-5.38765400	1.61826900
H	-8.66050600	-1.83600800	-1.33423100
Te	-0.84734900	-3.60654200	1.36501700
O	1.03392800	-3.55716500	0.43493700
O	-2.91757300	-3.39106200	1.62199200
Se	6.20071900	1.08050100	0.36109300
Se	0.43780600	3.22949300	-1.98869800
Se	-0.16715200	3.06343100	1.94754800
Se	-6.10354200	1.37782700	-0.37319600